



Direct numerical simulation of turbulent flows over acoustic liners

**EUROHPC
USER DAY
2023** Brussels
11.12.23



Project: “ENTRAIN”

EuroHPC used: Meluxina

Speaker: *Davide Modesti (TU Delft)*

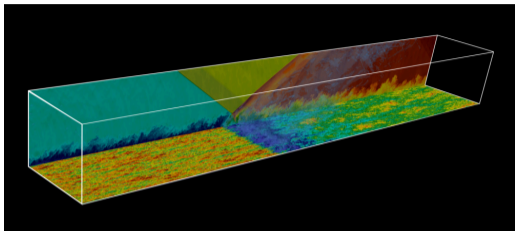
Introduction

Pre-exascale EU supercomputers




Rank	System	RPeak (ExaFlop/s)	Power (MW)
1.	Frontier (US)	1.6	23
2.	Aurora (US)	1.0	25
5.	LUMI (Finland)	0.4	7
6.	Leonardo (Italy)	0.3	7


The flow solver: STREAMS-2



Follow us on social media:

 @streams_cfd

 @streamscfd6365

 streamsdns

Documentation: <https://streams-cfd.github.io/STREAMS-2/>

Github: <https://github.com/STREAMS-CFD/STREAMS-2>

Main features:

- Open source GPL-3.0 license
- Direct numerical simulation of wall bounded flows
- Three different backends: CPU, NVIDIA GPU, AMD GPU
- Object oriented framework, modern Fortran



Developers team



Davide Modesti, TU Delft



Francesco Salvatore, Cineca



Matteo Bernardini, Sapienza



Srikanth Sathyanarayana, MPC

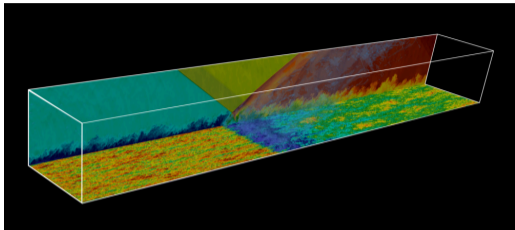


Sergio Pirozzoli, Sapienza

Research topics:

- Turbulent high-speed flows
- Wall turbulence
- Aeroacoustics
- Numerical methods
- High performance computing

STREAmS-2: numerics



Discretization:

- Hybrid energy conserving/shock capturing finite difference¹
- High order WENO reconstruction close to discontinuities
- Arbitrary order of accuracy for spatial derivatives
- Explicit time step integration, 3rd order low storage R–K

¹S. Pirozzoli J. Comput. Phys. 229.19 (2010): 7180-7190.

Acoustic liners



Haris Shahzad



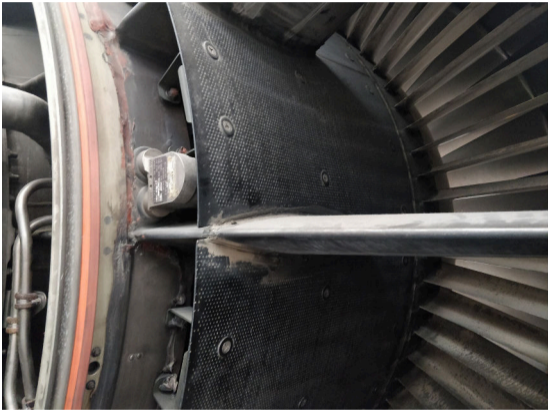
Stefan Hicel

TU Delft

Acoustic liners



Acoustic liners



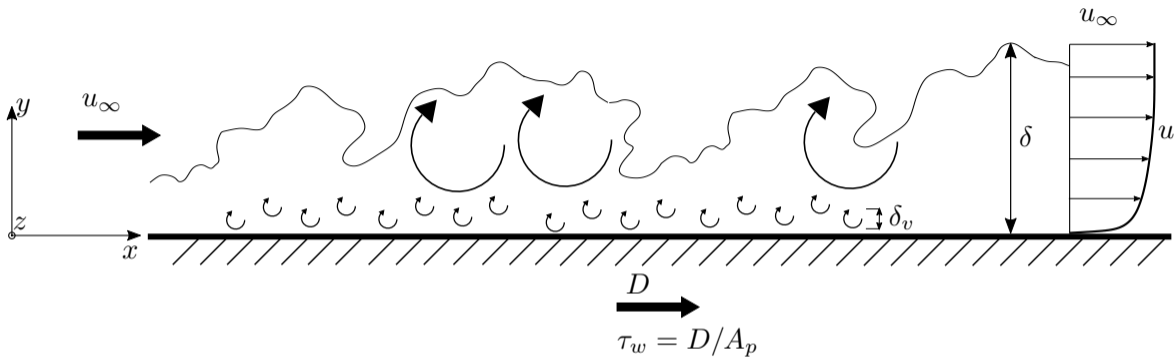
Acoustic liners



Acoustic liners



Effect of roughness: review



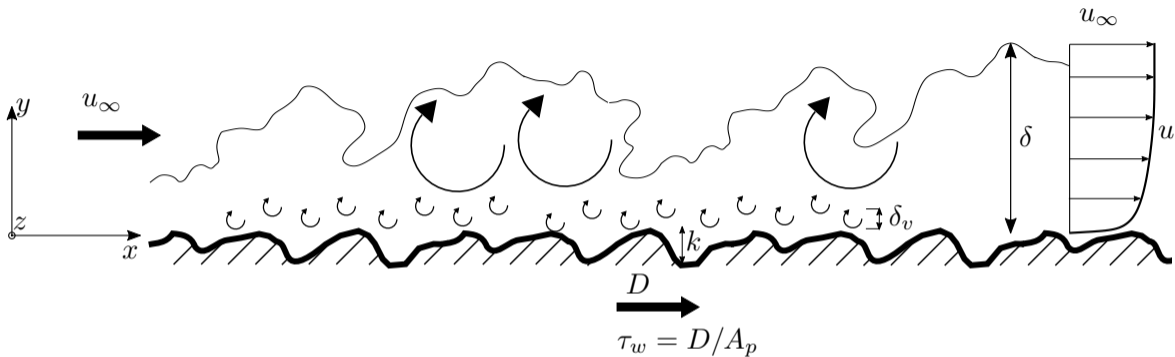
$$u_\tau = \sqrt{\tau_w / \rho_w}$$

$$\delta_v = \nu_w / u_\tau$$

$$Re_\tau = \delta / \delta_v$$

$$C_f = 2\tau_w / (\rho_\infty u_\infty^2)$$

Effect of roughness: review



$$u_\tau = \sqrt{\tau_w / \rho_w}$$

$$\delta_v = \nu_w / u_\tau$$

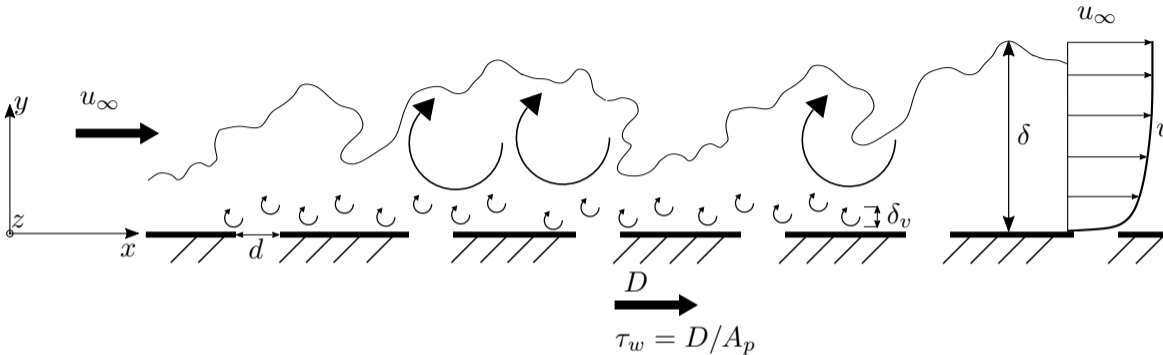
$$Re_\tau = \delta / \delta_v$$

$$k / \delta \ll 1$$

$$k^+ = k / \delta_v \gg 1$$

$$k^+ > 5 \text{ rough wall}$$

Effect of roughness: review



$$u_\tau = \sqrt{\tau_w / \rho_w}$$

$$\delta_v = \nu_w / u_\tau$$

$$Re_\tau = \delta / \delta_v$$

$$k / \delta \ll 1$$

$$k^+ = k / \delta_v \gg \gg 1$$

$$k^+ > 5 \text{ rough wall}$$

$$d / \delta = ?$$

$$d^+ = d / \delta_v = ?$$

Effect of roughness: review



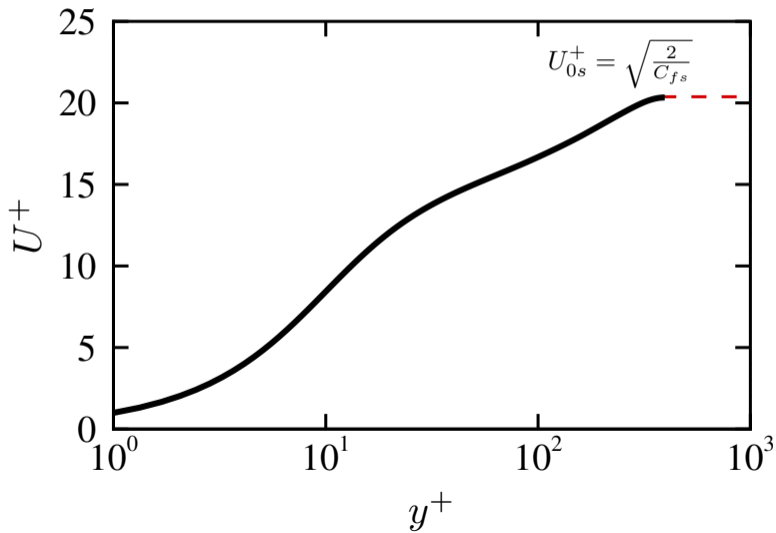
Noise reduction of about 8–10dB

$$d/\delta \approx 0.1$$

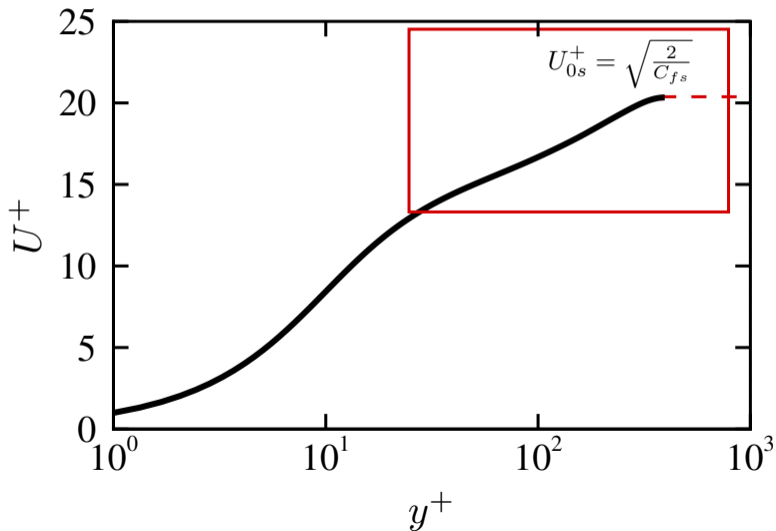
$$d^+ = d/\delta_v \approx 120\text{--}500$$

$$\sigma = 0.08\text{--}0.3$$

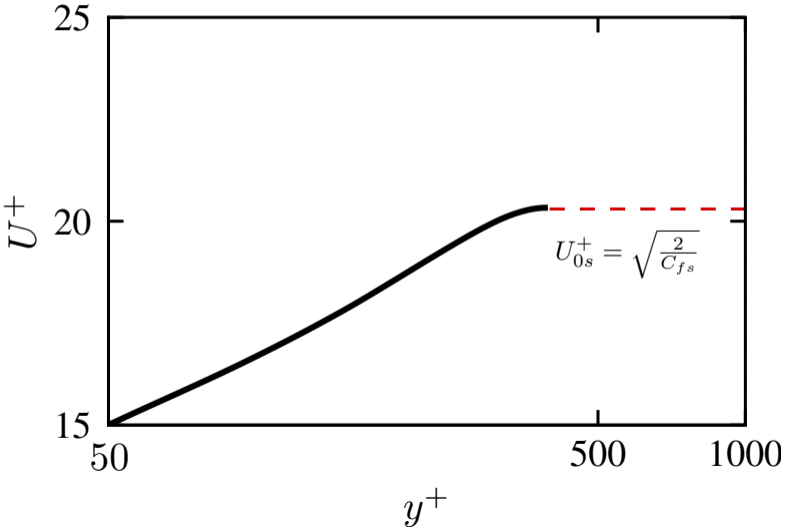
Effect of roughness: review



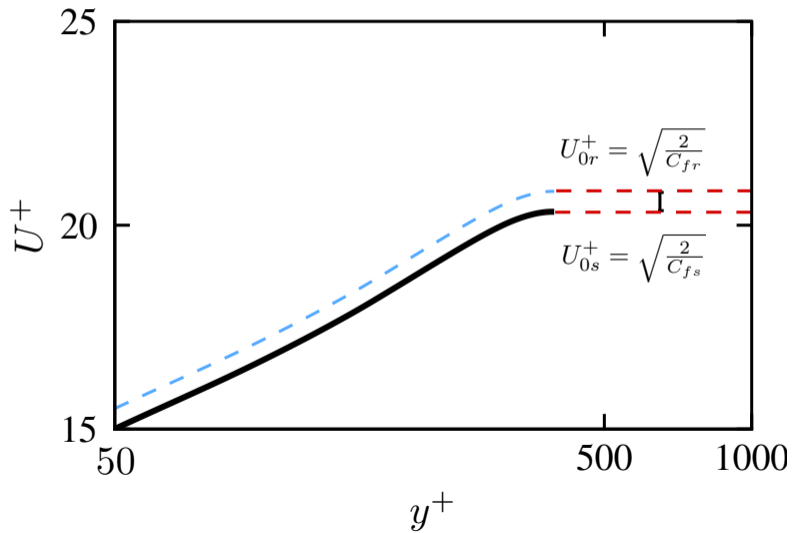
Effect of roughness: review



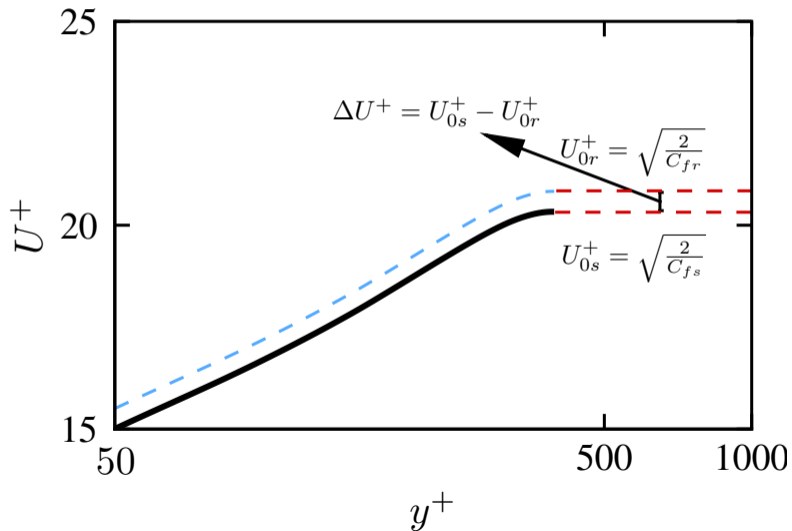
Effect of roughness: review



Effect of roughness: review

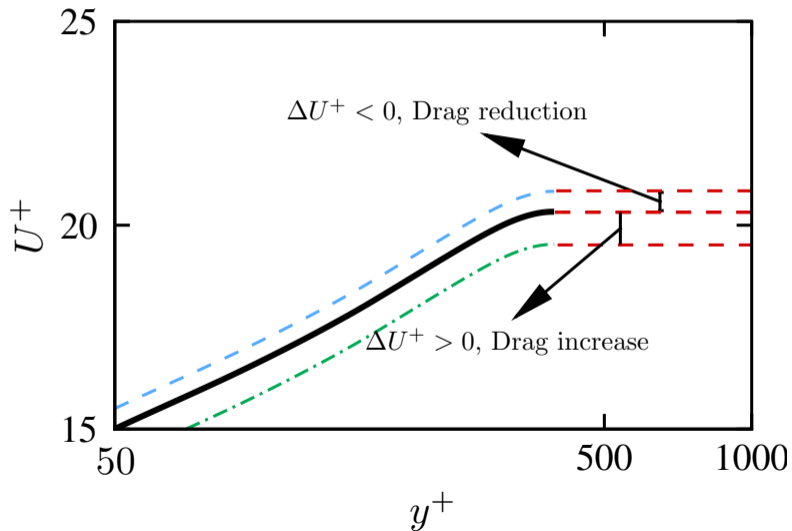


Effect of roughness: review

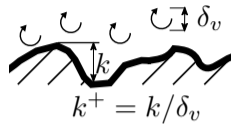
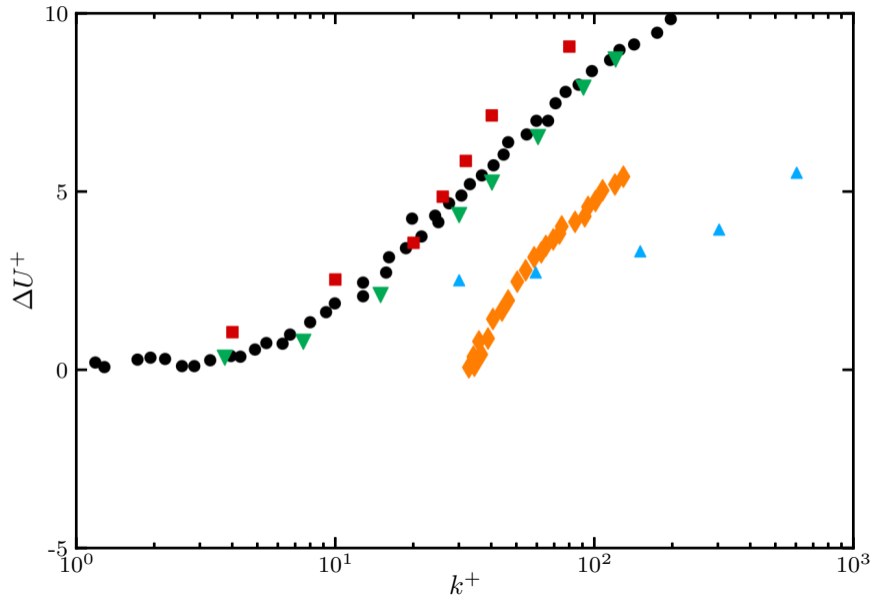


Effect of roughness: review

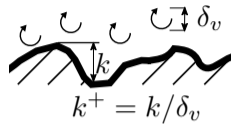
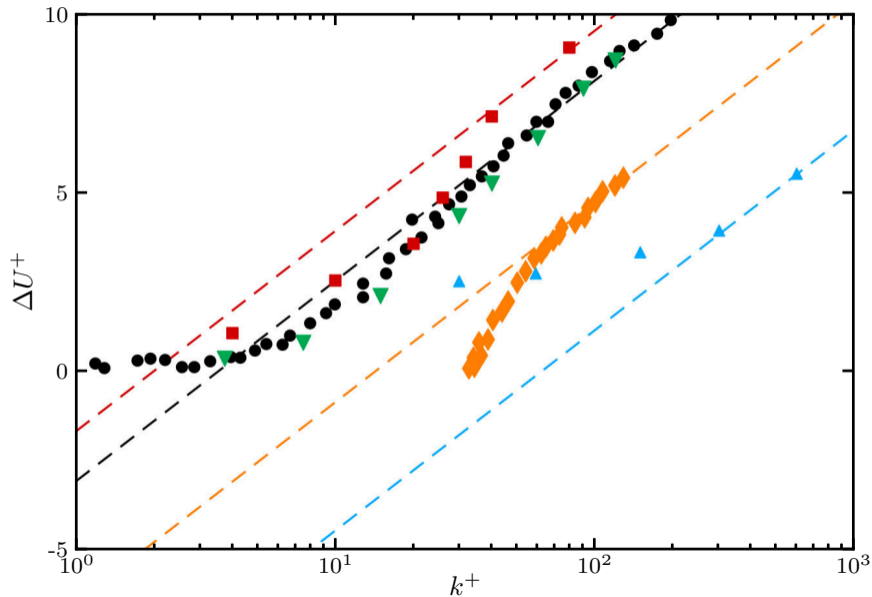
$$\mathcal{DV} = 1 - C_{fr}/C_{fs} \sim \sqrt{2C_{fs}}\Delta U^+$$



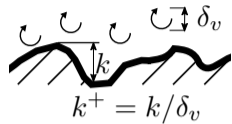
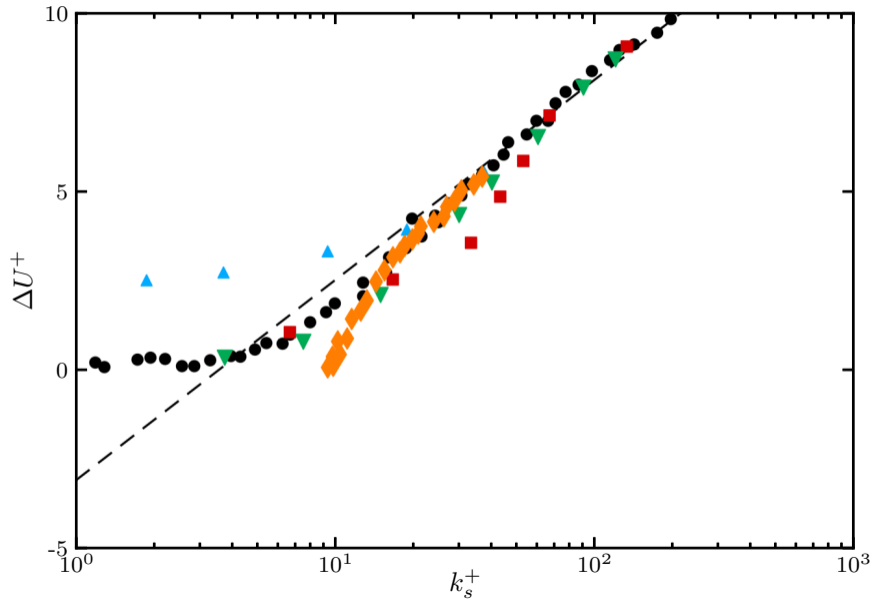
Effect of roughness: review



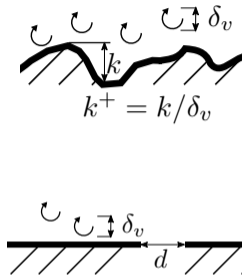
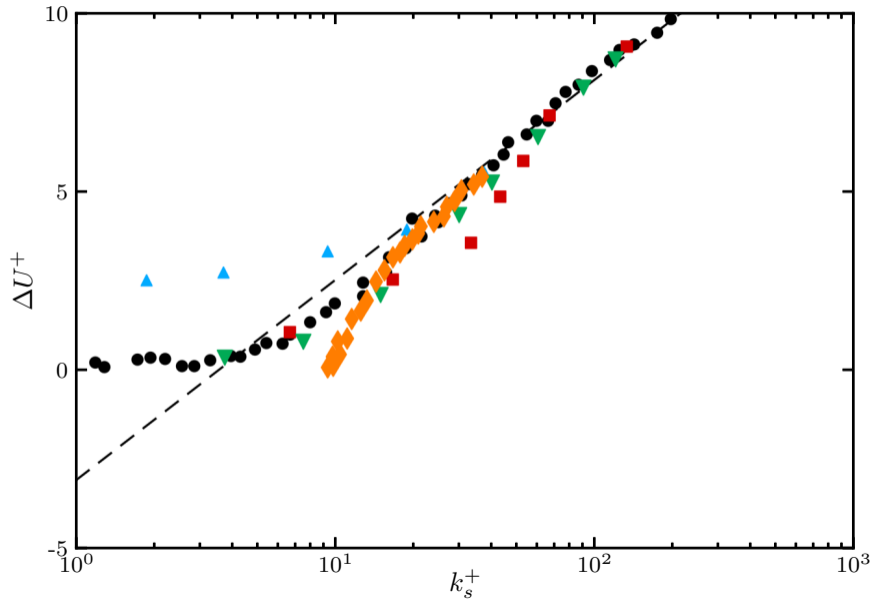
Effect of roughness: review



Effect of roughness: review



Effect of roughness: review



Effect of roughness: review

	d^+	σ	ΔD
GFIT ^{2,3,4}	180 – 660	0.08 – 0.3	10 – 350%
Wilkinson (1983) ⁵	9 – 150	0.047 – 0.14	2 – 60%
Gustavsson <i>et al.</i> (2019) ⁶	350 – 550	0.0853	30 – 50%
Zhang and Bodony (2016) ⁷	114	0.0099	4 – 100%
Scalo <i>et al.</i> (2015) ⁸	Impedance B.C		$\leq 325\%$
Sebastian <i>et al.</i> (2019) ⁹	Impedance B.C		$\leq 575\%$

²B.M. Howerton and M.G. Jones (2015), AIAA Paper 2015-2230

³B.M. Howerton and M.G. Jones (2016), AIAA Paper 2016-2979

⁴B.M. Howerton and M.G. Jones (2017), AIAA Paper 2017-4190

⁵Wilkinson (1983), AIAA Paper 1983-0294

⁶Gustavsson *et al.* (2019), AIAA Paper 2019-2683

⁷Q. Zhang and D.J. Bodony (2016), J. Fluid Mech. 792, pp 936–980

⁸C. Scalo, J. Bodart, S.K. Lele (2015). Phys. Fluids 27.3, p. 035107

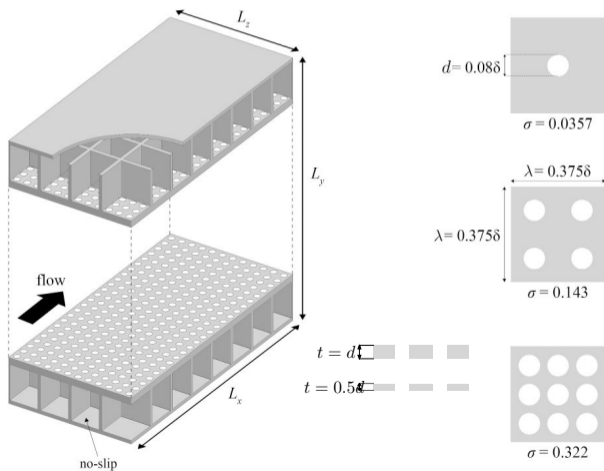
⁹R. Sebastian, D. Marx, and V. Fortuné (2019), J. Sound Vib. 306–330

Methodology and dataset

DNS of turbulent channel flow

Domain size $3\delta \times 2(\delta + h) \times 1.5\delta$

Bulk Mach number $M_b = 0.3$



Methodology and dataset



$\sigma = 0.0357$

	Re_b	Re_τ	d^+	σ	t/d	$1/\alpha^+$	Δx^+	Δy_{\min}^+	Δz^+
L_1	9139	503.5	40.3	0.0357	1	0.0528	1.1	0.80	1.1

Methodology and dataset



$\sigma = 0.142$

	Re_b	Re_τ	d^+	σ	t/d	$1/\alpha^+$	Δx^+	Δy_{\min}^+	Δz^+
L_1	9139	503.5	40.3	0.0357	1	0.0528	1.1	0.80	1.1
L_2	8794	496.4	39.7	0.142	1	0.859	1.0	0.80	1.0
L_4	19505	1038	83.0	0.142	1	1.80	2.1	0.81	2.1

Methodology and dataset



$\sigma = 0.322$

	Re_b	Re_τ	d^+	σ	t/d	$1/\alpha^+$	Δx^+	Δy_{\min}^+	Δz^+
L_1	9139	503.5	40.3	0.0357	1	0.0528	1.1	0.80	1.1
L_2	8794	496.4	39.7	0.142	1	0.859	1.0	0.80	1.0
L_3	8264	505.3	40.4	0.322	1	5.14	1.0	0.81	1.0
L_4	19505	1038	83.0	0.142	1	1.80	2.1	0.81	2.1
L_5	17810	1026	82.1	0.322	1	10.4	2.1	0.82	2.1
L_6	35470	2044	164.0	0.322	1	20.8	4.1	0.82	4.1

Methodology and dataset



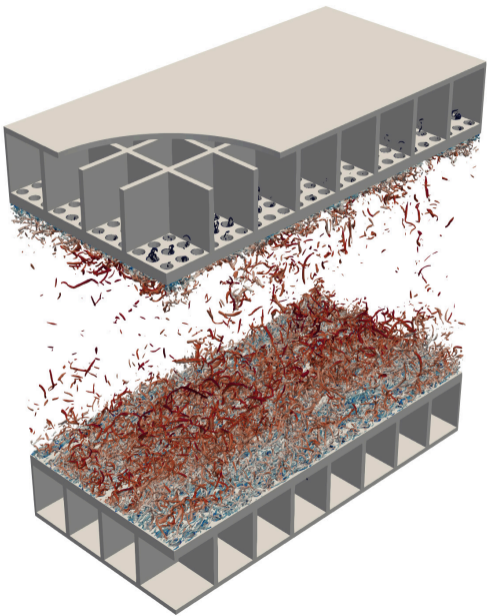
	Re_b	Re_τ	d^+	σ	t/d	$1/\alpha^+$	Δx^+	Δy_{\min}^+	Δz^+
L_1	9139	503.5	40.3	0.0357	1	0.0528	1.1	0.80	1.1
L_{t1}	9139	508.8	40.7	0.0357	0.5	0.0533	1.5	0.81	1.1
L_2	8794	496.4	39.7	0.142	1	0.859	1.0	0.80	1.0
L_{t2}	8794	520.8	41.6	0.142	0.5	0.901	1.6	0.83	1.1
L_3	8264	505.3	40.4	0.322	1	5.14	1.0	0.81	1.0
L_4	19505	1038	83.0	0.142	1	1.80	2.1	0.81	2.1
L_{t4}	19505	1031	82.5	0.142	0.5	1.78	3.1	0.82	1.1
L_5	17810	1026	82.1	0.322	1	10.4	2.1	0.82	2.1
L_{t5}	17810	1057	84.6	0.322	0.5	10.7	3.2	0.85	1.1
L_6	35470	2044	164.0	0.322	1	20.8	4.1	0.82	4.1

Methodology and dataset

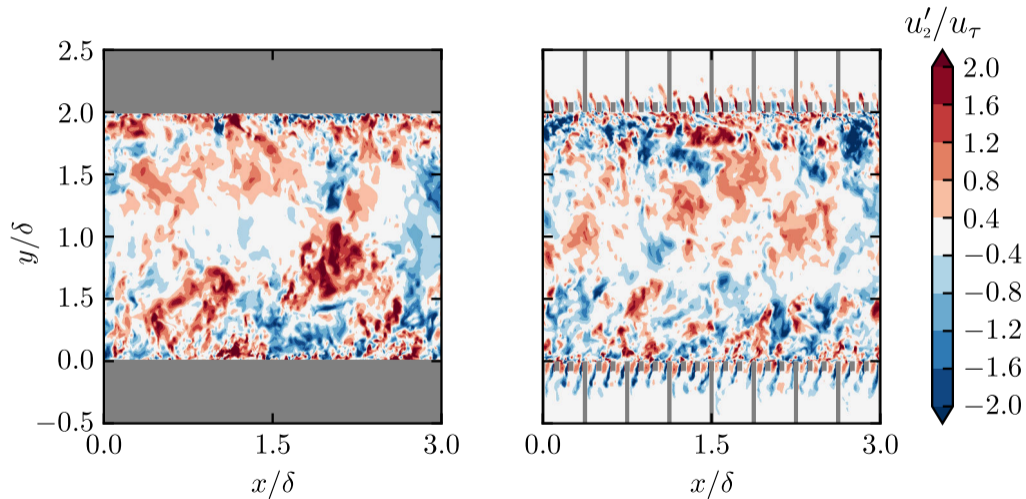
//////////

	Re_b	Re_τ	d^+	σ	t/d	$1/\alpha^+$	Δx^+	Δy_{\min}^+	Δz^+
S_1	9268	506.1	0	0	0	0	5.1	0.80	5.1
S_2	21180	1048	0	0	0	0	5.2	0.80	5.2
S_3	45240	2060	0	0	0	0	5.2	0.80	5.2
L_1	9139	503.5	40.3	0.0357	1	0.0528	1.1	0.80	1.1
L_{t1}	9139	508.8	40.7	0.0357	0.5	0.0533	1.5	0.81	1.1
L_2	8794	496.4	39.7	0.142	1	0.859	1.0	0.80	1.0
L_{t2}	8794	520.8	41.6	0.142	0.5	0.901	1.6	0.83	1.1
L_3	8264	505.3	40.4	0.322	1	5.14	1.0	0.81	1.0
L_4	19505	1038	83.0	0.142	1	1.80	2.1	0.81	2.1
L_{t4}	19505	1031	82.5	0.142	0.5	1.78	3.1	0.82	1.1
L_5	17810	1026	82.1	0.322	1	10.4	2.1	0.82	2.1
L_{t5}	17810	1057	84.6	0.322	0.5	10.7	3.2	0.85	1.1
L_6	35470	2044	164.0	0.322	1	20.8	4.1	0.82	4.1

Instantaneous flow field channel flow

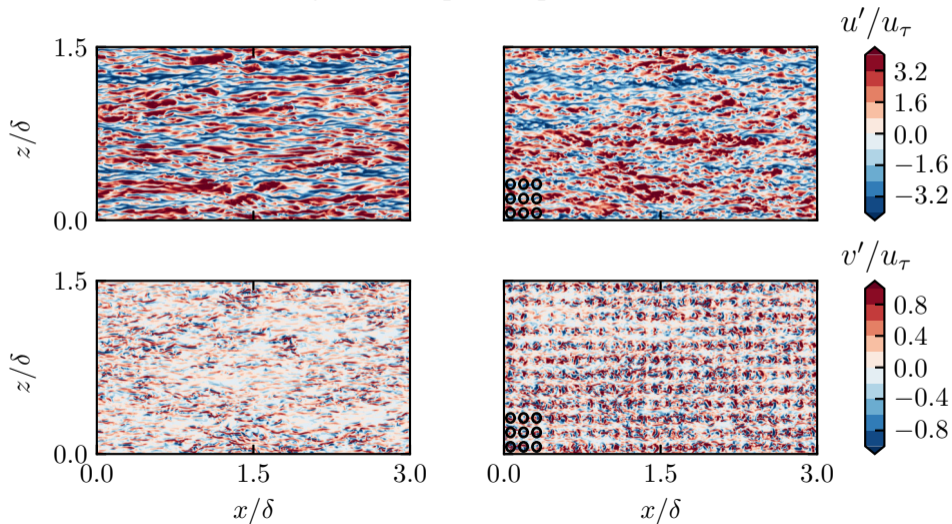


Instantaneous flow field channel flow

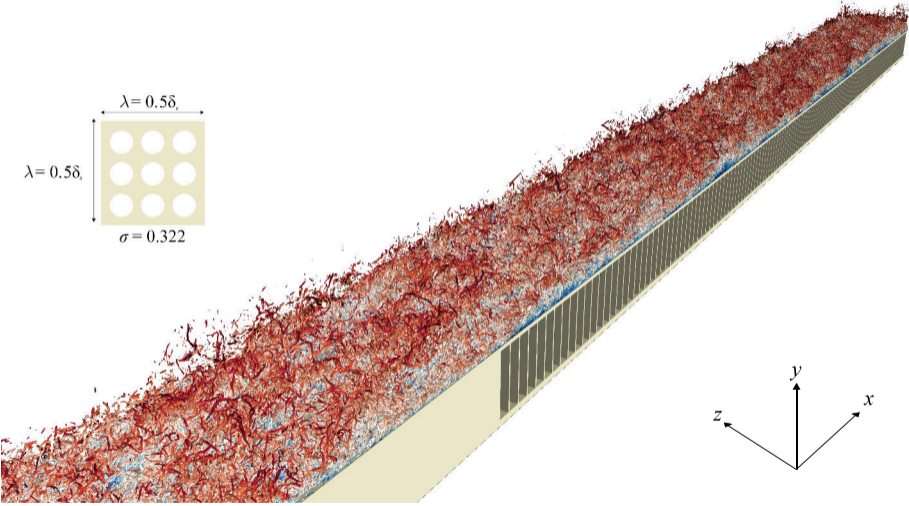


Instantaneous flow field channel flow

Instantaneous velocity in a wall-parallel plane at $y^+ = 12$, $Re_\tau = 2044$

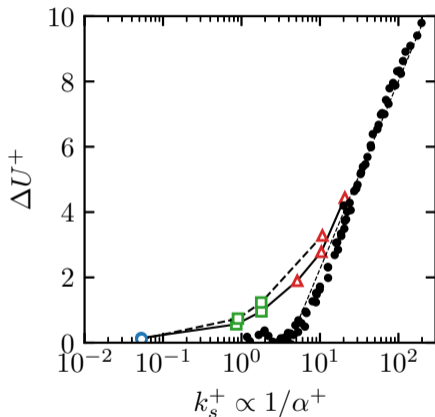
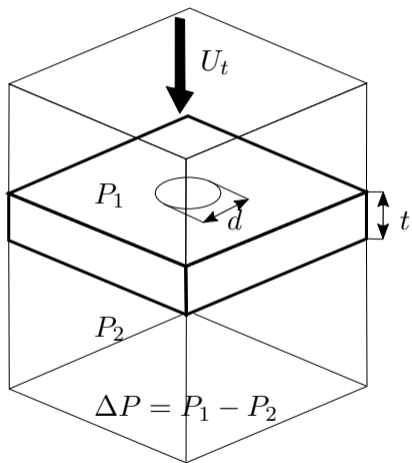


Turbulent boundary layer over acoustic liners¹⁰



Added drag

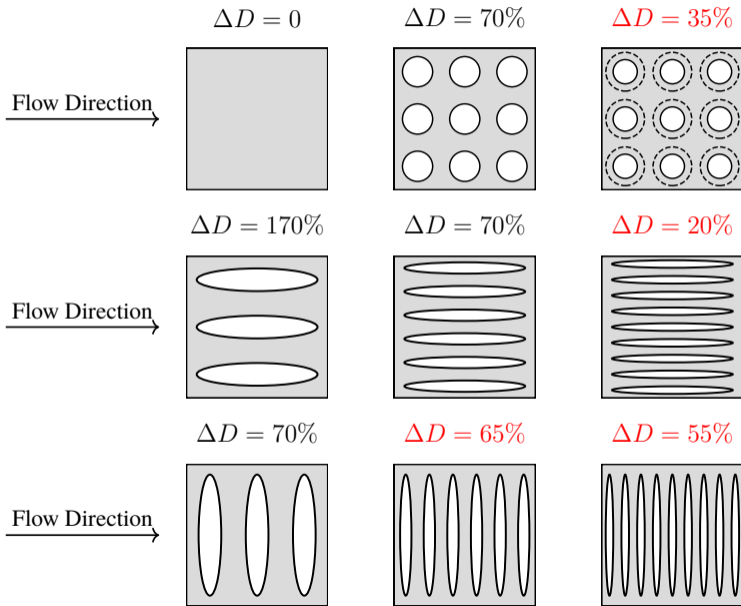
ΔU^+ depends on wall-normal permeability of the plate^{11 12}.



¹¹H. Shahzad, S. Hickel, D. Modesti Flow Turbul. Combust. 109.4 (2022): 1241-1254.

¹²H. Shahzad S. Hickel D. Modesti J. Fluid Mech. 965 (2023): A10.

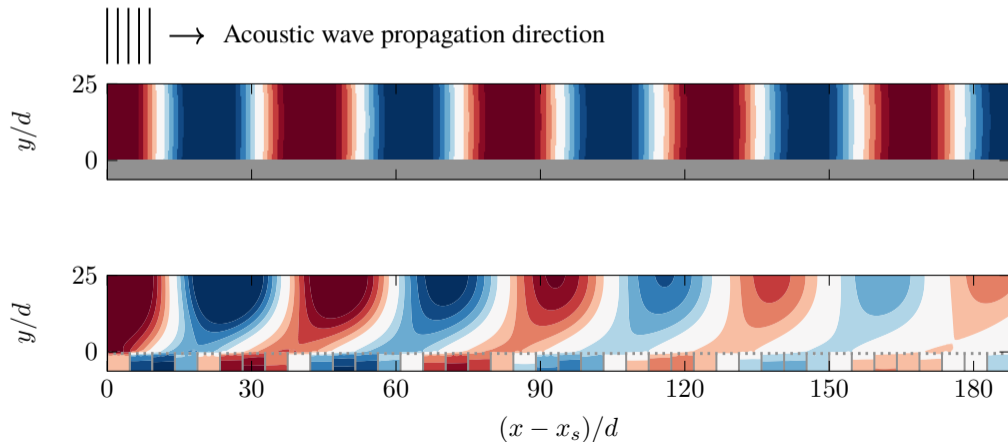
Acoustic liners: optimized geometries



Acoustic liners: optimized geometries

Acoustic Performance

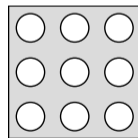
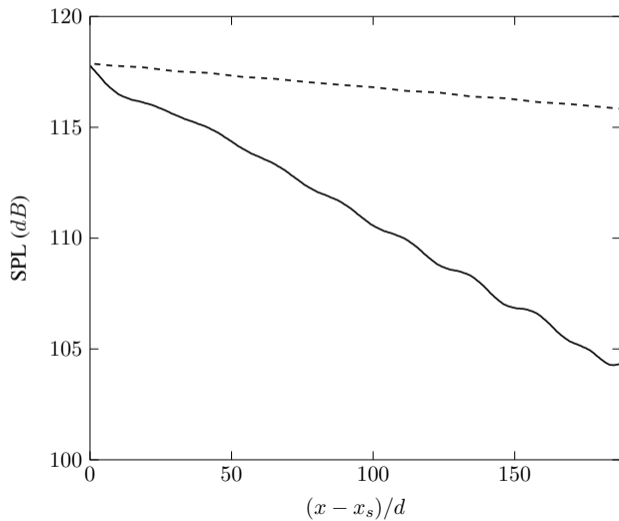
No grazing flow, array of 40 cavities¹³



¹³H. Shahzad, S. Hickel, D. Modesti AIAA J. (Under review)

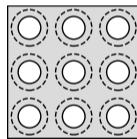
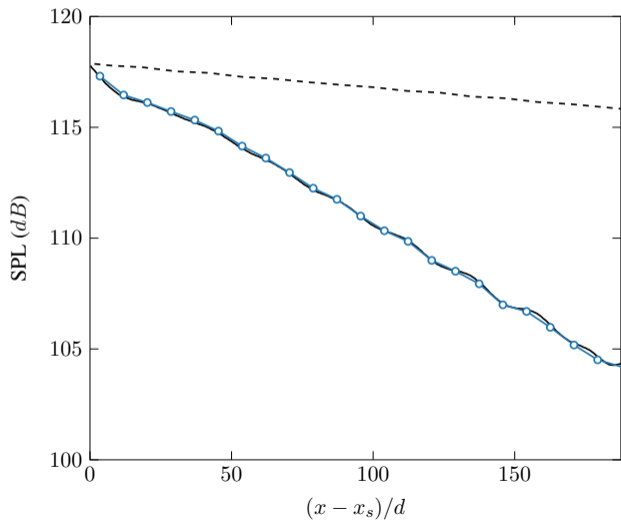
Acoustic liners: optimized geometries

SPL Loss



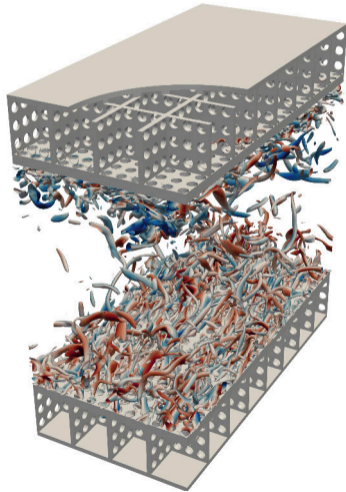
Acoustic liners: optimized geometries

SPL Loss



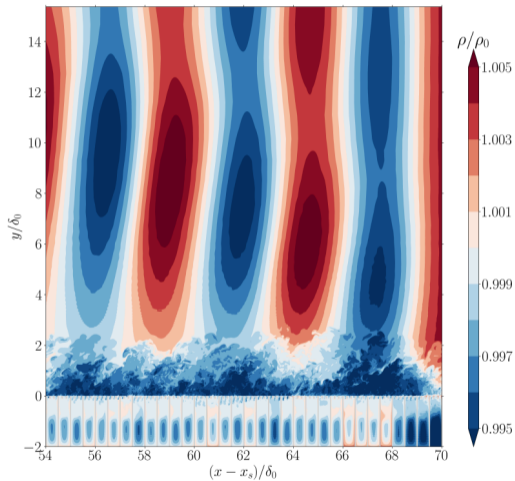
Ongoing work

Broadband acoustic liners



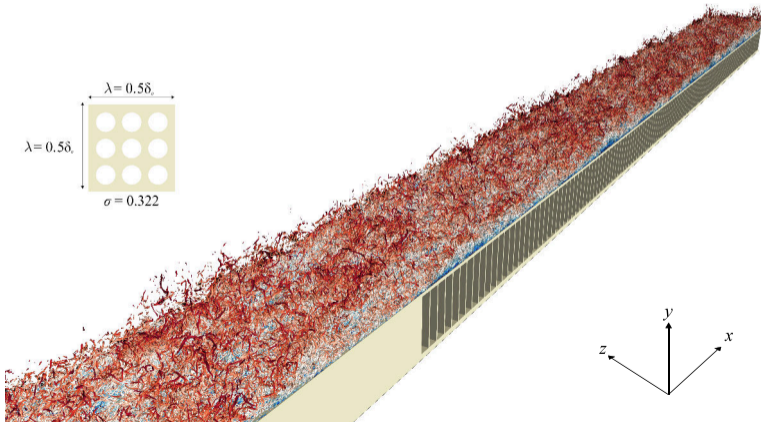
Ongoing work

Turbulent boundary layer with incoming sound wave, currently running on Meluxina



Final Remarks

- STREAMS-2 targets CPU and multiple GPU backends
- DNS at engineering Reynolds numbers are becoming accessible
- EuroHPC facilities are key



Interview for the general public

Science | Mechanics +... | 2022

Quiet Query: Scientists model how noise-reducing aircraft liners are a drag on efficiency

Aircraft noise is reduced by acoustic liners covering the inner surfaces of its engines. However, these components also add to aerodynamic drag – but by how much, and how this can be mitigated, was unclear. Thanks to simulations performed on the CSCS supercomputer “Piz Daint”, scientists have now deciphered the acoustic liners’ impact and how to improve them.

November 21, 2022 - by Santina Russo



QR code





Scale-resolving flow simulations for gaining physical insight in the flow and improving turbulence models for turbomachinery applications

**EUROHPC
USER DAY
2023** Brussels
11.12.23



Projects: *RoundedStepData4ML* + BE share on LUMI
+ Early access on LUMI + *TurbData4ML* (PRACE)
EuroHPC used: VEGA@IZUM, LUMI@CSC
Speaker: *Michel RASQUIN (Cenaero)*

- Author list: M. Rasquin, T. S. Cação Ferreira, T. Toulorge, K. Hillewaert



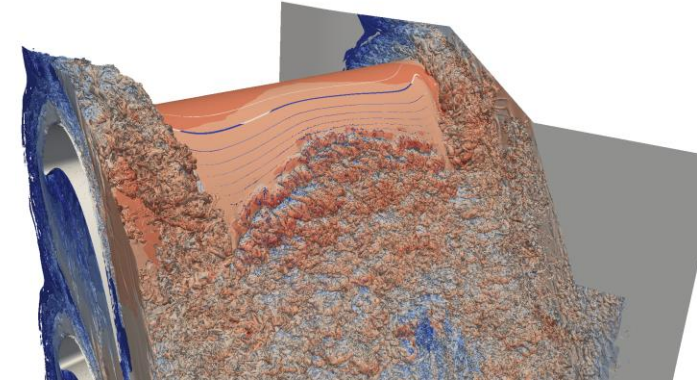
- High-resolution DNS and wall-resolved LES on realistic geometries

- Accurate representation of flow phenomena in boundary layers near solid surfaces

- Separation
- Shocks
- Transition and turbulence

- Main enablers

- Superior accuracy of high-order methods like DGM
- Access to and efficient exploitation of supercomputers



- Research themes for the application of DNS and LES

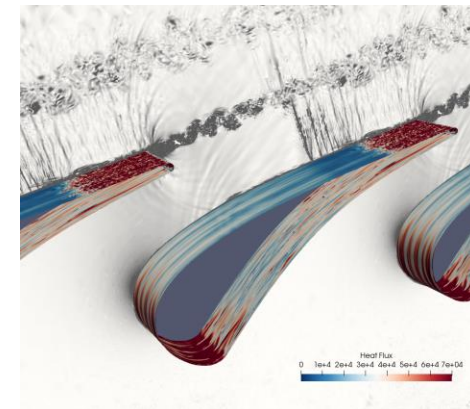
- Development of high-resolution numerical methods & tools

- Applications: high fidelity CFD of complex flows

- High-pressure turbine vane LS89

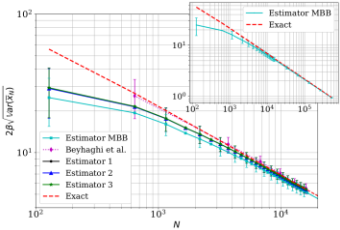
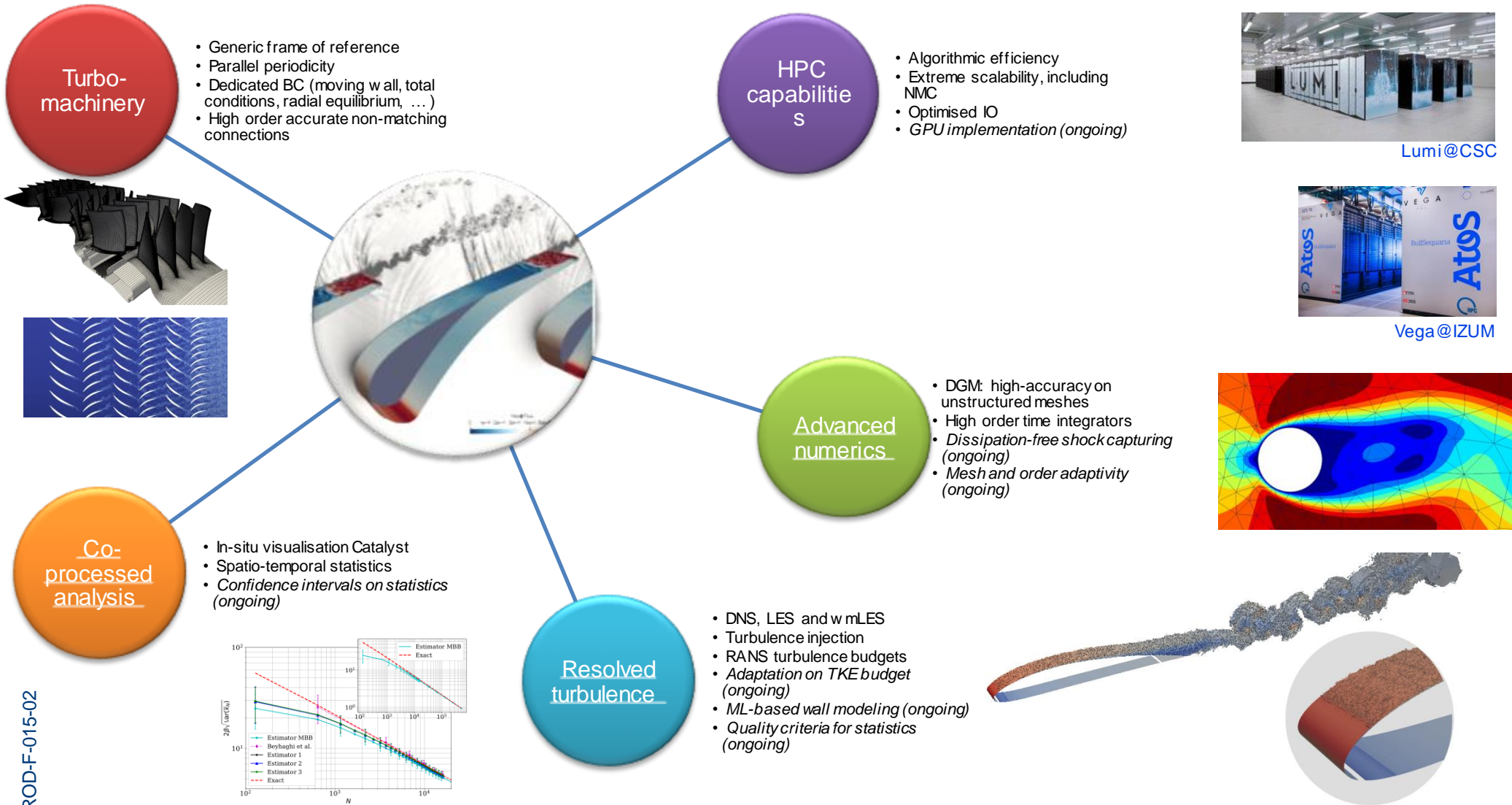
- Data-driven turbulence modeling

- HiFi-Turb-DLR rounded step



Development of high-resolution numerical tools

Highly accurate numerical wind tunnel for turbulence in turbomachinery

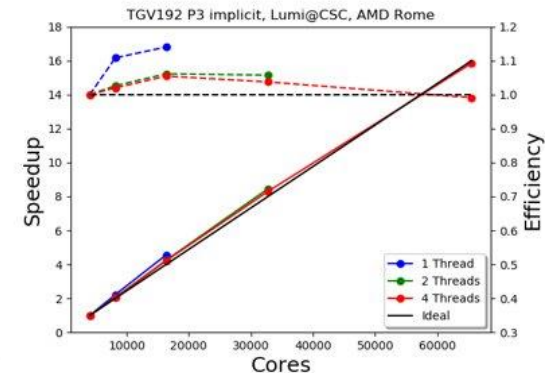
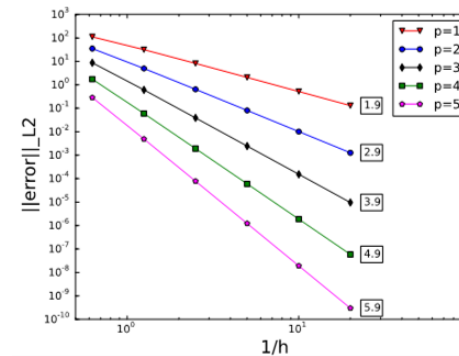
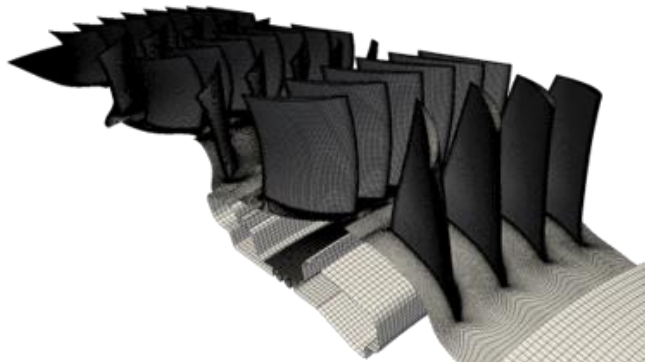
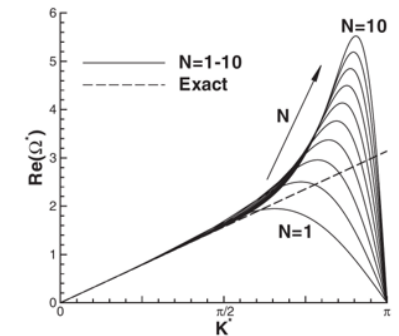
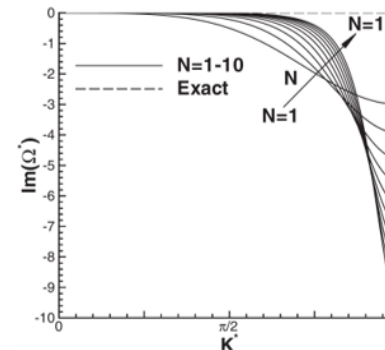
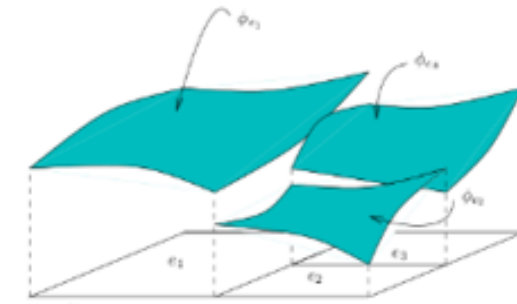
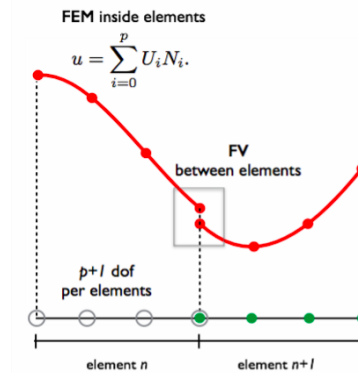


PROD-F-015-02

High-order Discontinuous Galerkin Method

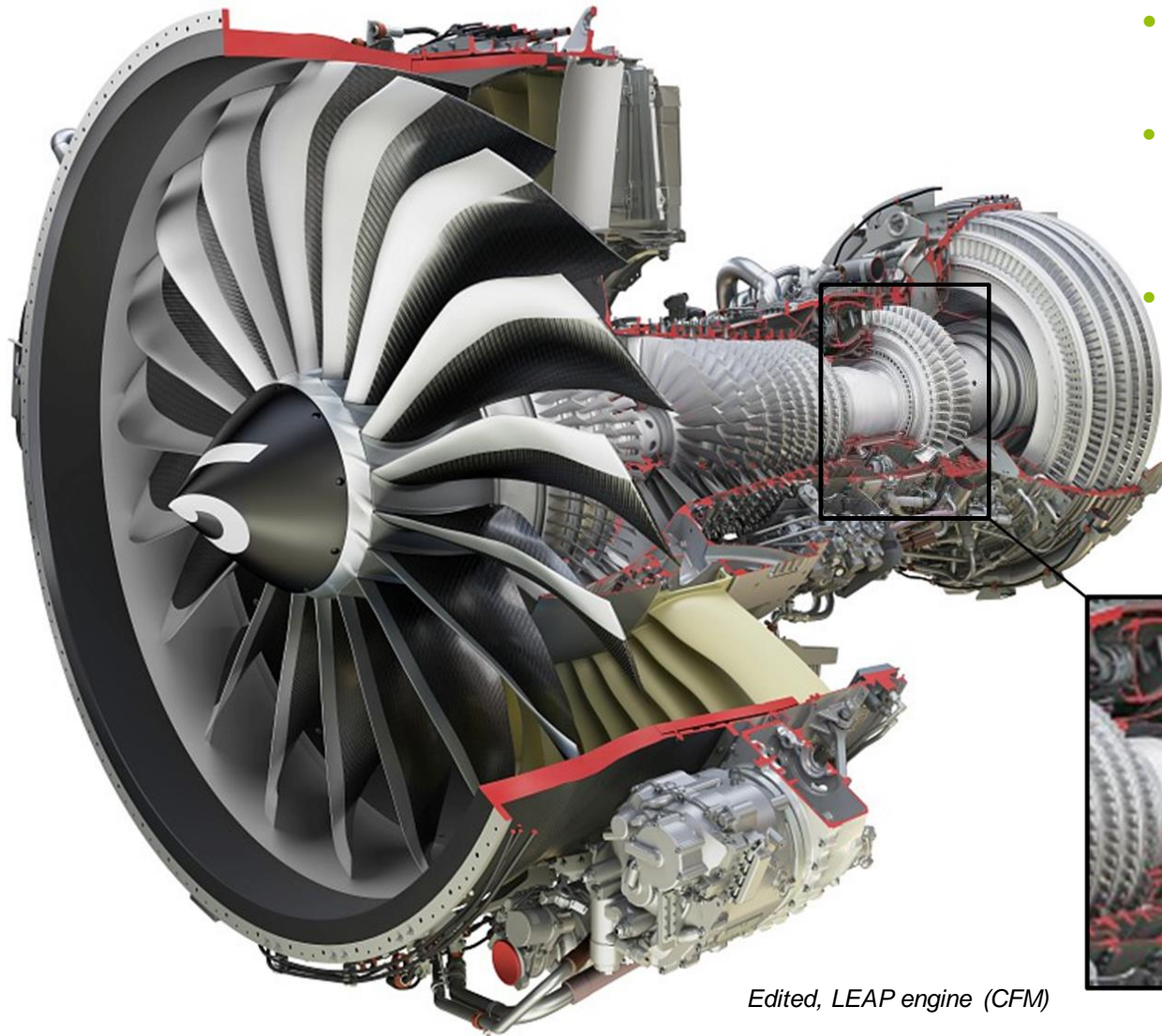
Why DG?

- Unstructured meshes and complex geometries
- High accuracy
 - Guaranteed order of convergence $p+1$
 - No degradation near size jumps/walls
 - Low dissipation/dispersion error
- High efficiency
 - Data locality
 - Compact matrix-matrix operations
 - High scalability (MPI/OpenMP/GPU)



Aircraft gas turbine engine

High pressure turbine vane LS89



- 2021 PhD thesis Tânia Sofia Cação Ferreira + follow up
- Boundary layer transition and convective heat transfer of the high-pressure turbine vane LS89
- Complementary experimental and numerical work

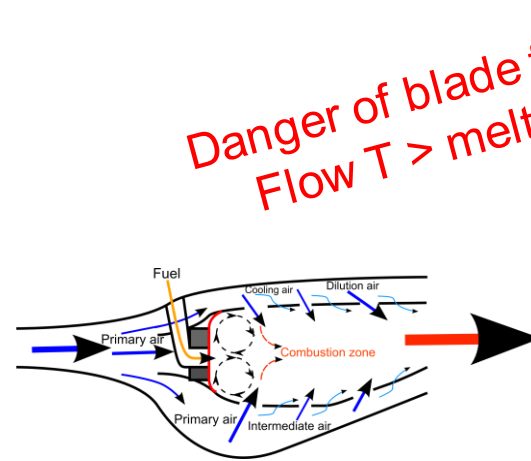
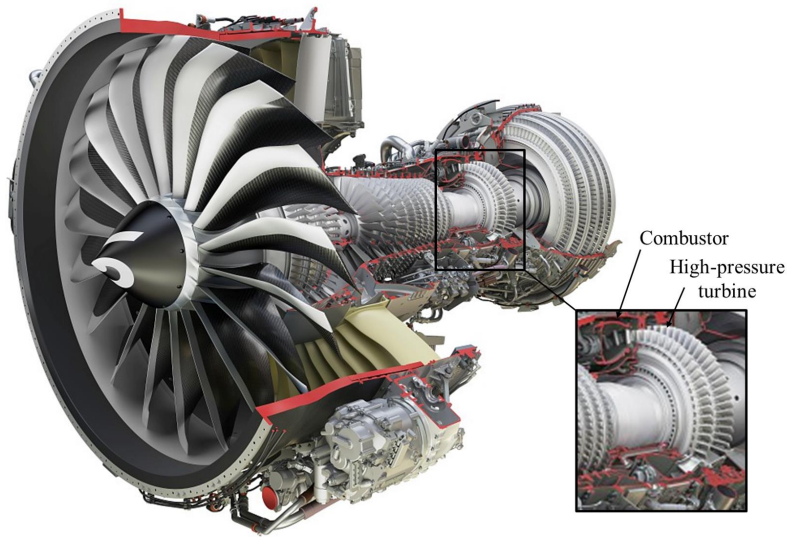
Combustor
High-pressure turbine



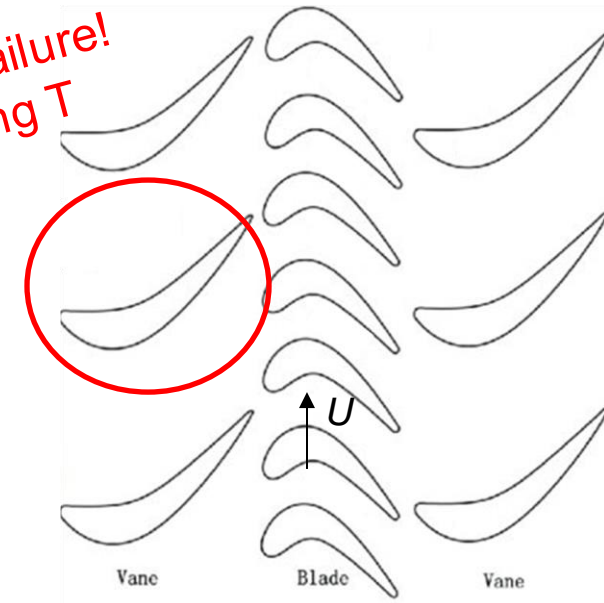
Edited, LEAP engine (CFM)

High-pressure aircraft gas turbine

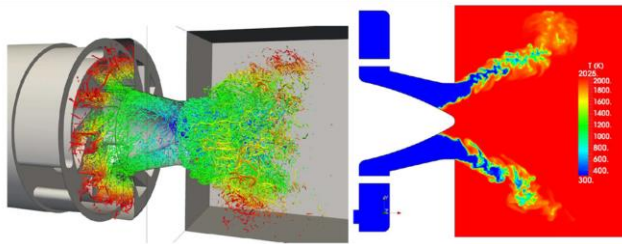
Highest temperature during engine cycle



Danger of blade failure!
Flow $T >$ melting T



DNS of an isothermal and reacting combustion swirler (Moureau et al. 2010)



Combustor exit/HPT inlet flow:

- **Temperature = 500-2000K**
- **Turbulence intensity = 10-30%**

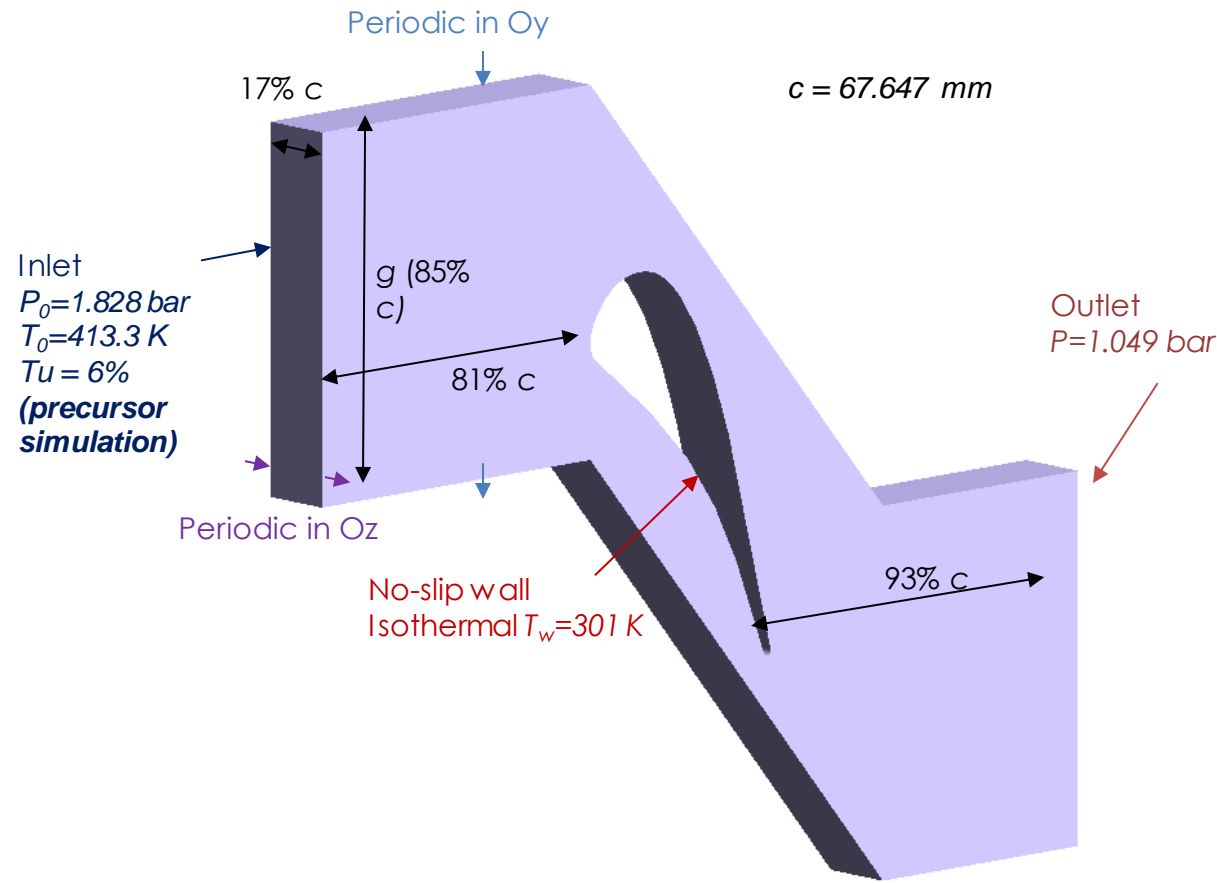
1st turbine stator

faces the **hot turbulent** combustion flow

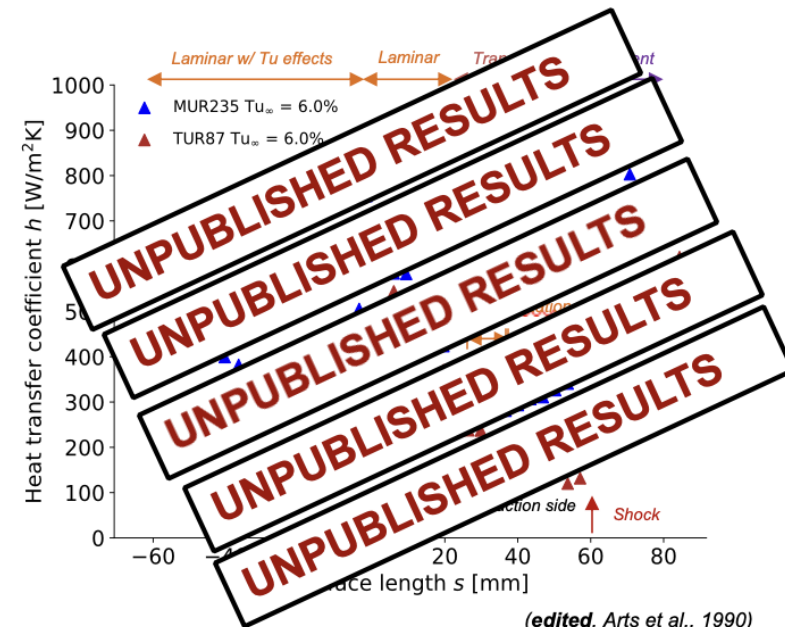
- **Accurate heat transfer predictions are crucial for efficiency and safety!**
- **Requires accurate prediction of the boundary layer**

PROD-F-015-02

Domain and boundary conditions MUR235/TUR87 configuration



Experiments	MUR235	TUR87
$M_{i,s,out}$	0.93	0.92
$Re_{i,s,out}$	1.15×10^6	1.15×10^6
$T_{0,in}/T_{s,wall}$	1.37	1.37
Tu_∞	6%	6%
	Arts et al. 1990	Ferreira & Arts 2021



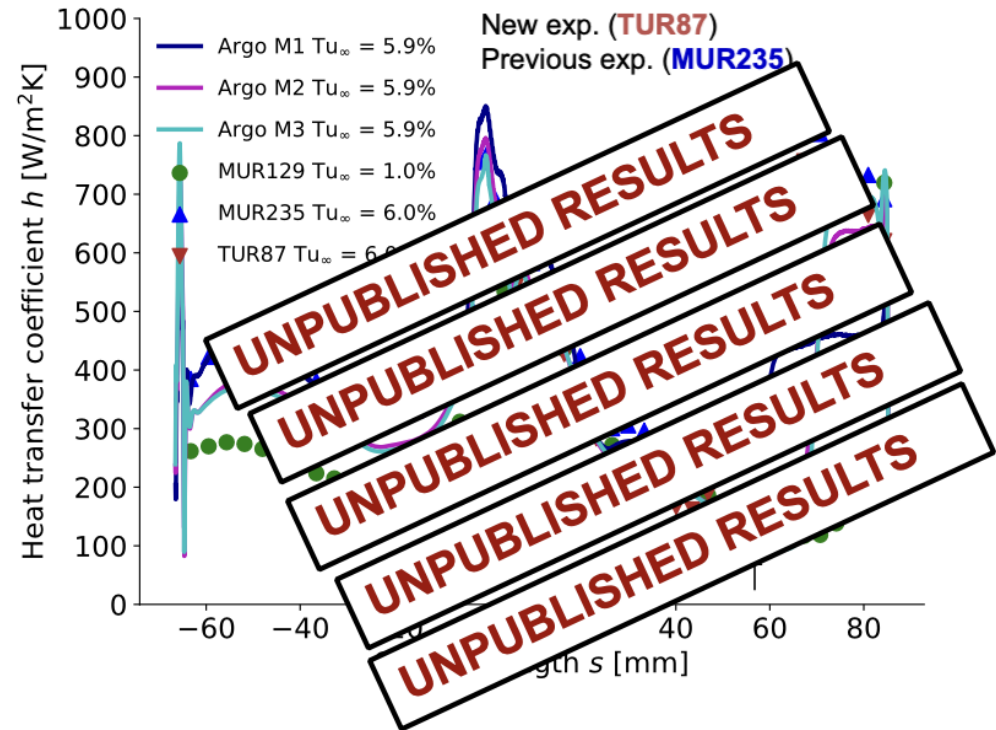
PROD-F-015-02



EuroHPC
Joint Undertaking



Heat transfer for meshes M1, M2, M3



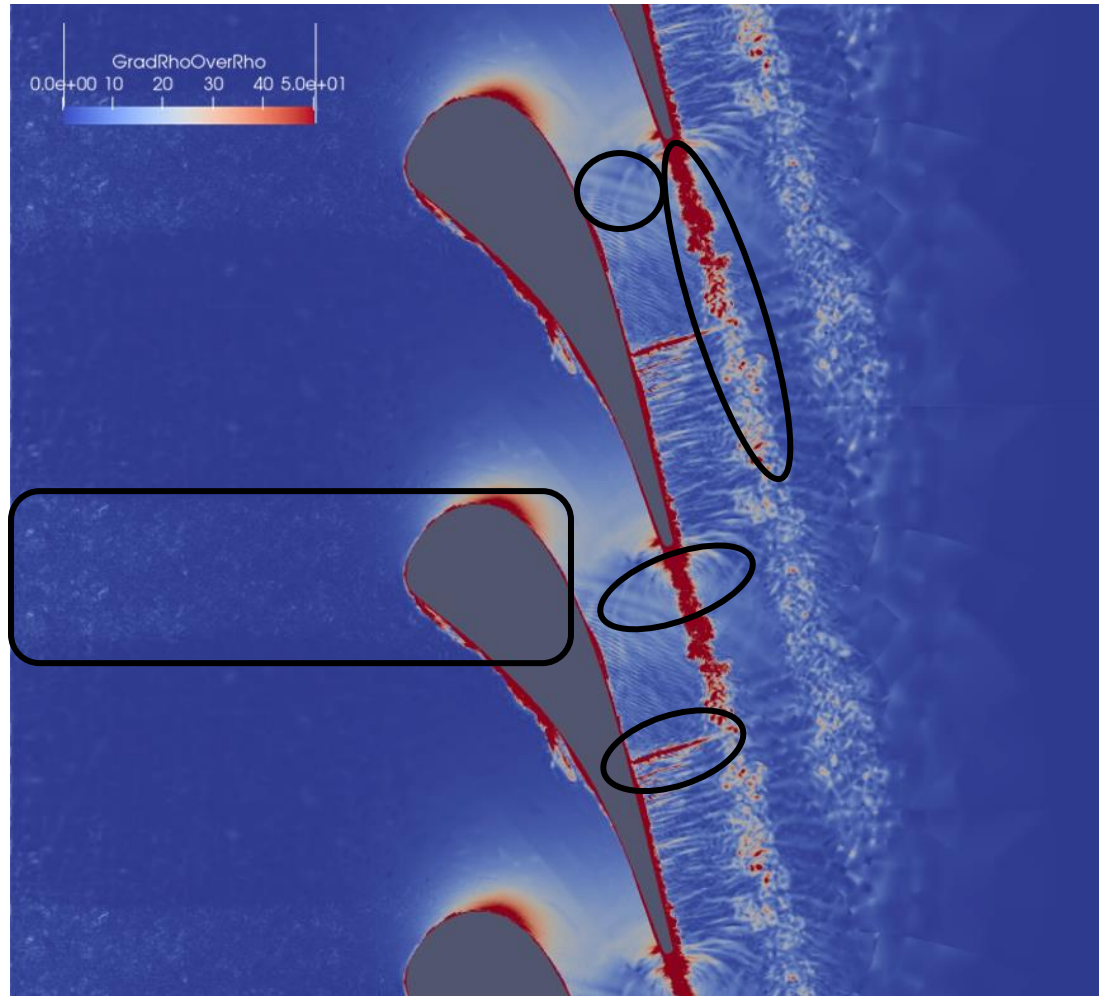
Parameters	M1	M2	M3	New mesh! M4
Mesh	M1	M2	M3	M4
Oz layers	40	74	85	153
Prism elements	80	148	510	918
Hexahedron elements	2M	3.7M	3.3M	10.9M
Degrees of freedom	127M	236M	212M	700M
x^+	83	83	50	25
y^+ (max)	~1	~1	~1	~1
z^+	~100	~50	~45	25
Partitions	2160	3960	3456	9984
CPU hours/flow over inlet + chord**	1M Zenobe	0.95M Galileo	0.8M Zenobe + Lumi	Lumi

Observations:

- Experiments: highly sensitive boundary layer to the facility environment
- Simulations: strong dependence on the mesh resolution (and on the artificial viscosity)
- 2nd experimental campaign with updated facility (TUR87) and refined numerical simulations tend to converge towards the same heat flux prediction

Flow visualisation

Density gradient



Acoustic waves reflection on the suction side

Wake vortex shedding

Acoustic waves formation at the trailing edge

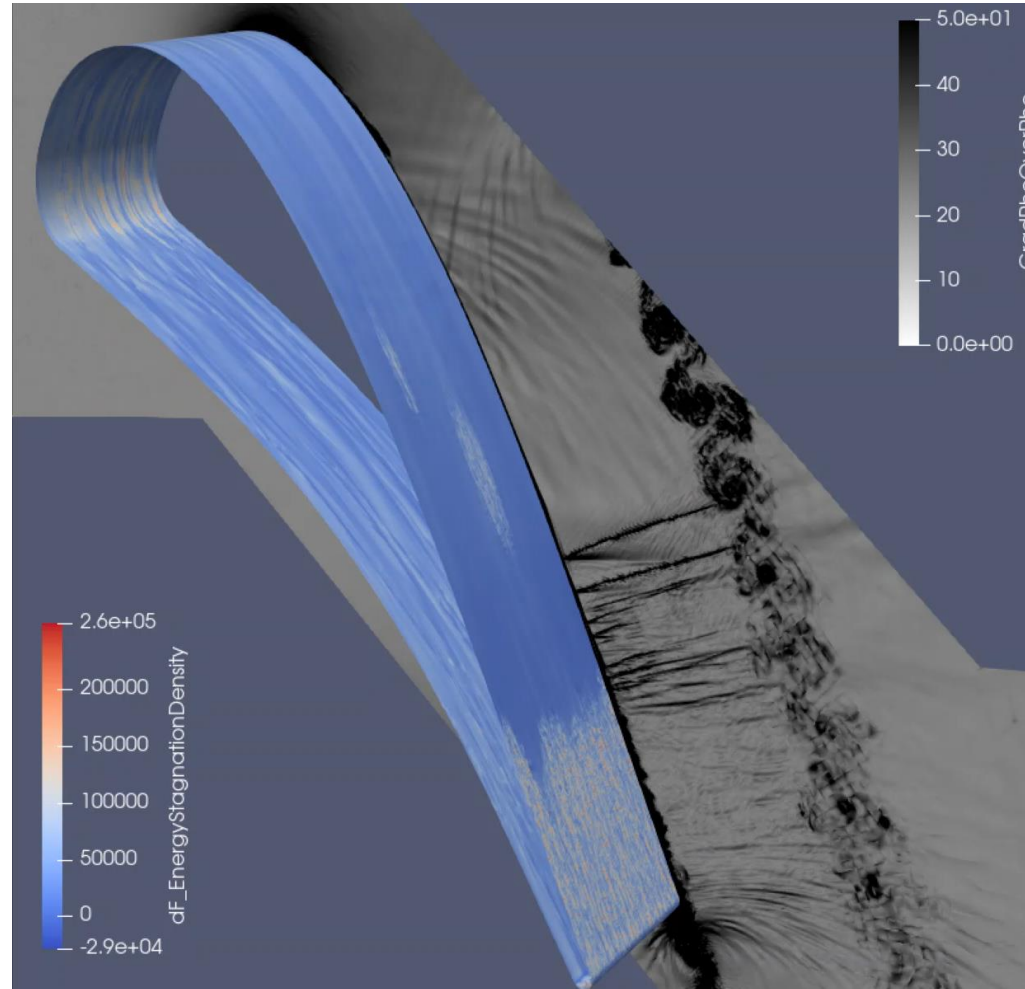
Normal shock

Refined inlet turbulent structures

PROD-F-015-02

Heat transfer

Mesh M2



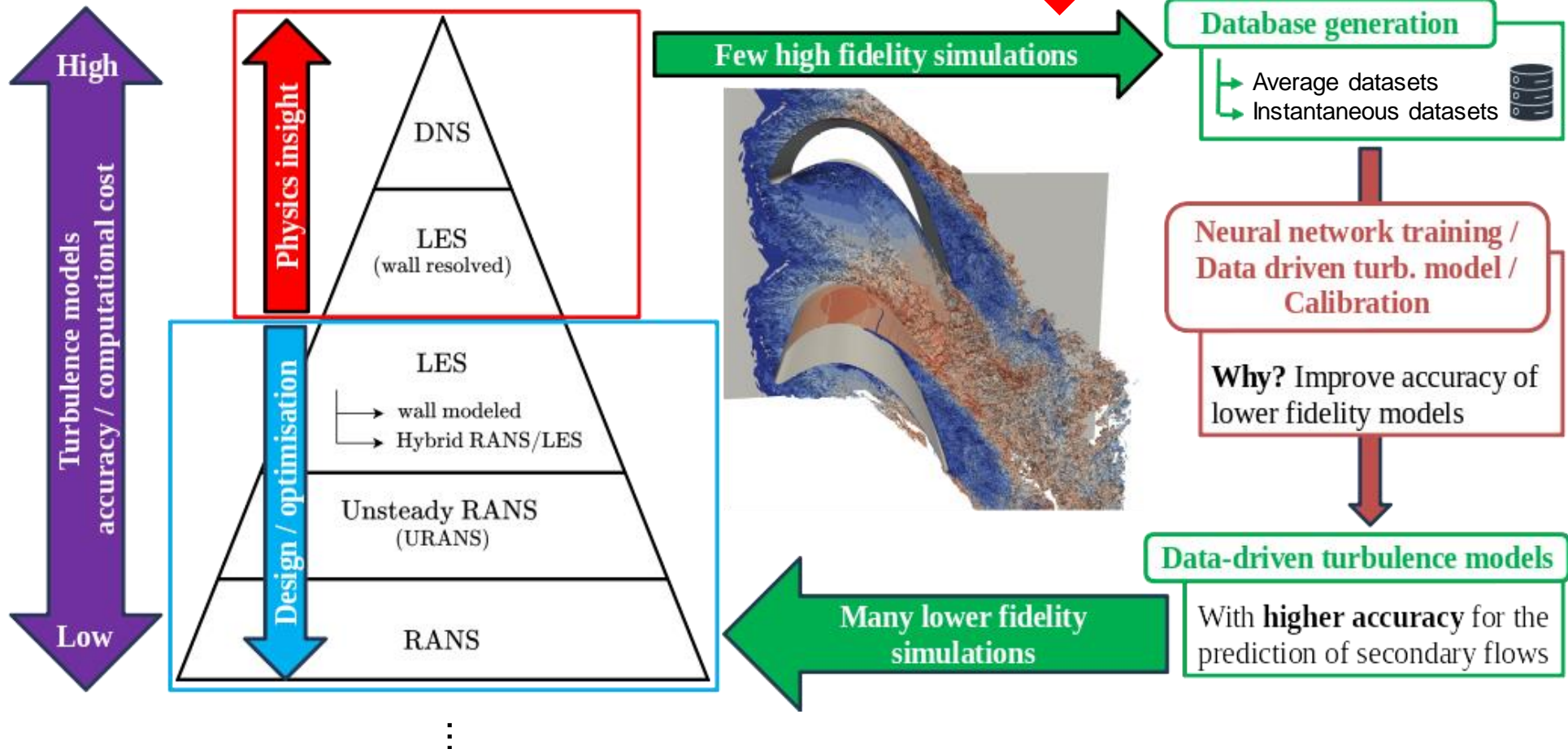
PROD-F-015-02

Data-driven turbulence modeling

Generic methodology



Access to EuroHPC systems is essential

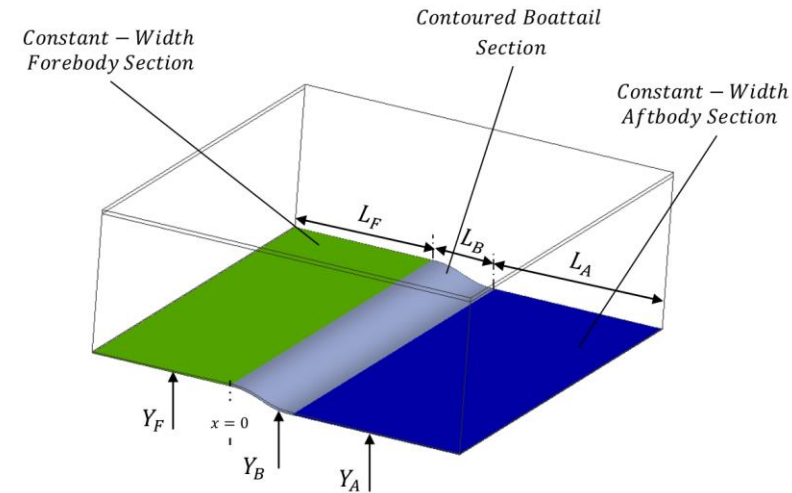


PROD-F-015-02

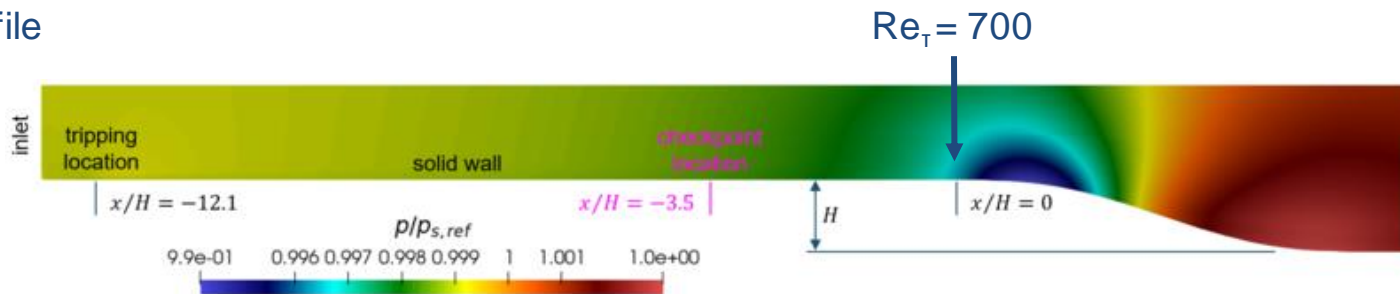
HiFi-Turb-DLR rounded step

Test case definition

- Test case proposed within H2020 HiFi-Turb project
 - Documented in the ERCOFTAC Knowledge Base wiki
 - https://www.kbwiki.ercoftac.org/w/index.php/DNS_1-5
- Features an adverse pressure gradient on a turbulent boundary layer
 - 3 step heights
 - Incipient, moderate ($Re_h=98113$) and full separation



Blasius BL profile



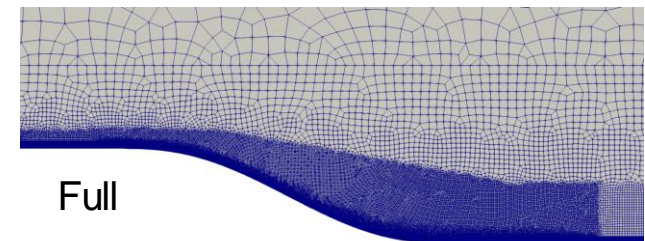
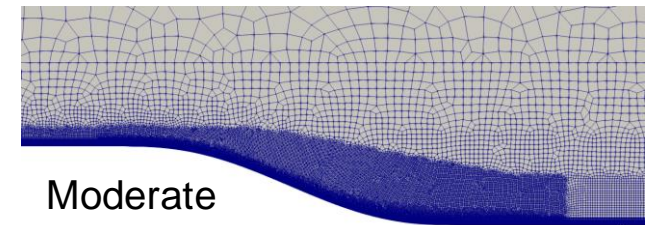
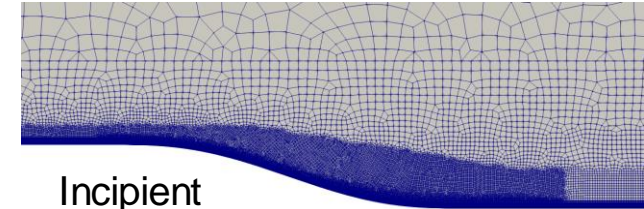
Courtesy of UniBG and ERCOFTAC

Outlet pressure

HiFi-Turb-DLR rounded step

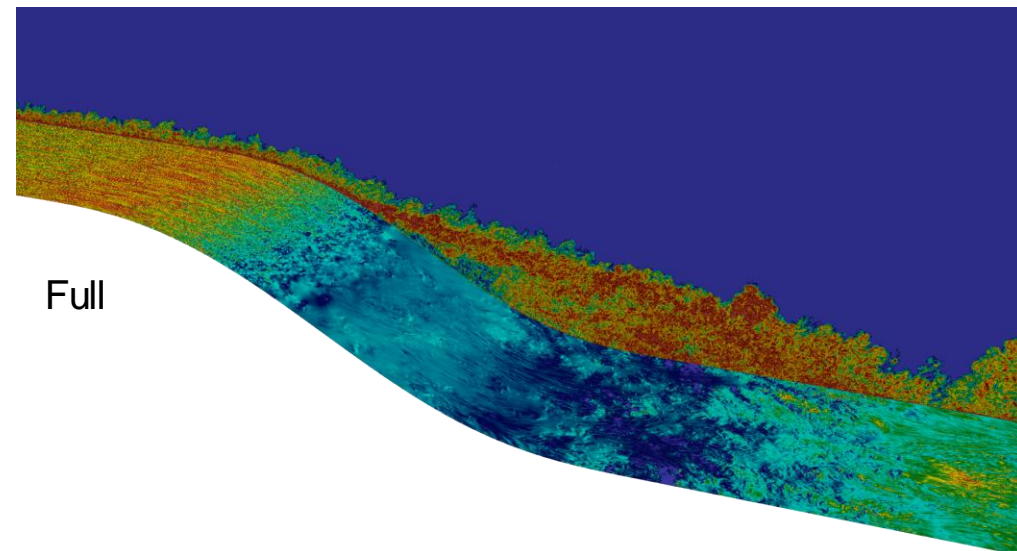
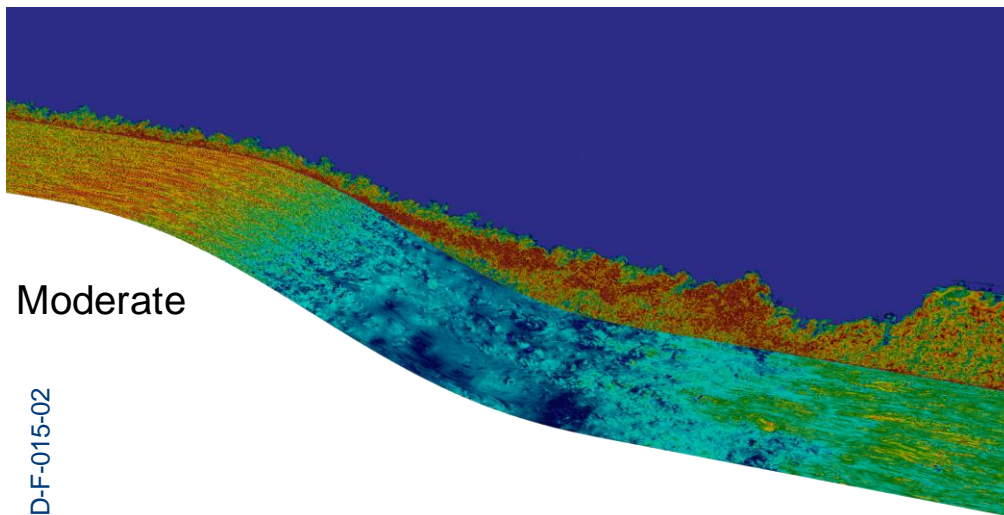
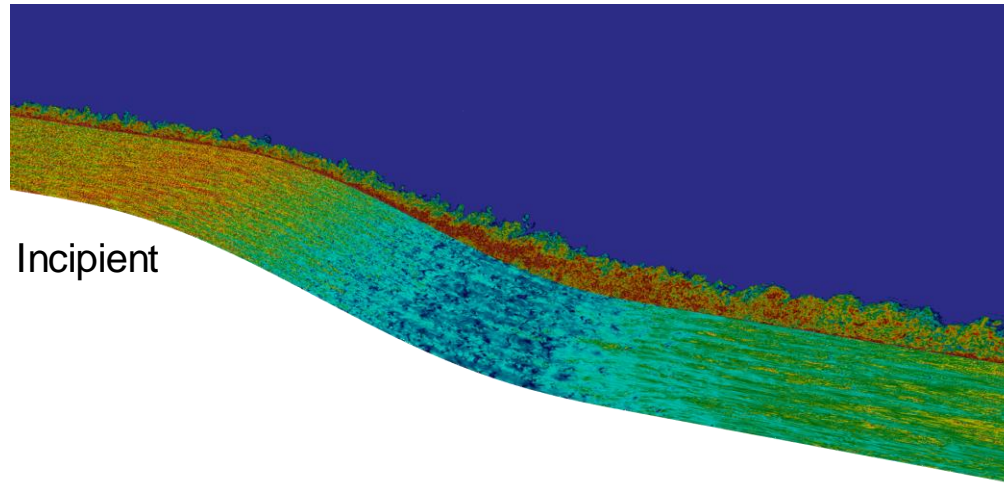
Mesh characteristics

	Incipient	Moderate	Full
Hexes	10.3 M	10.8 M	11.6 M
Dof	1.30 B	1.35 B	1.45 B
Height (m)	2.90e-2	3.62e-2	4.38e-2
Span (m)	8.69e-2		
Span/height	3	2.4	2
Nz	188		
Δz	4.10e-4 m		
Upstream bump			
Δx^+	<20		
Δy_{1+}	<1		
Δz^+	<14.8		
Bump			
Δx	*0.5 w.r.t. upstream bump		



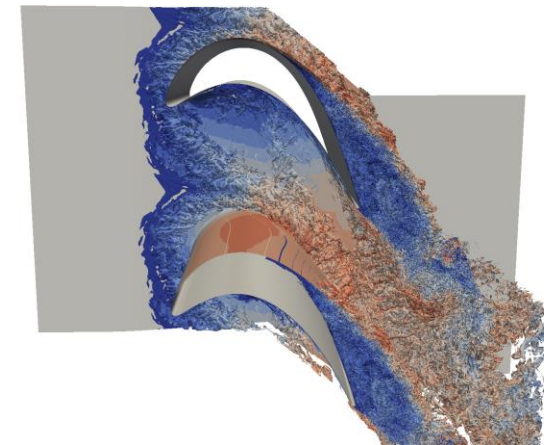
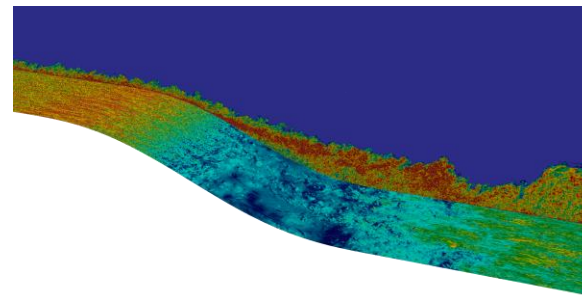
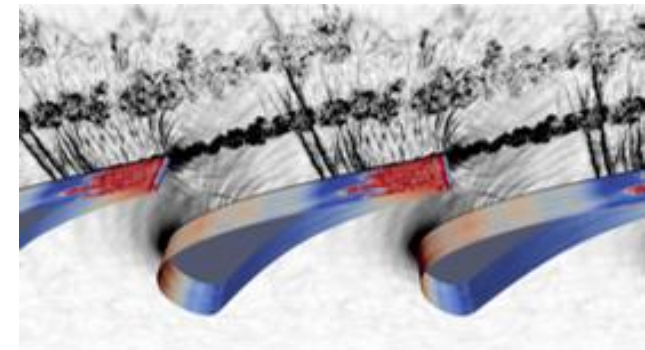
Flow visualisation

Wall shear stress + Vorticity



PROD-F-015-02

- **High-resolution simulations as part of a "multi-fidelity" paradigm**
 - Physical understanding to support and complement experimental testing
 - Performance prediction in off-design conditions
 - Data generation for lower-fidelity model calibration (RANS, wall models)
- **Advanced numerical framework**
 - High-order numerical scheme
 - Scalable
 - Post-processing and statistical analysis
- **Applications**
 - Academic aerodynamic flows
 - Turbomachinery flows



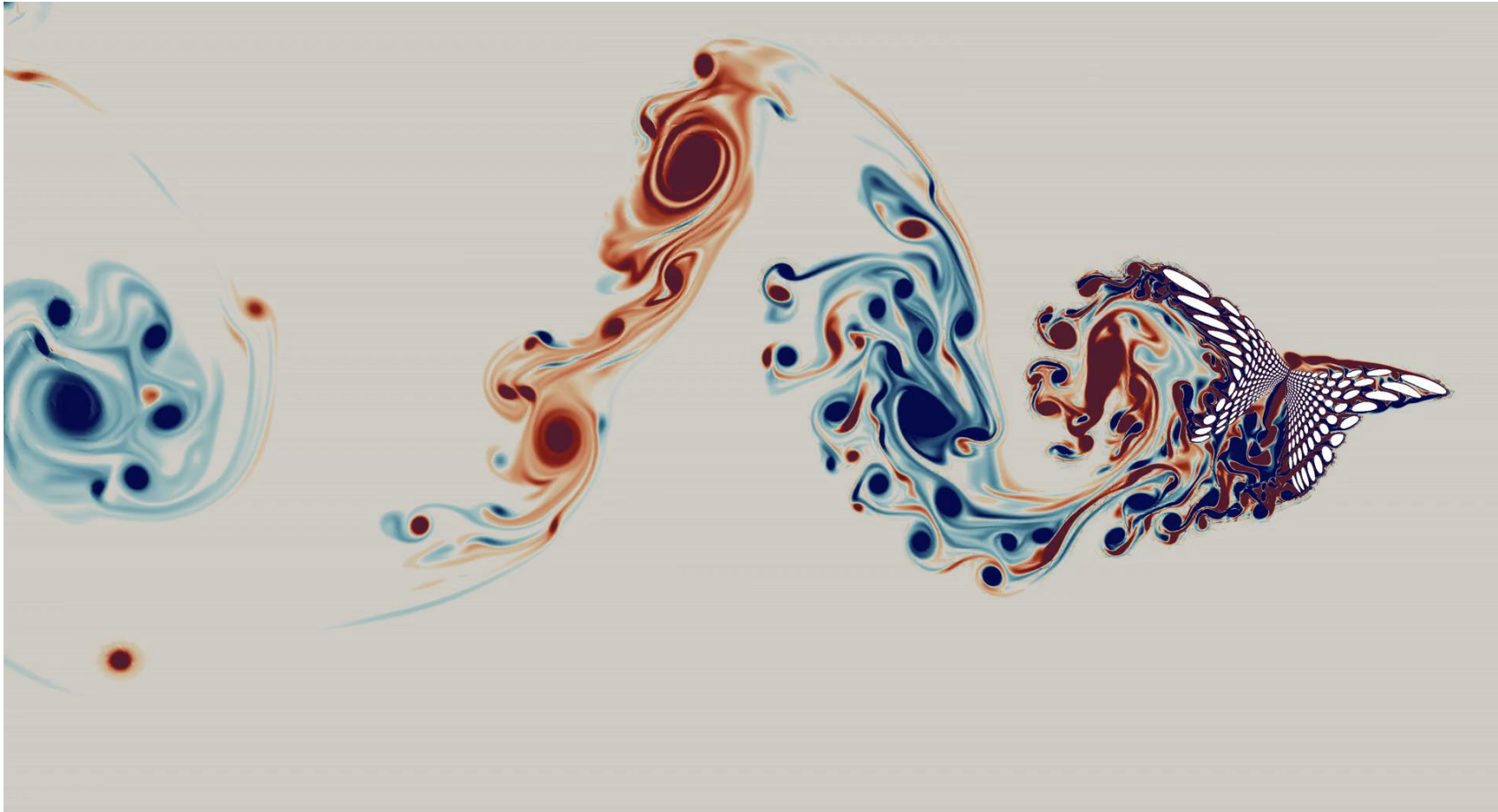
➔ Access to large computational resources is essential

Acknowledgments

- We acknowledge **EuroHPC JU** for awarding us access to
 - LUMI hosted by CSC in Kajaani, Finland
 - VEGA hosted by IZUM in Maribo, Slovenia
- We acknowledge **PRACE** for awarding us access to
 - Galileo hosted by CINECA in Bologna, Italy
 - Hawk hosted by HLRS in Stuttgart, Germany
- The present research benefited from computational resources made available on the Tier-1 supercomputer of the Fédération Wallonie-Bruxelles, infrastructure funded by the **Walloon Region** under grant agreement numbers 1117545 and 1910247



Thank you for your attention



PROD-F-015-02



A Portable Drug Discovery Platform for Urgent Computing

**EUROHPC
USER DAY
2023** Brussels
11.12.23



Project: *EHPC-BEN-2022B12-001*

EuroHPC used: LUMI-G

Speaker: *Davide GADIOLI (Politecnico di Milano)*



Drug discovery

- Target at least one protein that represents the disease
- The goal is to find a small molecule that has a strong interaction
 - Expected to yield a therapeutic effect in clinical trials

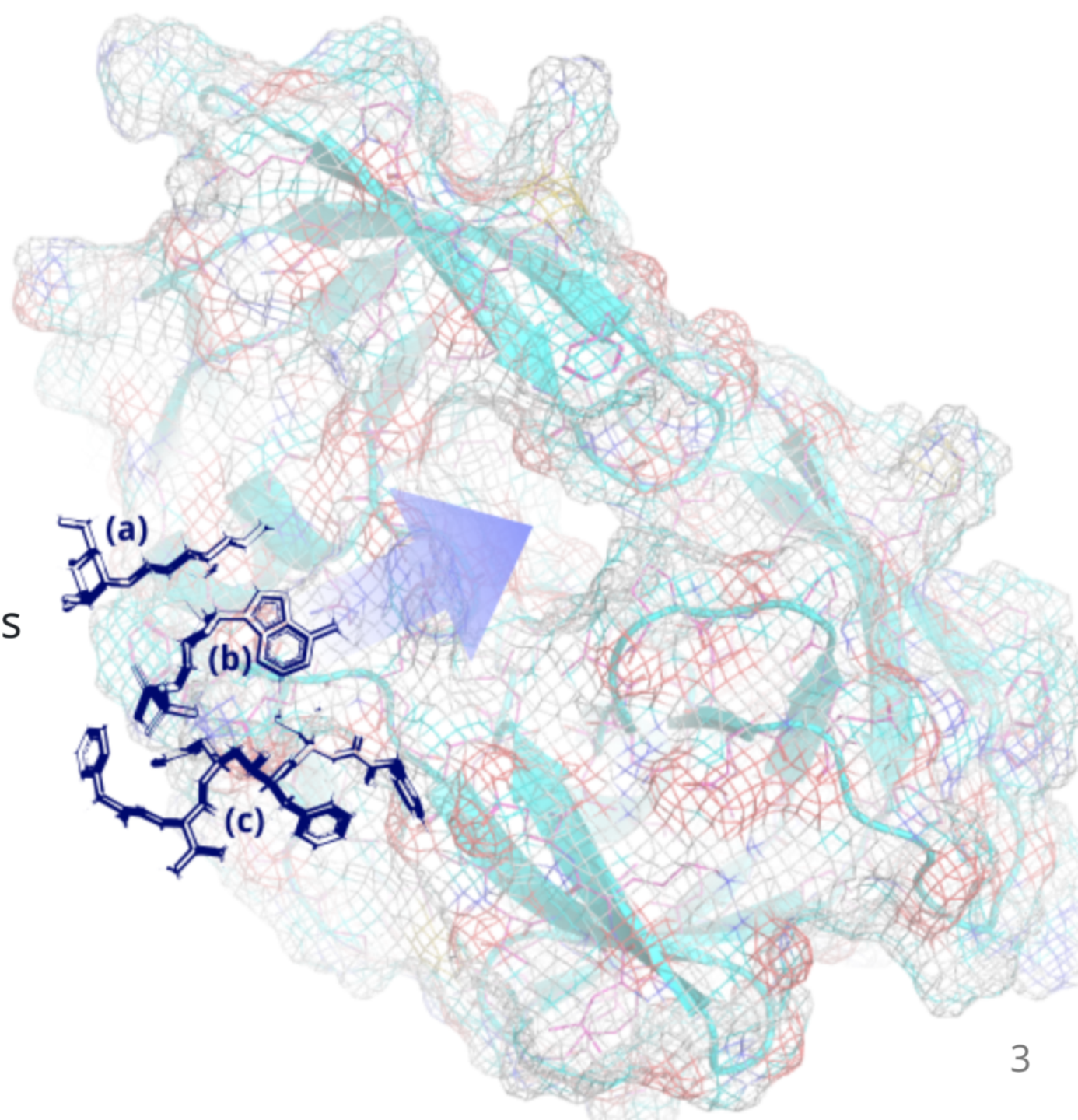
Virtual screening

Problem input

- Target protein
- Huge database of virtual molecules

Expected output

- Molecules to test *in-vitro*





Why High Performance Computing?

- The interaction strength estimation is complex
- The evaluation of each molecule-protein pair is independent
 - Embarrassing parallel problem
- Simulation of known chemical reactions grants access to huge chemical space
 - increasing the probability of finding good candidates



LiGen Virtual Screening Application



- Component of the EXSCALATE drug discovery platform
- Designed from scratch to hinge on modern supercomputer nodes
- Used to perform extreme-scale virtual screening campaign

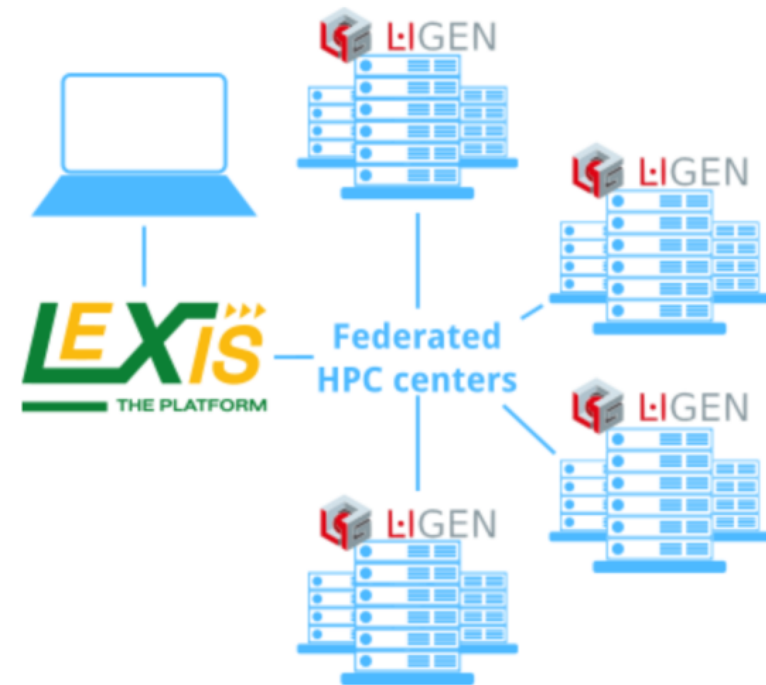
ANTAREX^{10¹⁸} 4ZIKA

EXSCALATE
4COV



HPCaaS: The Urgent Computing Scenario

- LiGen deployed on multiple EU HPC centers
- Integration in the LEXIS platform
- Virtual screening on multiple locations





Manage Hardware Heterogeneity

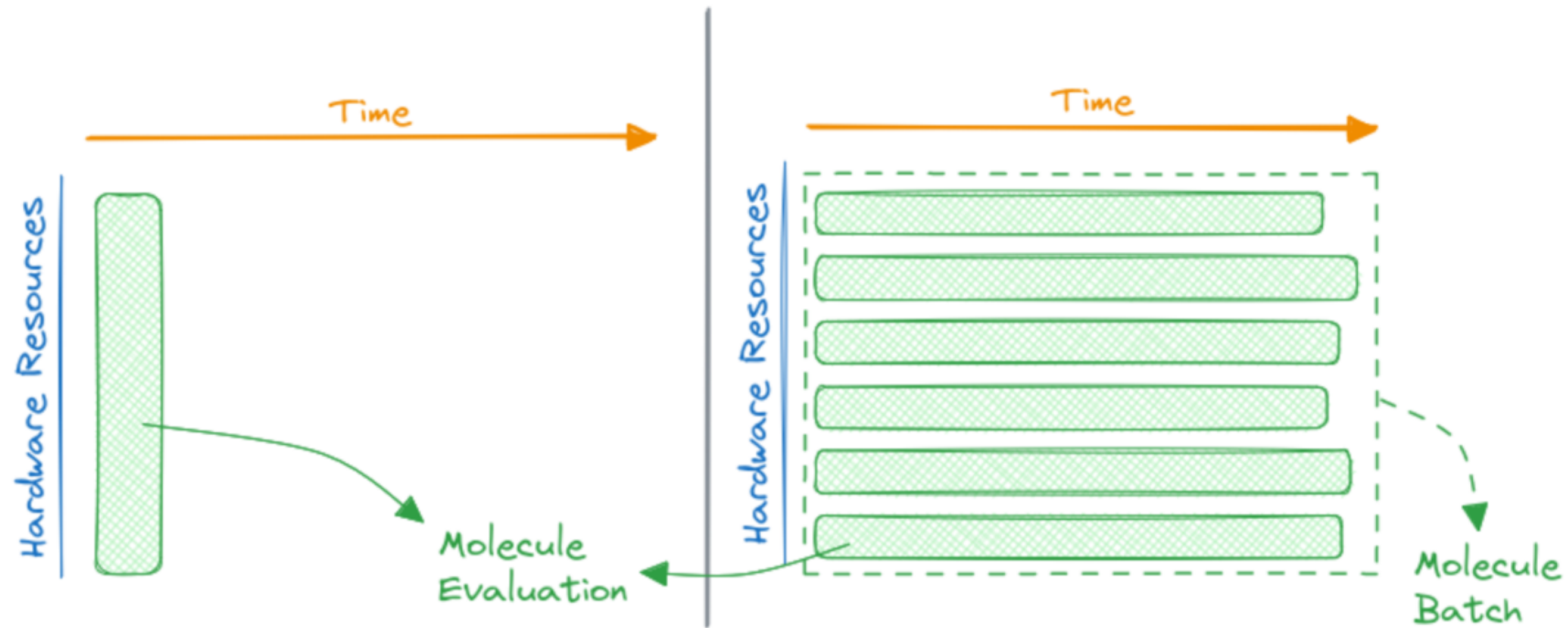
- Efficient CUDA implementation
 - Support from NVIDIA engineers
- We introduced a SYCL porting
 - Computation kernels
 - Out-of-order input computation



LIGATE



LiGen Computation parallelism





LiGen Batched Approach

1. Write kernels with non-type template parameters for atom number
 - Different hardware requirements

```
template<size_t num_atoms>
__global__ void kernel( ... ) {
    ...
}
```



LiGen Batched Approach

1. Write kernels with non-type template parameters for input features
2. Define input features clusters that impact the kernel's complexity
 - The ligands computation should last for a similar period

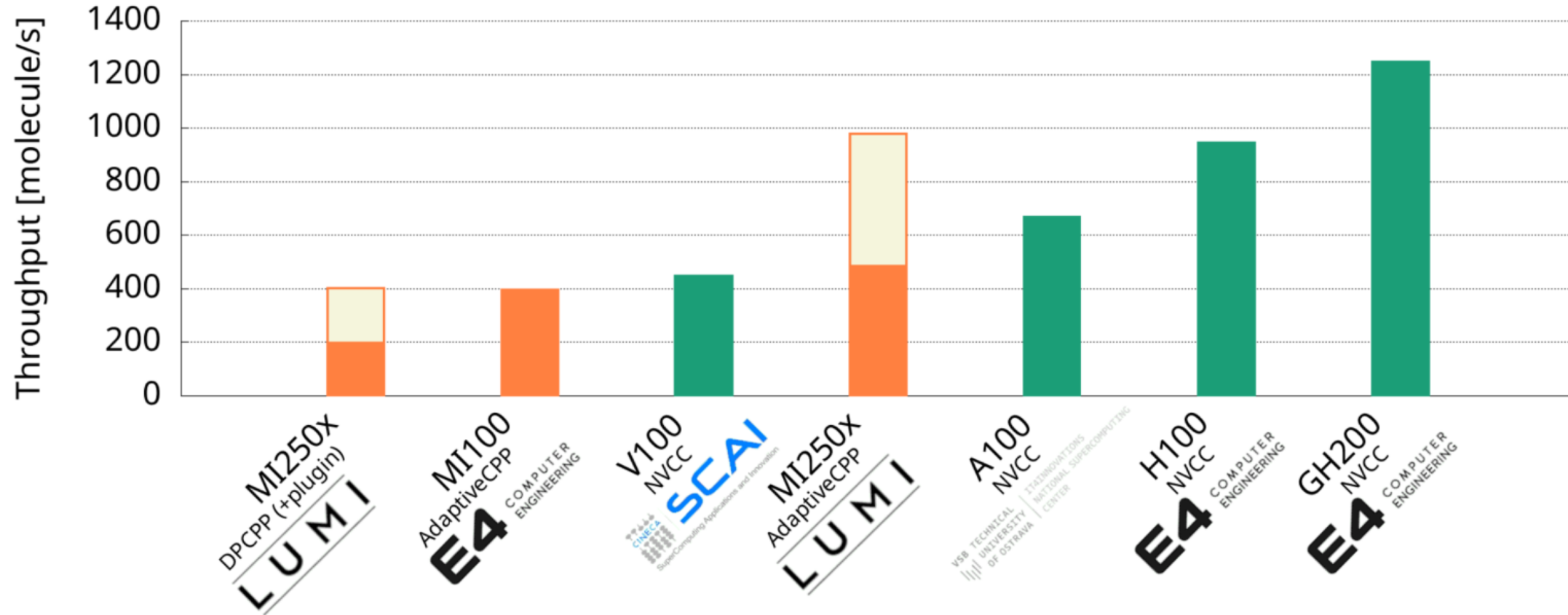


LiGen Batched Approach

1. Write kernels with non-type template parameters for input features
2. Define input features clusters that impact the kernel's complexity
3. Use Hardware characteristics to size each ligand batch at runtime
 - Automatic tuning using CUDA or SYCL query API



Performance on the single logical GPU card

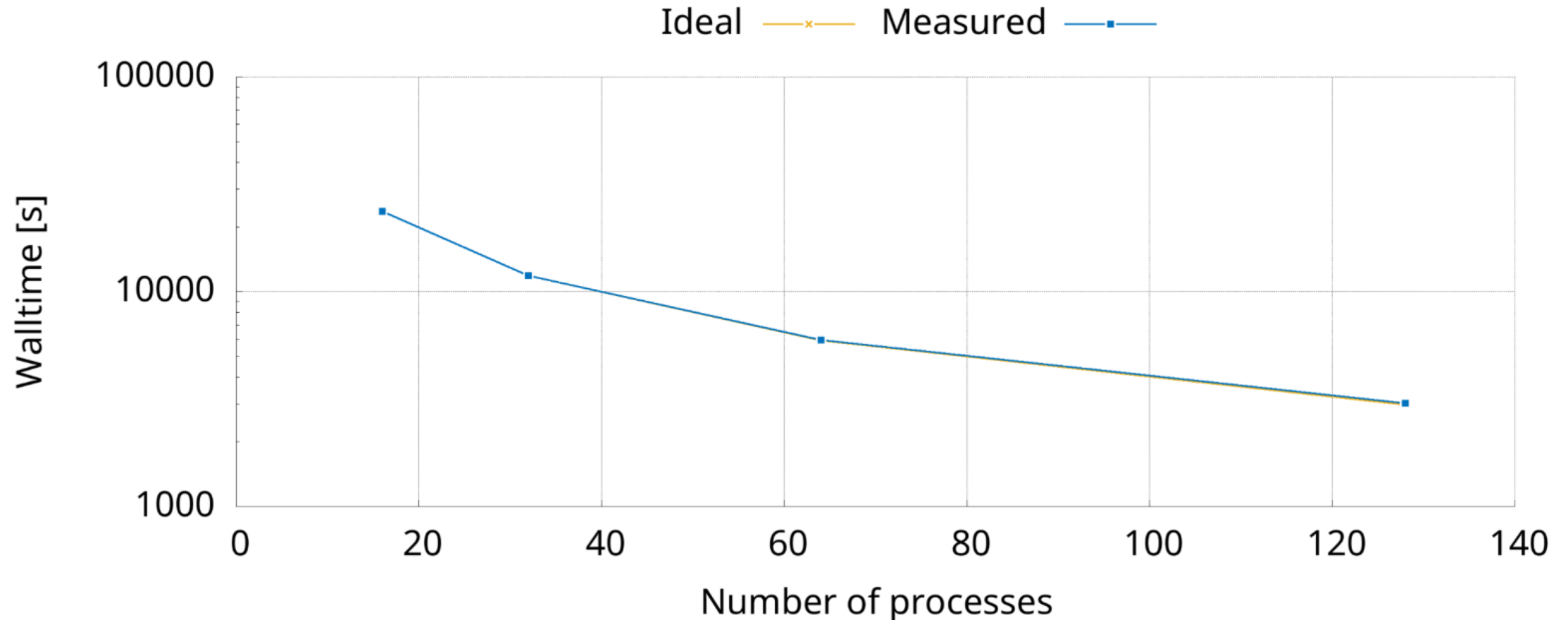




Scaling on the number of GPUs (LUMI-G)

Num nodes	Num GPUs/node	Throguhput [molecule/s]	Speed-up
16	1	7'808.96	1
16	8	60'566.672	7.756

Strong Scaling on the number of nodes (LUMI-G)



NOTE: due to a technical problem with the FS, we used only 1 GPU per node



Acknowledgement

EuroHPC JU for awarding this project access to LUMI and Karolina

- We could optimize LiGen software-knobs
- We benchmarked on the LUMI machine
 - Ready to run a virtual screening campaign
- In the LIGATE context, we can provide access to LiGen through the LEXIS platform

- "EXSCALATE: an extreme-scale virtual screening platform for drug discovery targeting polypharmacology to fight SARS-CoV-2." IEEE Transactions on Emerging Topics in Computing
- "Understanding the I/O impact on the performance of high-throughput molecular docking." 2021 IEEE/ACM Sixth International Parallel Data Systems Workshop (PDSW).
- "Exploiting OpenMP and OpenACC to accelerate a geometric approach to molecular docking in heterogeneous HPC nodes." The Journal of Supercomputing
- "Improving computation efficiency using input and architecture features for a virtual screening application", arxiv, minor revision
- "GPU-optimized Approaches to Molecular Docking-based Virtual Screening in Drug Discovery: A Comparative Analysis", arxiv, minor revision



Large Eddy Simulations (LES) of a Three-Element High-Lift Wing: Exploring the Active Flow Control (AFC) Capabilities.

**EUROHPC
USER DAY
2023** Brussels
11.12.23



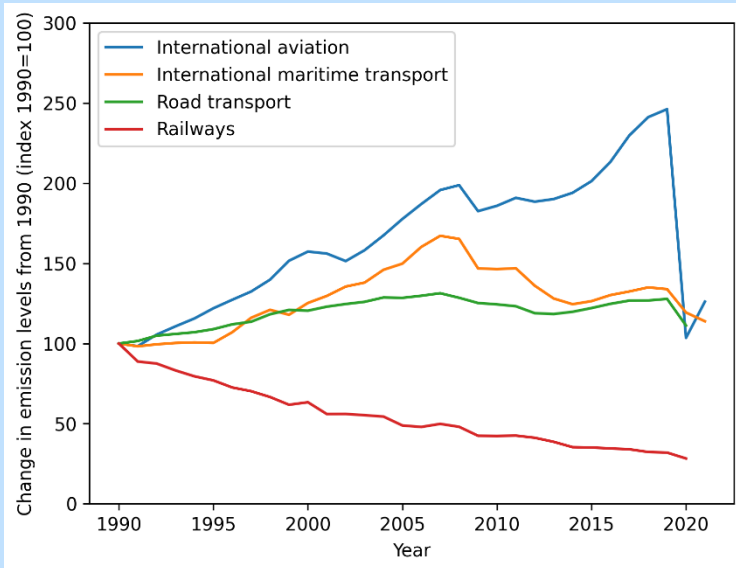
Project: “Active Flow Control of a 3-Element High-Lift Wing: The Role of Coherent Structures”

EuroHPC used: Vega CPU (IZUM)

Motivation

GOAL

Reduce drag in wings



[1] European Environment Agency, Greenhouse gas emissions from transport in Europe, accessed 6 June 2023, <https://www.eea.europa.eu/ims/greenhouse-gas-emissions-from-transport>

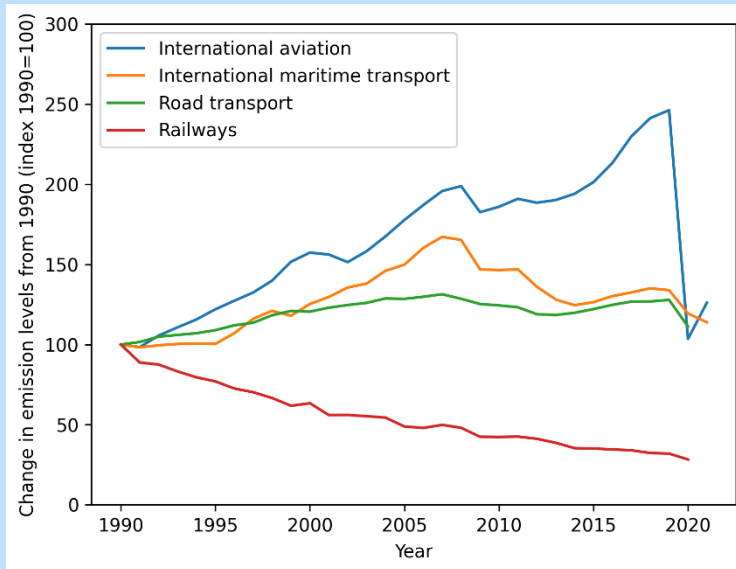
[2] B. Eiximeno, A. Miró, J.C. Cajas, O. Lehmkuhl, I. Rodriguez (2022). DOI: <https://doi.org/10.3390/fluids7090292>

[3] O. Lehmkuhl, A. Lozano-Durán, I. Rodriguez (2020). DOI: [10.1088/1742-6596/1522/1/012017](https://doi.org/10.1088/1742-6596/1522/1/012017)

Motivation

GOAL

Reduce drag in wings



[1] European Environment Agency, Greenhouse gas emissions from transport in Europe, accessed 6 June 2023, <https://www.eea.europa.eu/ims/greenhouse-gas-emissions-from-transport>

[2] B. Eiximeno, A. Miró, J.C. Cajas, O. Lehmkuhl, I. Rodriguez (2022). DOI: <https://doi.org/10.3390/fluids7090292>

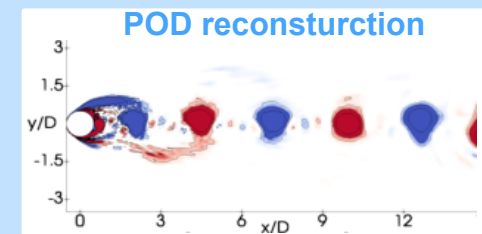
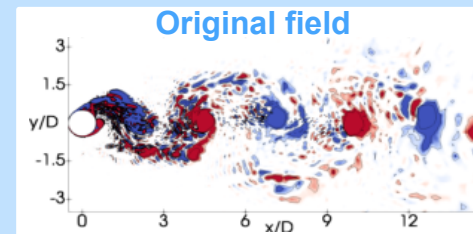
[3] O. Lehmkuhl, A. Lozano-Durán, I. Rodriguez (2020). DOI: [10.1088/1742-6596/1522/1/012017](https://doi.org/10.1088/1742-6596/1522/1/012017)

METHODOLOGY

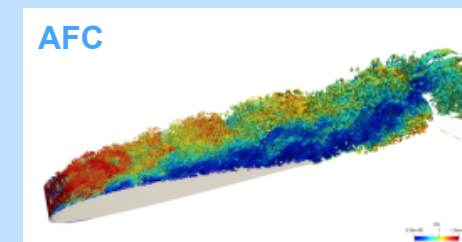
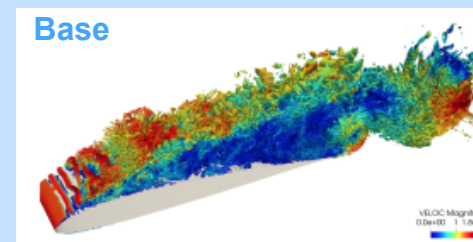
LES simulations of the baseline configuration

Understand the underlying physics of the problem

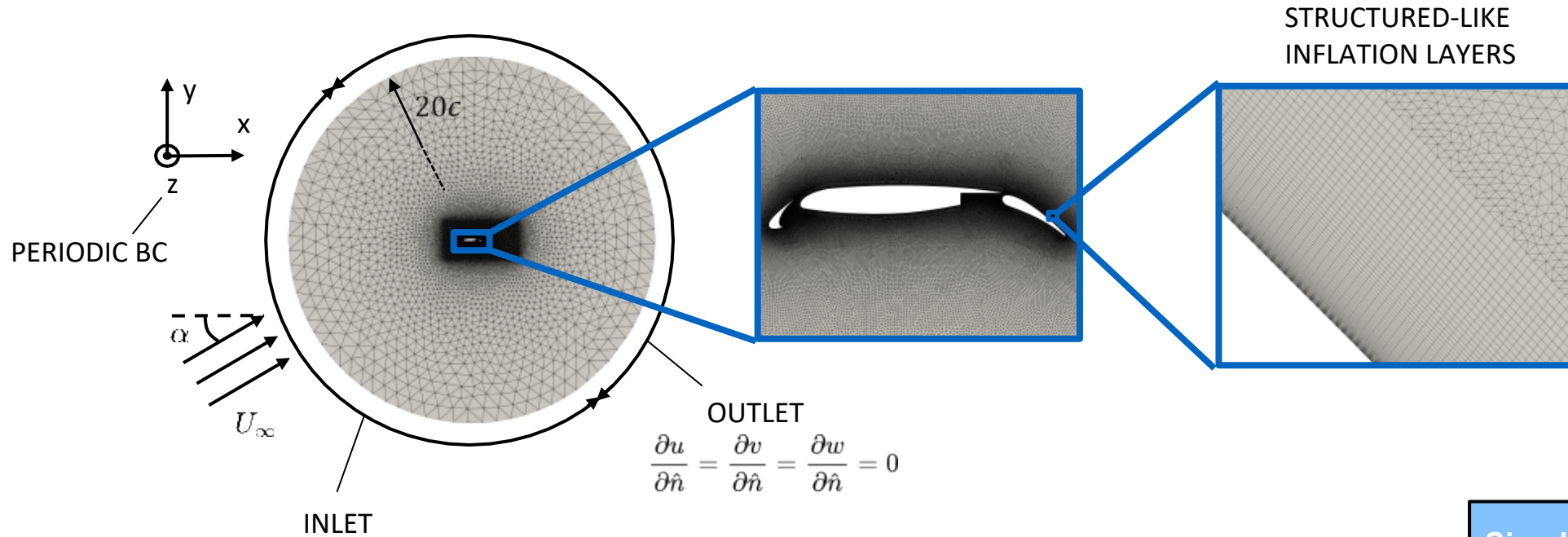
Apply reduce order models (ROMs): POD, DMD, Autoencoders...



Propose Active Flow Control (AFC) actuations



Baseline LES – Case Configuration



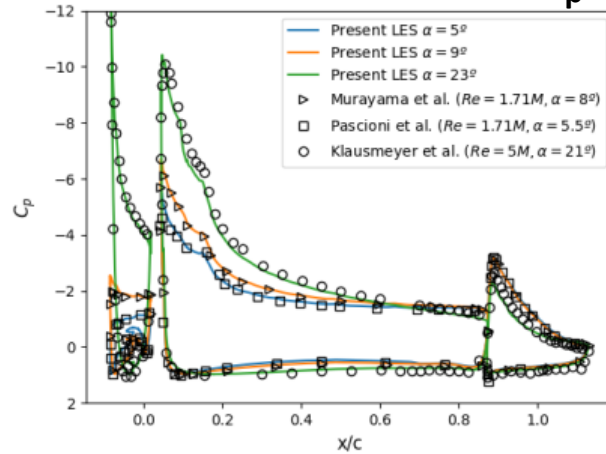
Simulation Code:

ALYA (FEM)

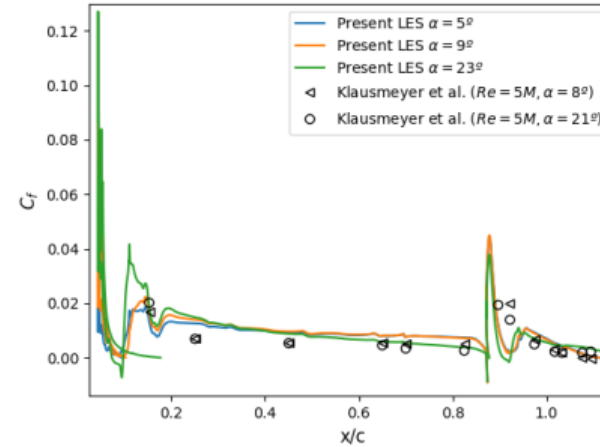
Flow Conditions		Domain			Mesh				
Re_c	α	Airfoil	$L_x = L_y$	L_z	N_{points}	N_{planes}	Δx^+_{max}	Δy^+_{max}	Δz^+_{max}
750,000	5, 9 and 23°	30P30N	20c	0.1c	58M	128	80	1	50

Baseline LES – Validation

Pressure Coefficient (C_p)



Skin Friction Coefficient (C_f)



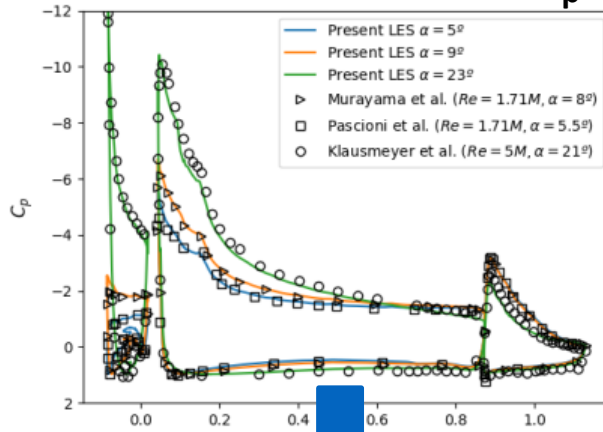
[6] M. Murayama, K. Nakakita, K. Yamamoto, H. Ura, Y. Ito, M. Choudhari (2014). DOI: <https://doi.org/10.2514/6.2018-3460>

[7] K. Pascioni, L.N. Cattafesta, M. Choudhari (2014). DOI: <https://doi.org/10.2514/6.2014-3062>

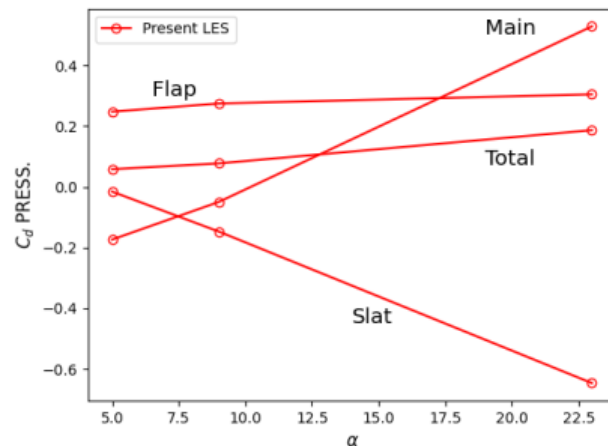
[8] S. Klausmeyer, J. Lin (1994). DOI: <https://doi.org/10.2514/6.1994-1870>

Baseline LES – Validation

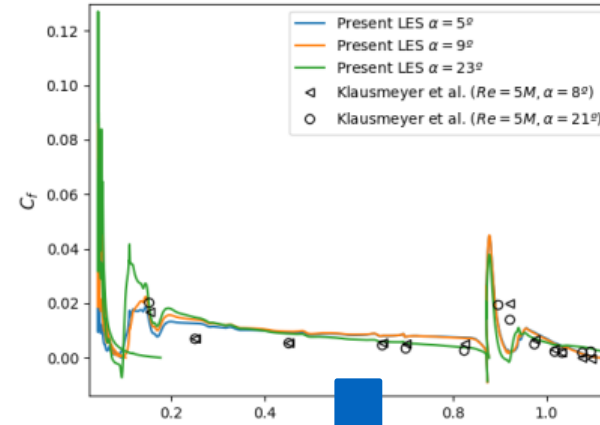
Pressure Coefficient (C_p)



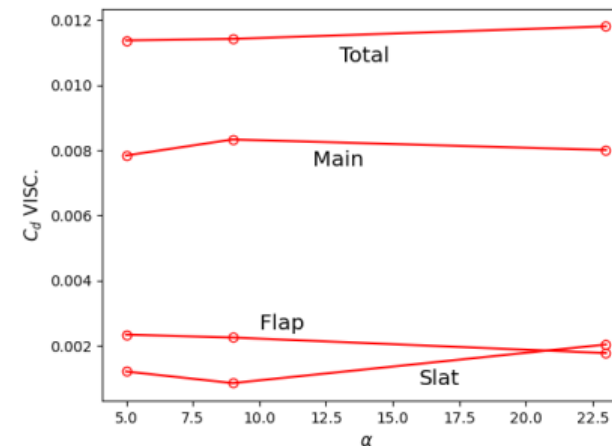
Pressure Drag Coefficient ($C_{d, pres.}$)



Skin Friction Coefficient (C_f)



Viscous Drag Coefficient ($C_{d, visc.}$)



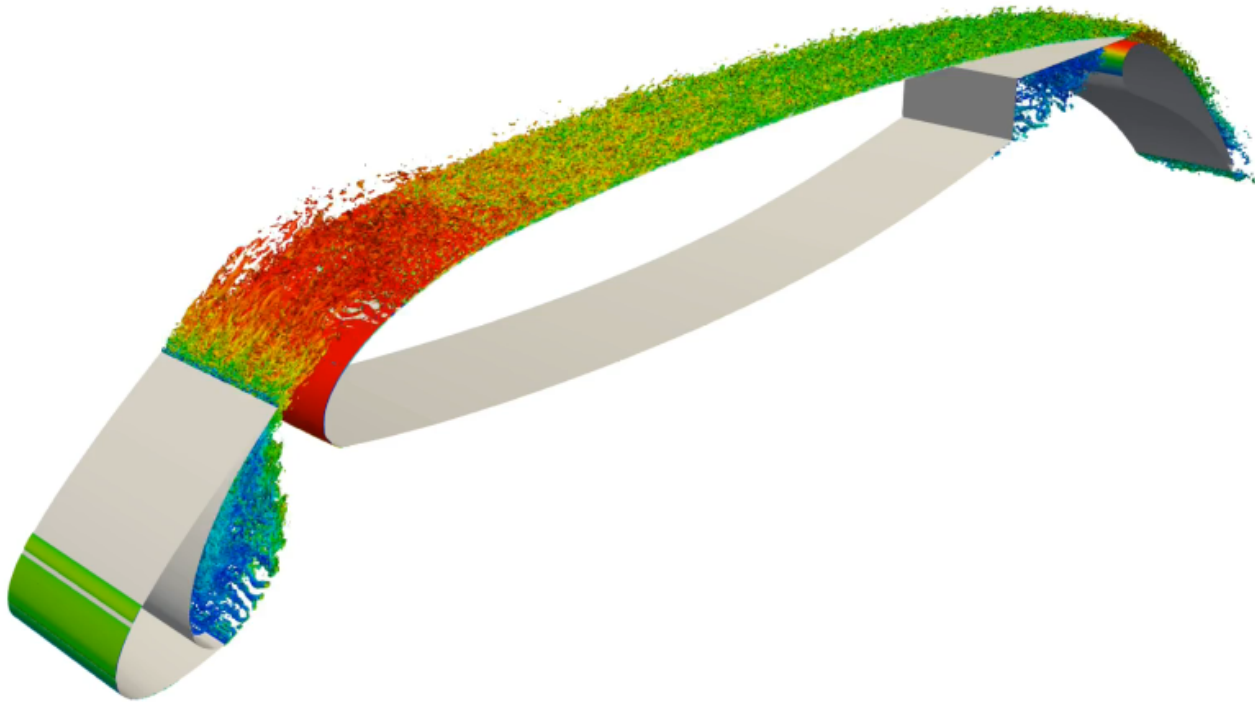
[6] M. Murayama, K. Nakakita, K. Yamamoto, H. Ura, Y. Ito, M. Choudhari (2014). DOI: <https://doi.org/10.2514/6.2018-3460>

[7] K. Pascioni, L.N. Cattafesta, M. Choudhari (2014). DOI: <https://doi.org/10.2514/6.2014-3062>

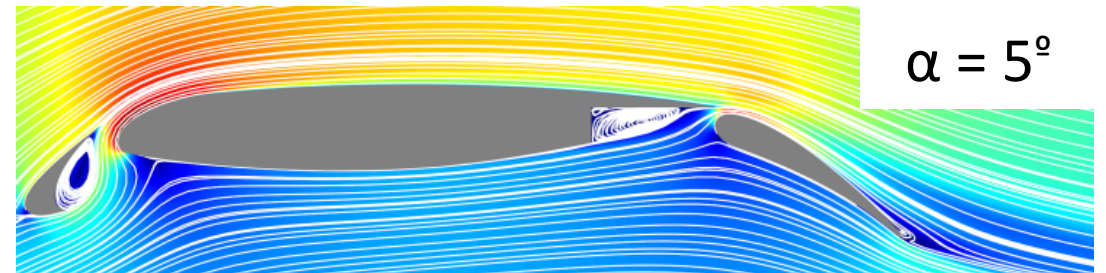
[8] S. Klausmeyer, J. Lin (1994). DOI: <https://doi.org/10.2514/6.1994-1870>

Baseline LES – Flow Overview

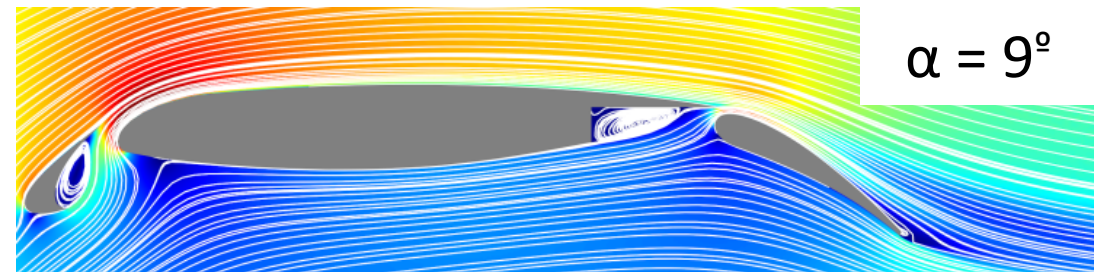
Q-criterion isocontours at $\alpha = 5^\circ$



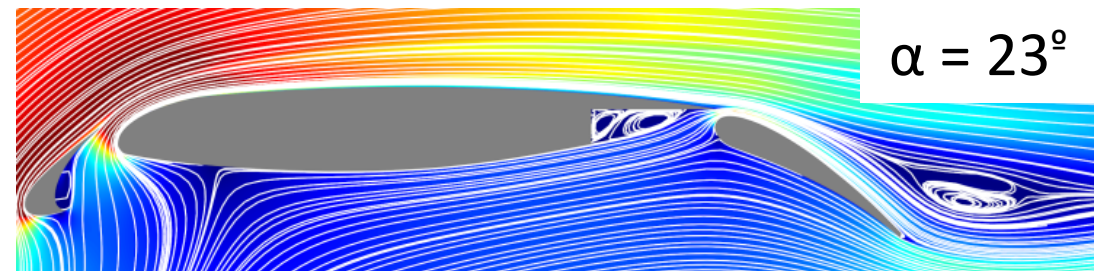
Streamlines Coloured by Velocity Magnitude



$\alpha = 5^\circ$



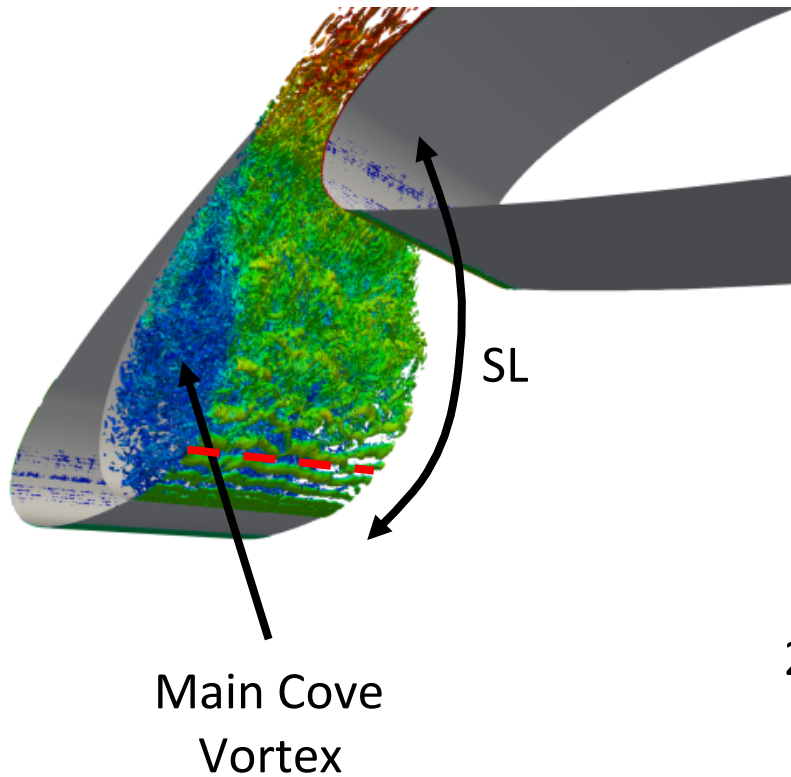
$\alpha = 9^\circ$



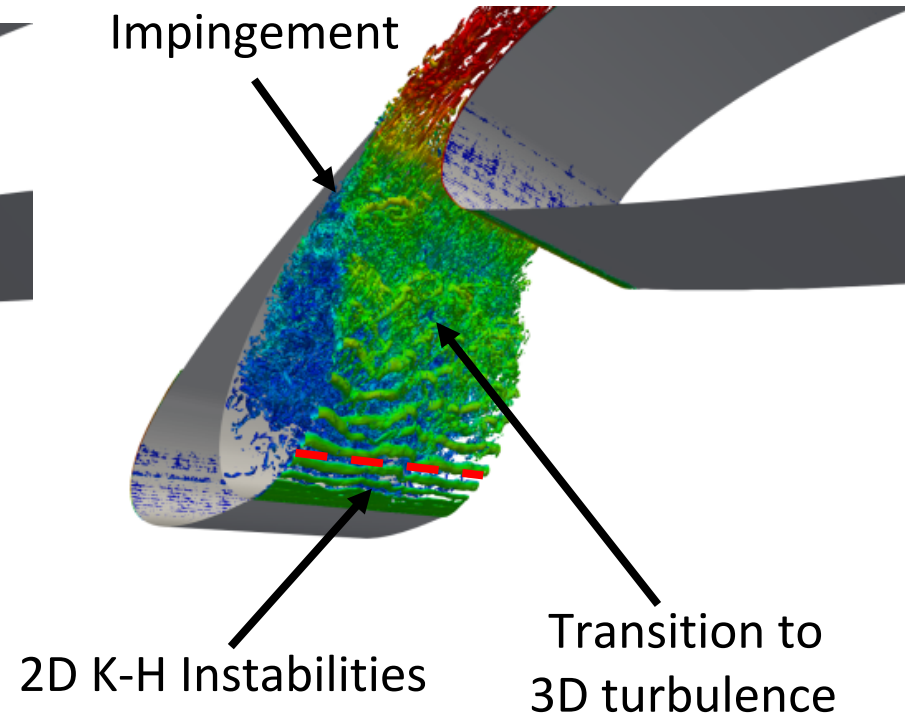
$\alpha = 23^\circ$

Baseline LES – Slat Cove Dynamics

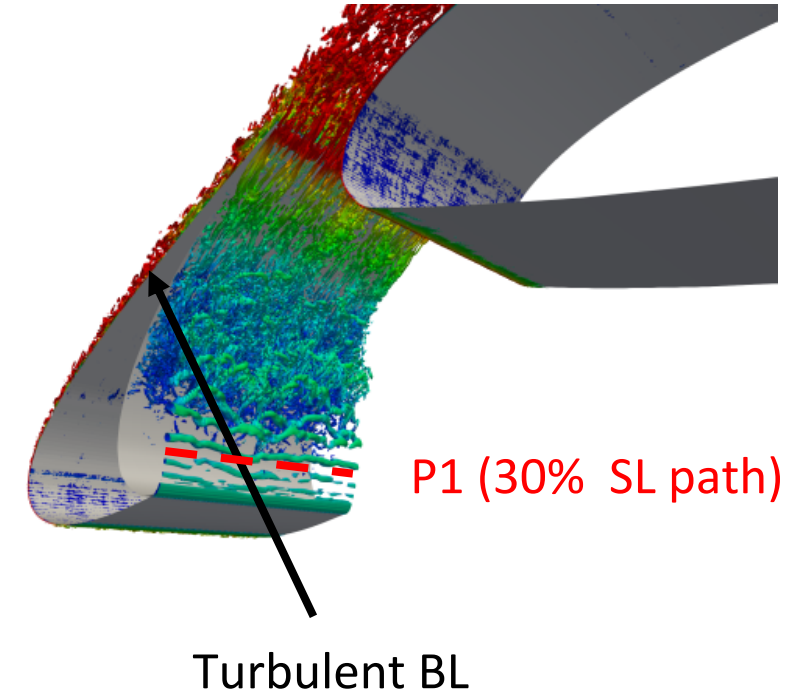
$\alpha = 5^\circ$



$\alpha = 9^\circ$

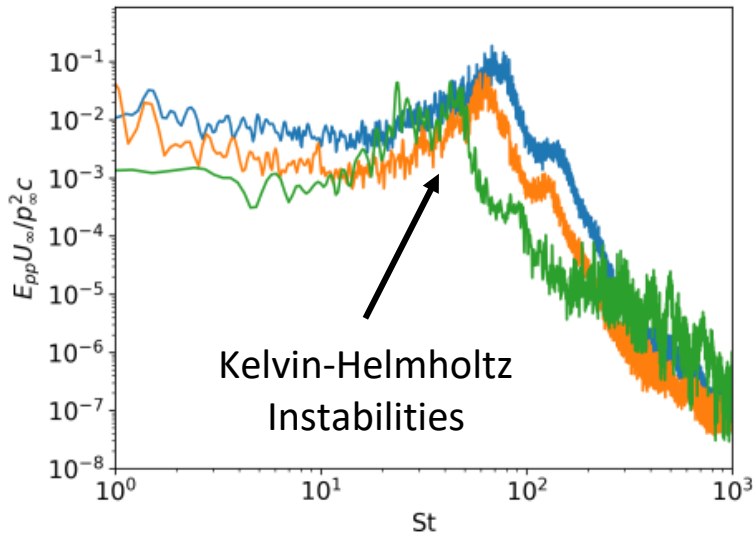


$\alpha = 23^\circ$



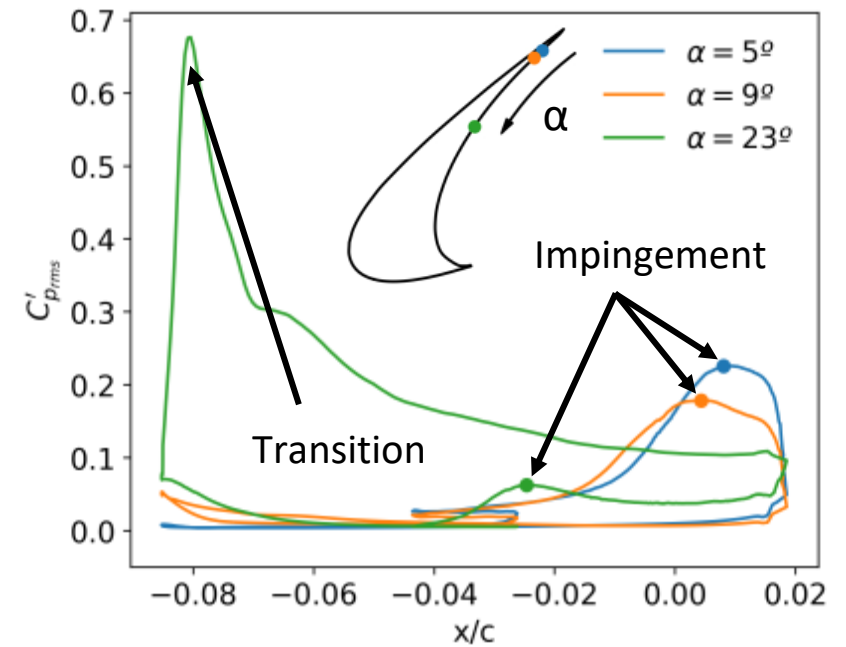
Baseline LES – Slat Cove Dynamics

Pressure Spectra at P1



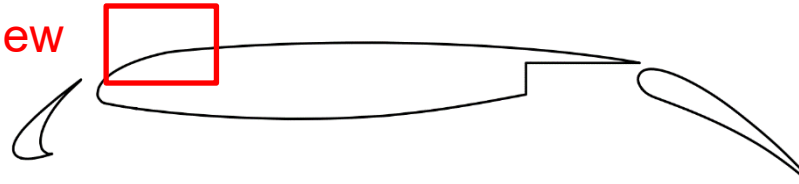
α [°]	St [-]
5	70
9	64
23	35

RMS of C_p'



Baseline LES – Turbulent Transition

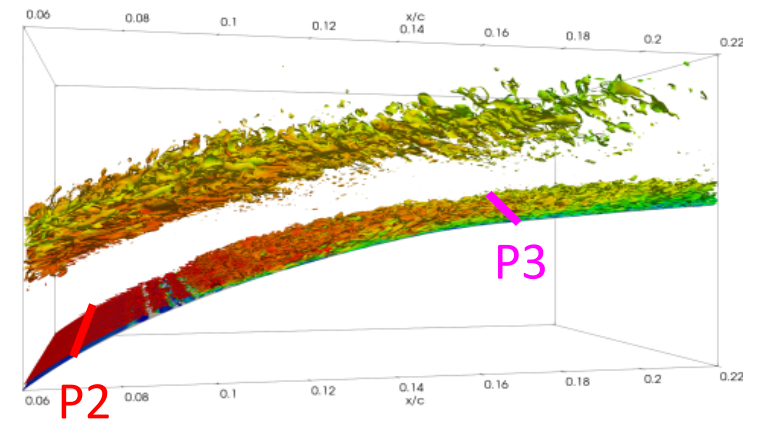
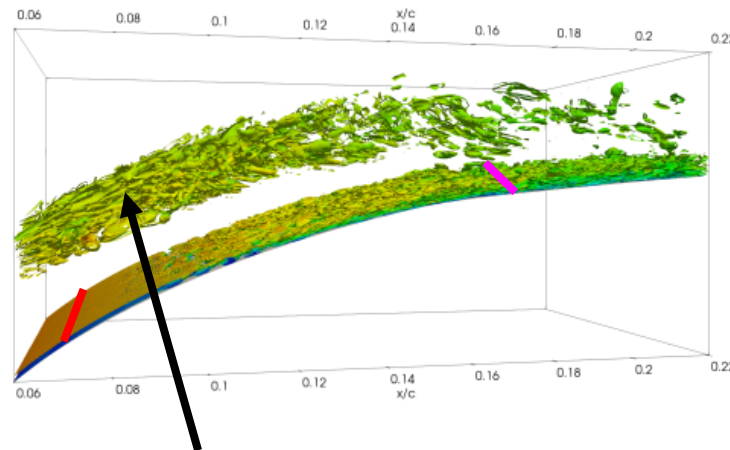
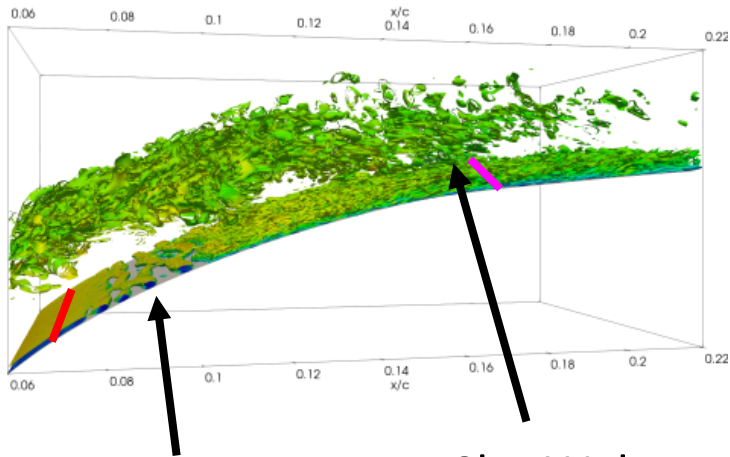
Zoomed view



$\alpha = 5^\circ$

$\alpha = 9^\circ$

$\alpha = 23^\circ$



T-S Instabilities

Slat Wake Interaction

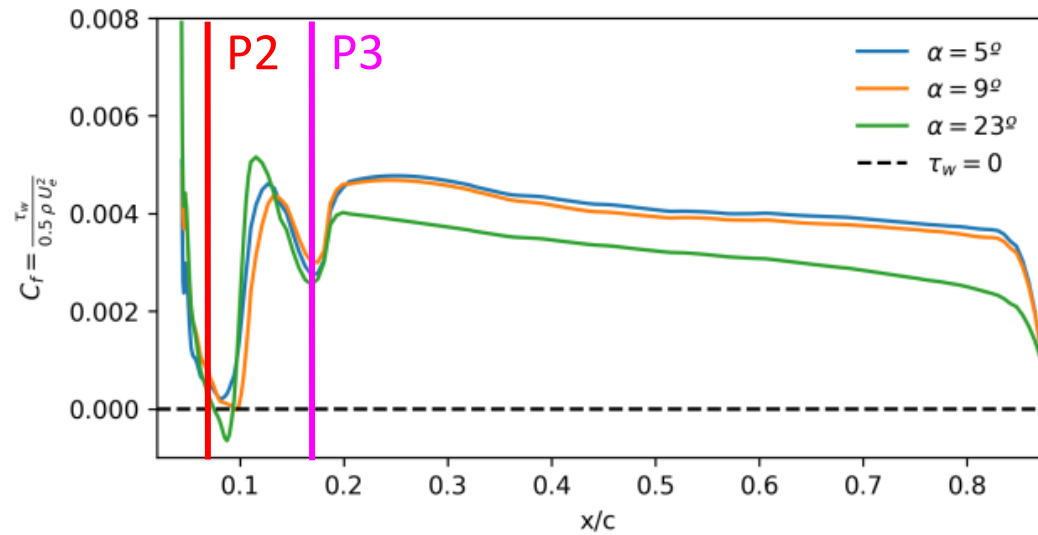
Slat Wake

P2

P3

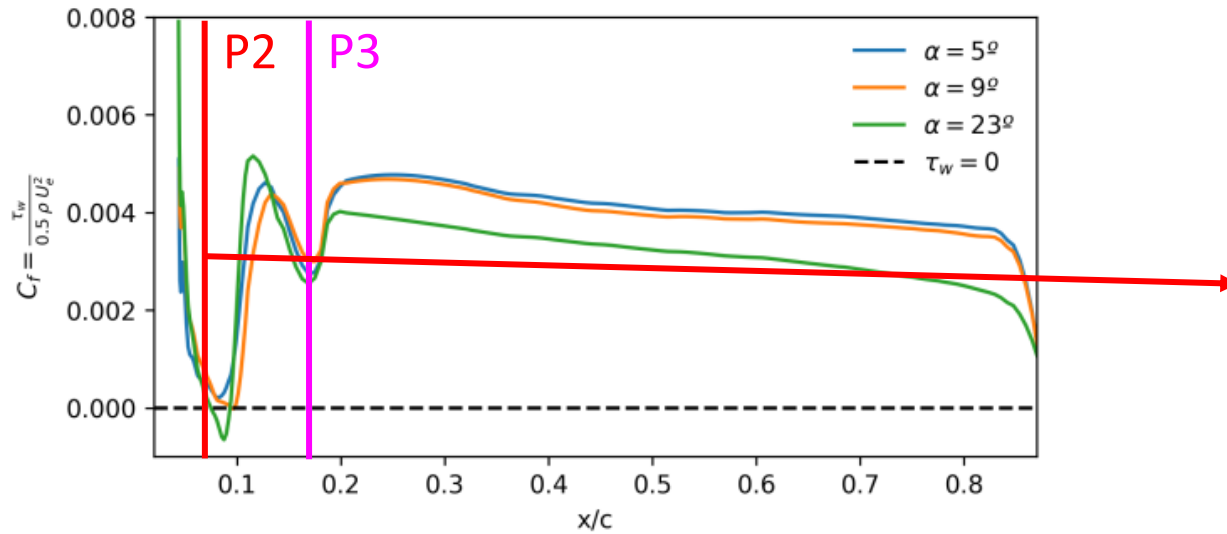
Baseline LES – Turbulent Transition

Skin Friction Coefficient

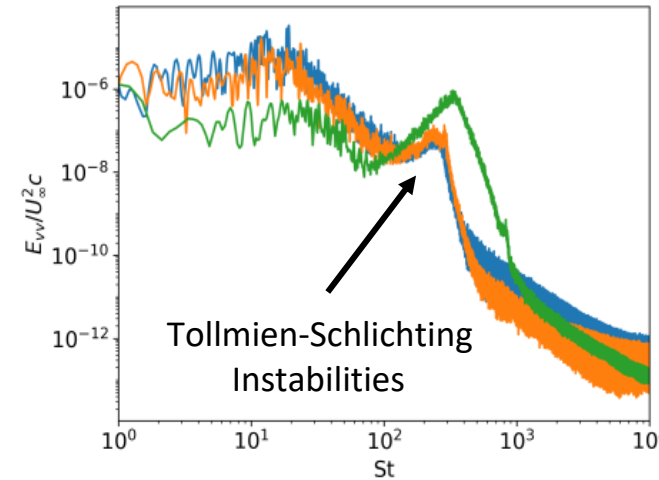


Baseline LES – Turbulent Transition

Skin Friction Coefficient



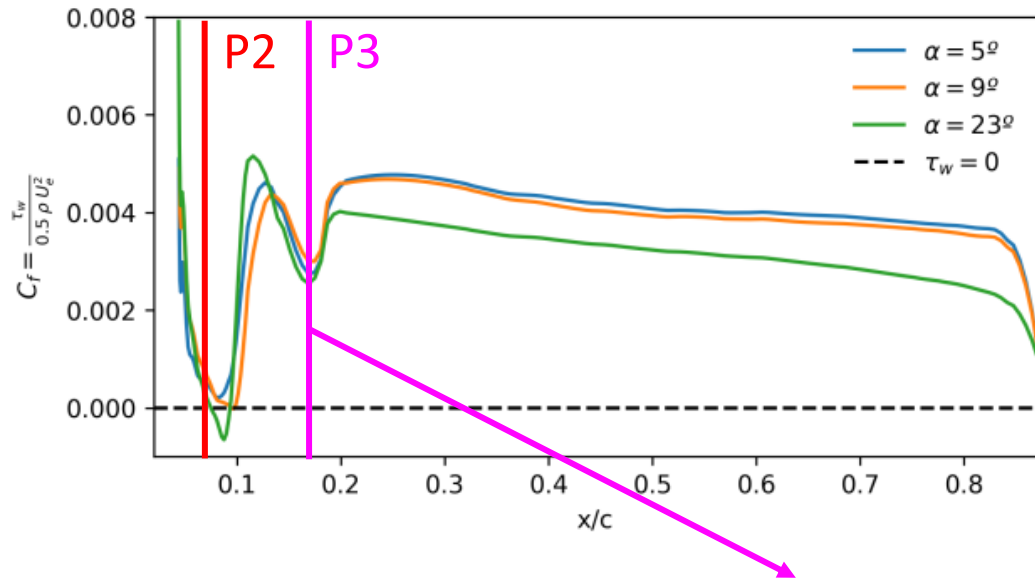
Velocity Magnitude Spectra at P2



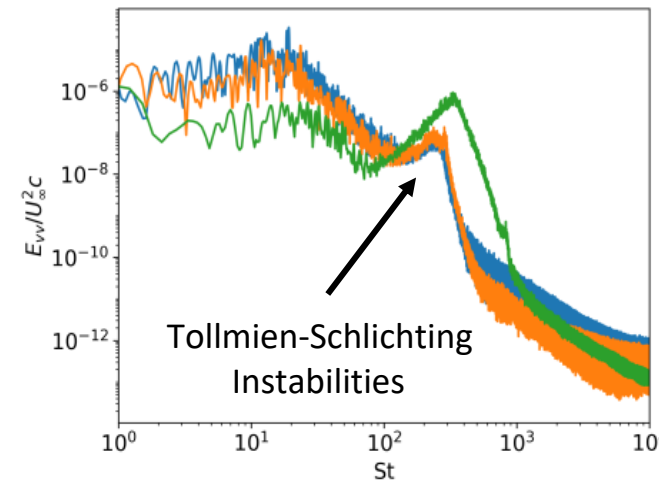
α [°]	St [-]
5	255
9	285
23	340

Baseline LES – Turbulent Transition

Skin Friction Coefficient

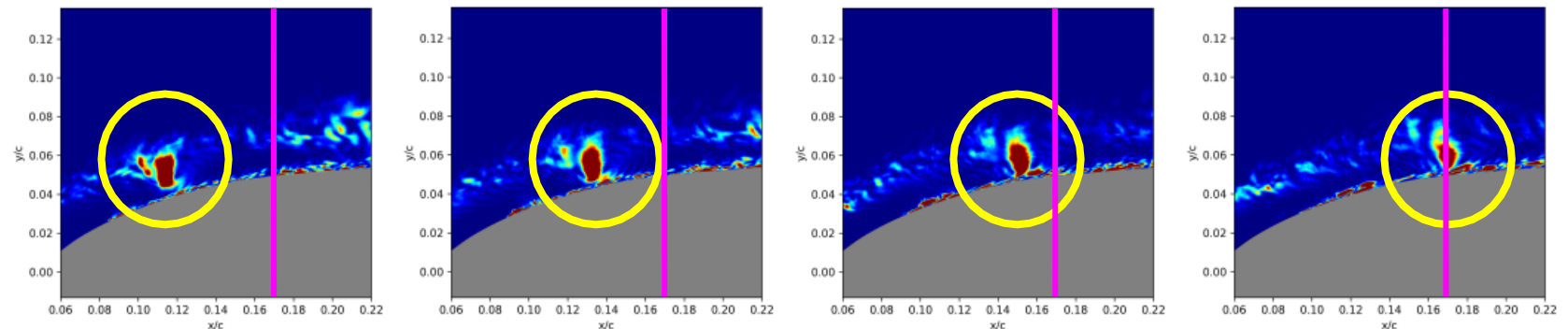


Velocity Magnitude Spectra at P2



α [°]	St [-]
5	255
9	285
23	340

Instantaneous TKE

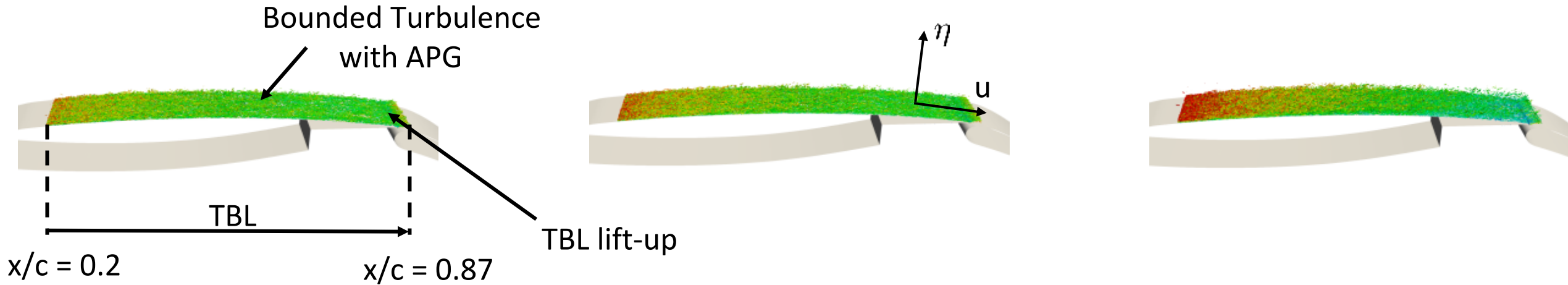


Baseline LES – Turbulent Boundary Layer

$\alpha = 5^\circ$

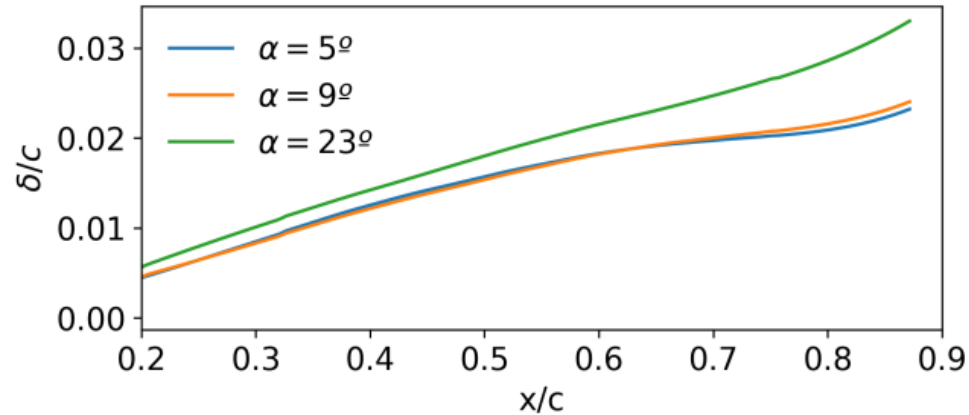
$\alpha = 9^\circ$

$\alpha = 23^\circ$

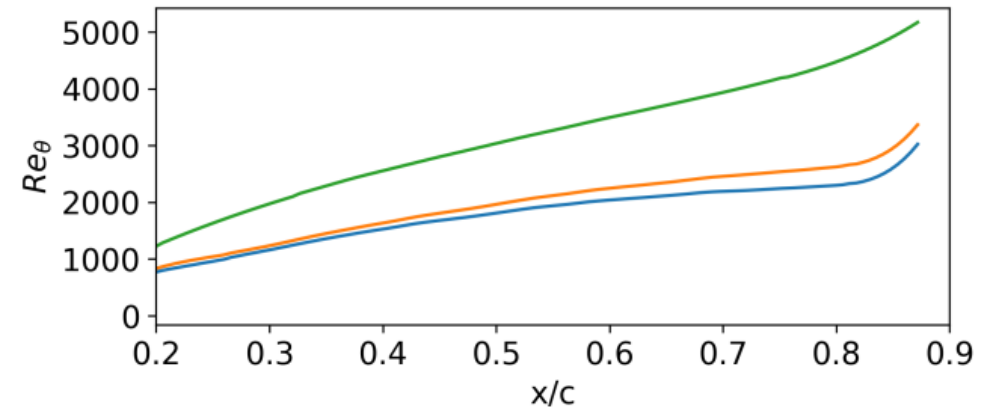


Baseline LES – Trubulent Boundary Layer

Boundary Layer Thickness

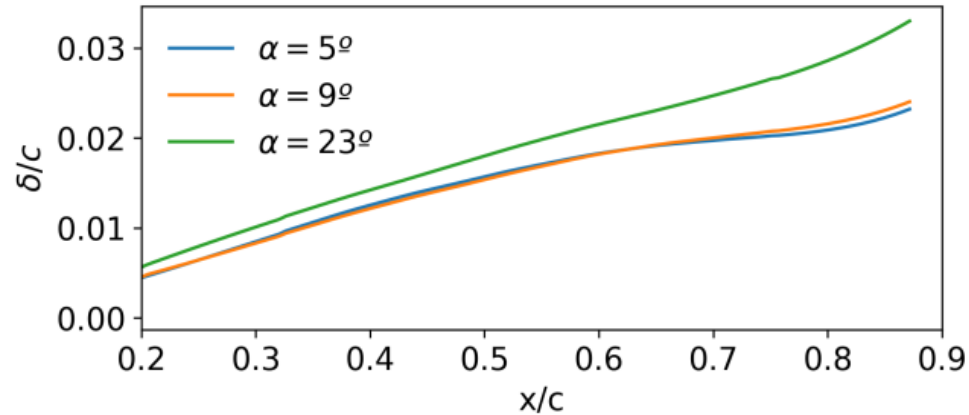


Momentum Thickness Reynolds

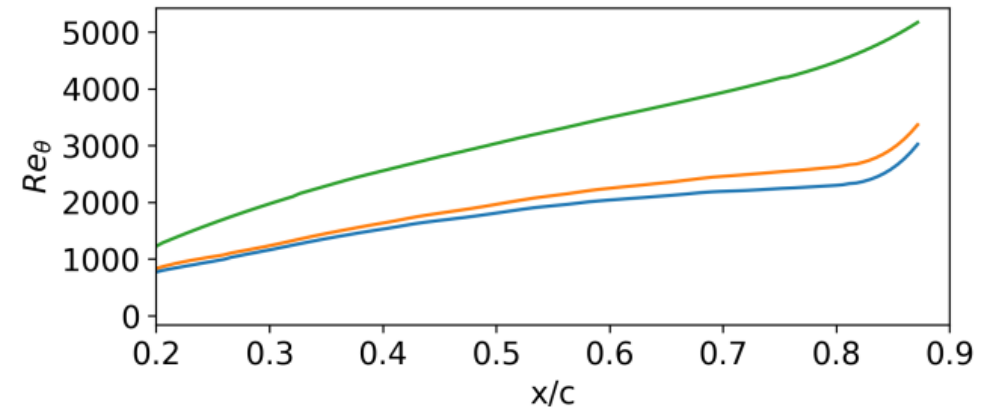


Baseline LES – Trubulent Boundary Layer

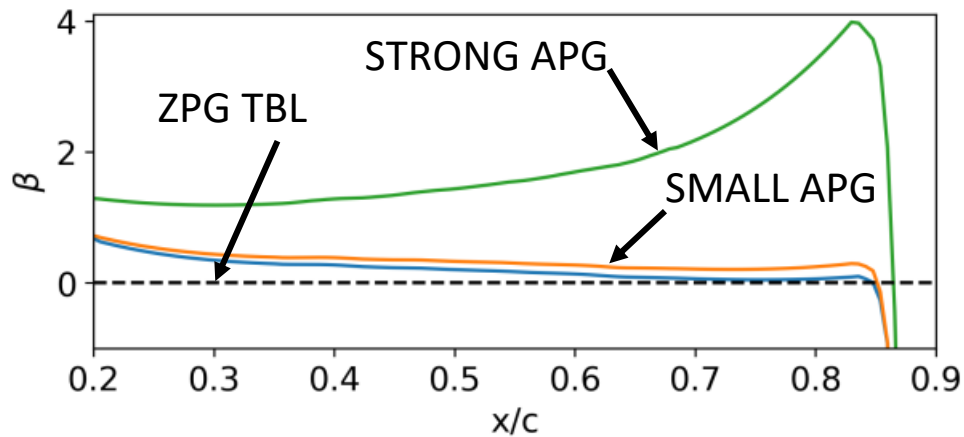
Boundary Layer Thickness



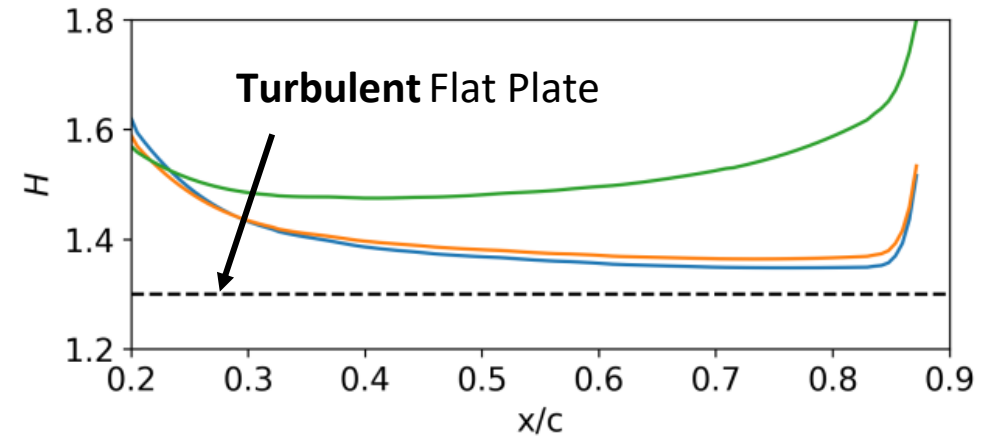
Momentum Thickness Reynolds



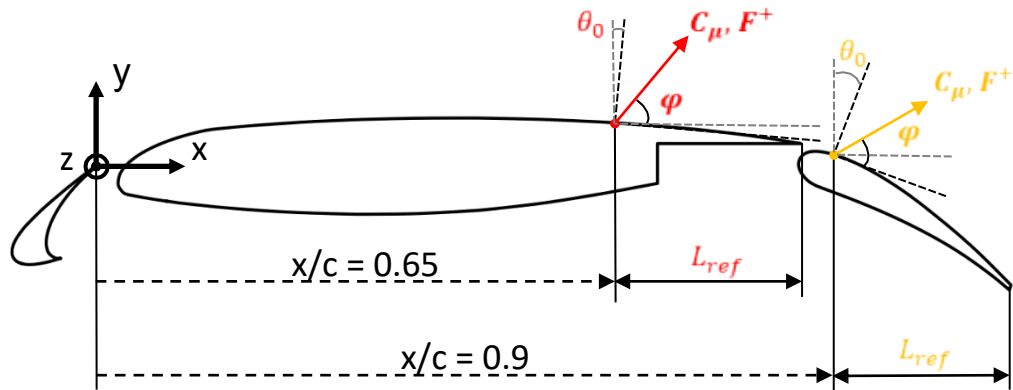
Clouser Pressure-Gradient Parameter



Shape Factor



AFC LES – Case Configuration

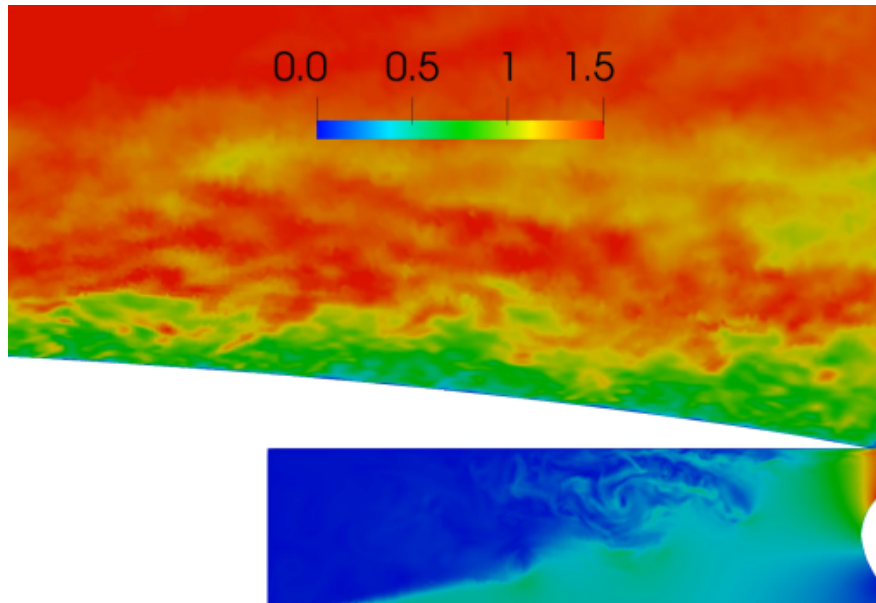


$$\begin{bmatrix} u \\ v \\ w \end{bmatrix}_{xyz, act} = U_\infty \sqrt{\frac{c}{h}} C_\mu \sin\left(2\pi \frac{F^+ U_\infty}{L_{ref}} t\right) \begin{bmatrix} \cos(\varphi - \theta_0) \\ \sin(\varphi - \theta_0) \\ 0 \end{bmatrix} = f(C_\mu, F^+, \varphi)$$

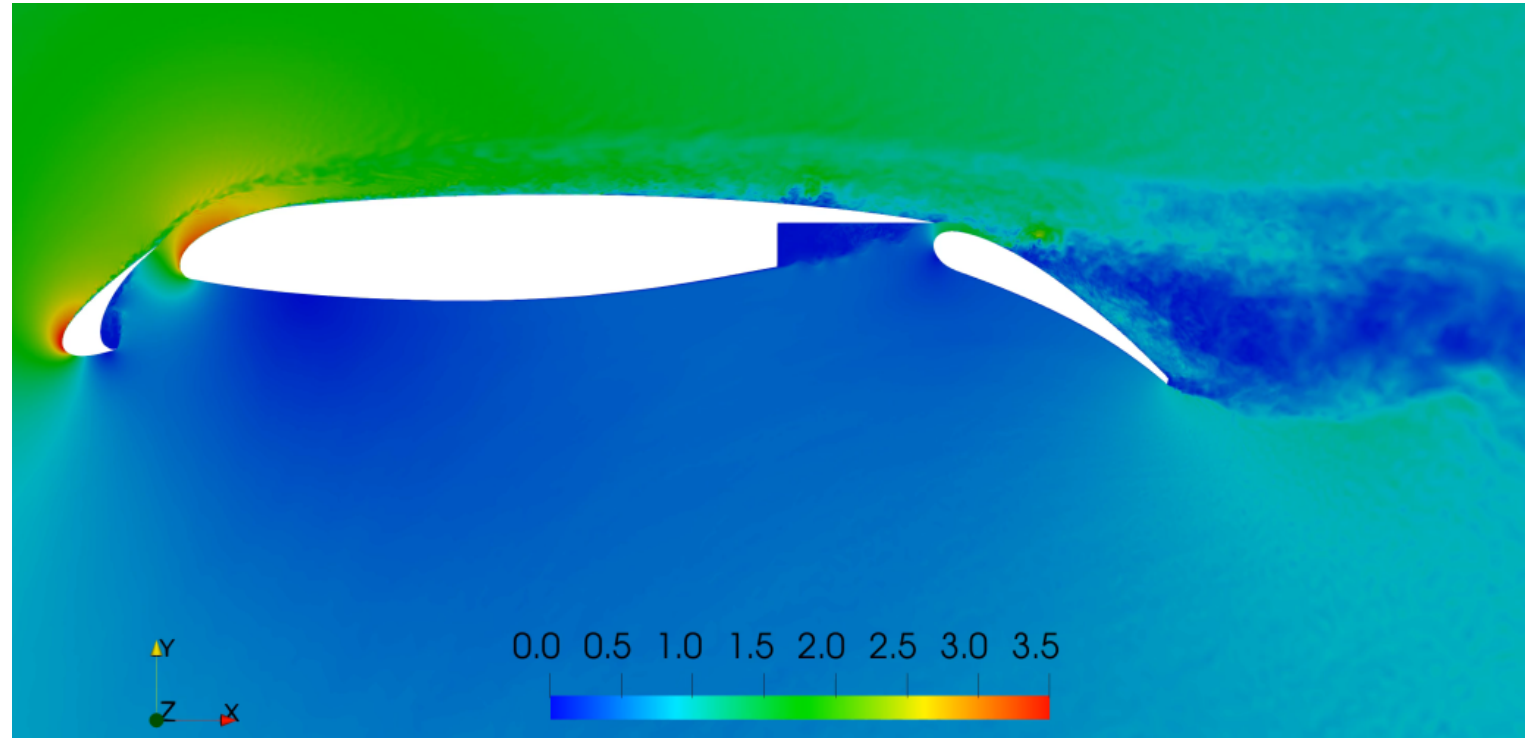
	CASE ID	Main Actuation			Flap Actuation		
		C_μ	F^+	φ	C_μ	F^+	φ
$Re_c = 750,000$ $\alpha = 23^\circ$	1	0.015	0.34	20°	- Not actuated -		
	2	- Not actuated -			0.025	0.34	20°
	3	0.015	1.52	90°	- Not actuated -		
	4	- Not actuated -			0.025	1.52	90°
	5	0.015	1.52	45°	0.025	1.52	90°

AFC LES - Results

Case ID 1



Case ID 5



Work in Progress!

Conclusions

- Computational data shows **good agreement** with the experimental observations.
- Evolution of flow dynamics **at increasing α** :
 - **Slat SL:** (i) Smaller recirculation area. (ii) Lower K-H frequencies. (iii) Weaker impingement strength. (iv) More pronounced wake (TBL on suction side).
 - **Main turb. transition:** (i) Nearly at constant locations. (ii) Higher T-S frequencies.
 - **Main TBL:** (i) Stronger APG. (ii) More pronounced main wake. (iii) Recirculation region (Stall conditions).
- **Viscous drag** remains nearly **constant** with α (from $C_{d\text{ visc.}} = 0.0114$ to 0.0118); while **pressure drag increases** noticeably (from $C_{d\text{ press.}} = 0.0580$ to 0.1865).
- **Pressure is the main contributor** to drag (Half or even one order of magnitude higher):
 - **Flap** has the highest $C_{d\text{ press.}}$ at lower α (curvature \rightarrow APG), but it remains approximately constant with α (constrained flow \rightarrow main-flap gap jet).
 - In the **slat**, $C_{d\text{ press.}}$ diminishes with α (Higher suction peak + element inclination \rightarrow Positive force).
 - The $C_{d\text{ press.}}$ in the **main** goes from the lowest value (behaves nearly as a flat plate) to the highest one (Strong APG along suction side).
- Two **actuators strategies** tested **with the idea of**:
 - **Main actuator:** Reduce the APG in the main TBL \rightarrow reduce its wake.
 - **Flap actuator:** Increase the vertical mixing of the main-flap gap jet flow.

Future Work

- Analyse the **AFC results** and assess the differences with the baseline case: Why /Why not improved?
- Build **ROMs models** (POD, DMD, Autoencoders...): Fruther understand the Flow features contributed by the actuations.
- **Exploit** the capabilities of machine learning (**Deep Reinforcement Learning**) to optimize the actuation parameters.

Thank you for your attention



EuroHPC
Joint Undertaking



RED ESPAÑOLA DE
SUPERCOMPUTACIÓN



GOBIERNO
DE ESPAÑA

MINISTERIO
DE CIENCIA
E INNOVACIÓN



**Barcelona
Supercomputing
Center**
Centro Nacional de Supercomputación



**Agència
de Gestió
d'Ajuts
Universitaris
i de Recerca**

A wireframe dinosaur, resembling a T-Rex, is positioned in the center of the image. The background is a server room with blue lighting and server racks. The dinosaur is composed of a network of white lines forming its body. The overall scene is a digital or data center environment.

Heat-transfer in drop-laden turbulence

**EUROHPC
USER DAY
2023** Brussels
11.12.23



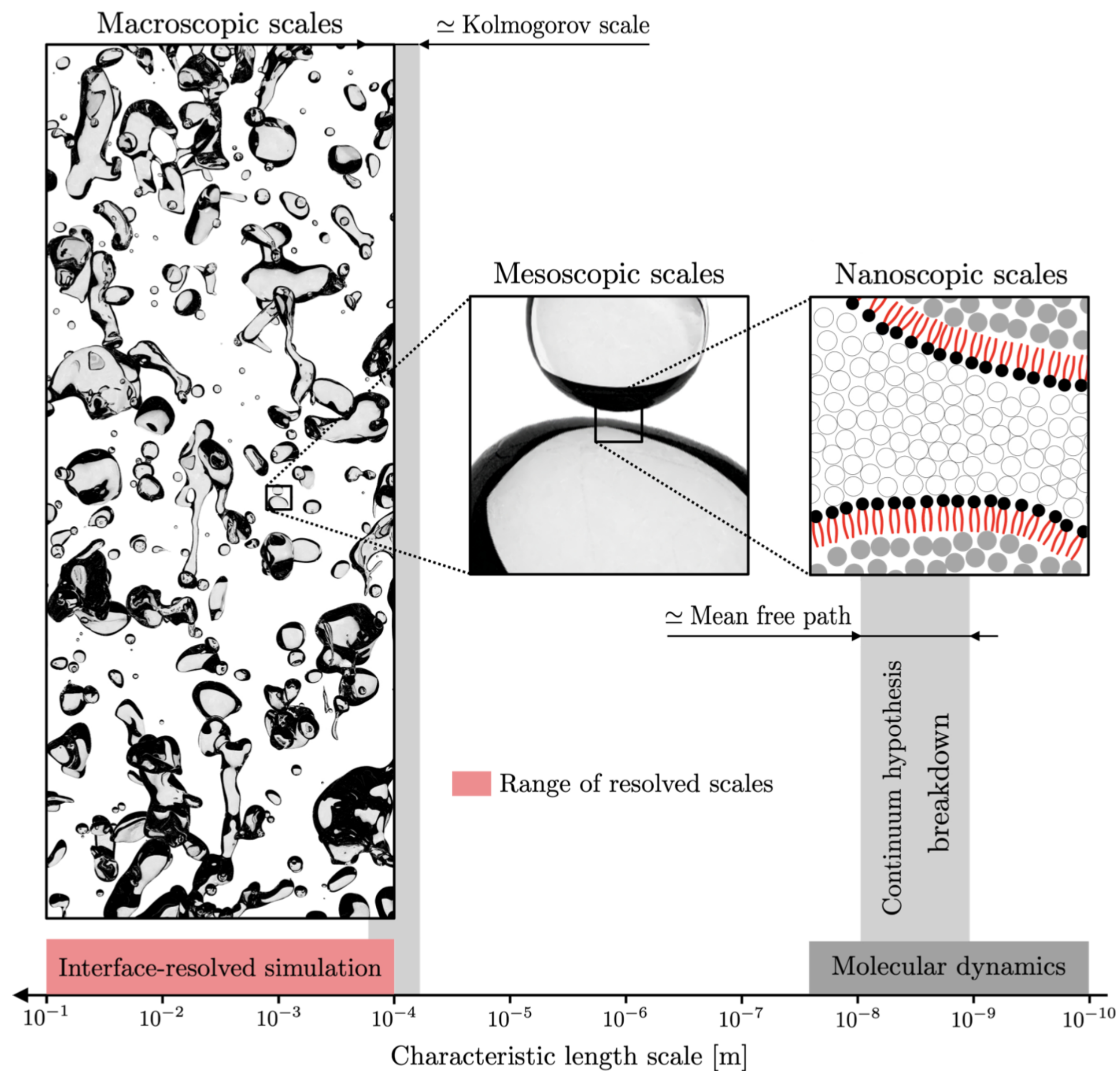
Project: *"BubbLe-modUlated Mixing in turbulENce (BLUMEN)"*

EuroHPC used: Discoverer

Speaker: *Alessio ROCCON (Univ. Udine)*

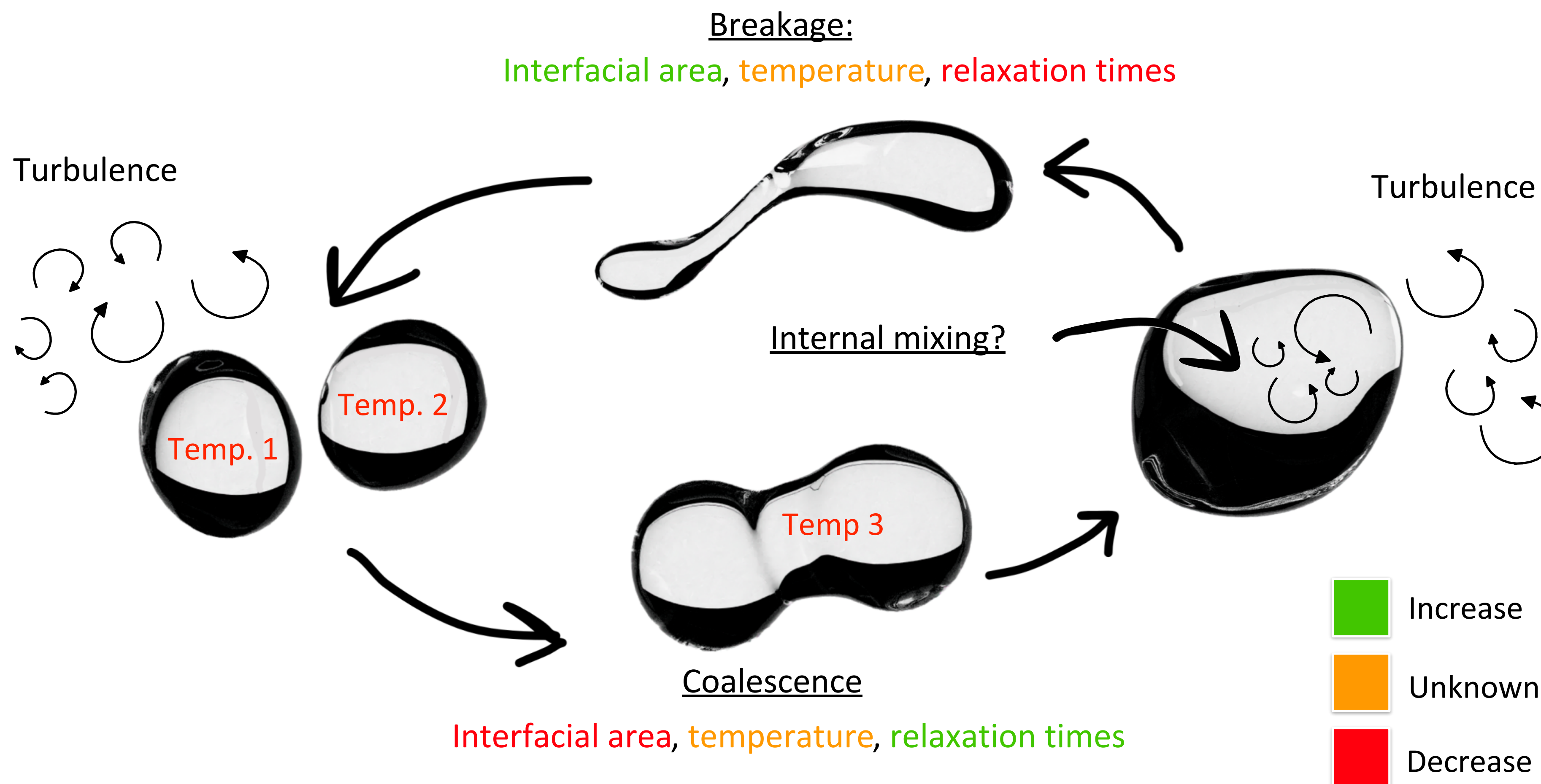
The problem involves a wide range of spatial and temporal scales:

- Largest scale of problem
- Kolmogorov scale
- Molecular scale of the interface



How does a passive scalar (e.g. temperature) behave in multiphase turbulence?

Internal/external turbulent transport and turbulence-interface interactions can modify the mixing:



Heat transfer?

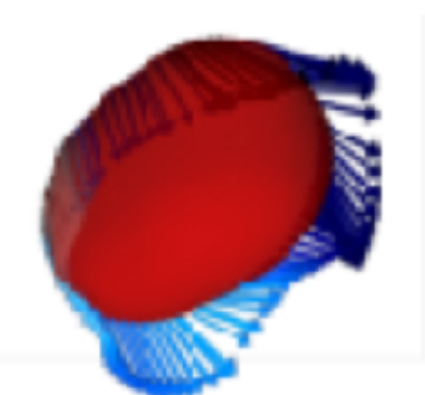
Assumptions:

- Same density/viscosity
- Small temperature difference
- Same thermal diffusivity

Prandtl number

$$Pr = \frac{\nu}{a} = \frac{\text{Momentum diffusivity}}{\text{Thermal diffusivity}}$$

Flow:



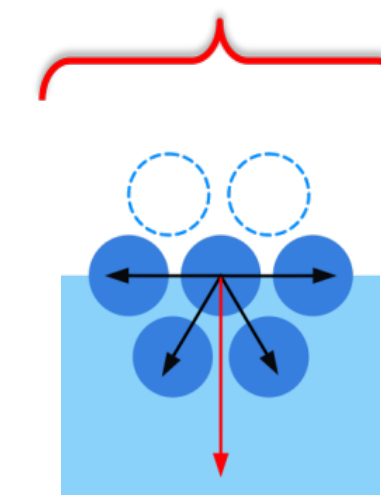
$$\nabla \cdot \mathbf{u} = 0$$

$$\rho(\phi) \left[\frac{\partial \mathbf{u}}{\partial t} + \mathbf{u} \cdot \nabla \mathbf{u} \right] = -\nabla p + \frac{1}{Re_\tau} \nabla \cdot [\eta(\phi)(\nabla \mathbf{u} + \nabla \mathbf{u}^T)] + \underbrace{\frac{3}{\sqrt{8}} \frac{Ch}{We} \nabla \cdot \boldsymbol{\tau}_e}_{\text{Surface tension forces}}$$

Interface:



$$\frac{\partial \phi}{\partial t} + \mathbf{u} \cdot \nabla \phi = \frac{1}{Pe_\phi} \nabla^2 \mu_\phi$$



Surface tension forces

Temperature:



$$\frac{\partial \theta}{\partial t} + \mathbf{u} \cdot \nabla \theta = \frac{1}{Re_\tau Pr} \nabla^2 \theta$$



Transport equation for a passive scalar, no feedback on NS

The **Cahn-Hilliard equation** is the principal governing equation in the phase-field method and includes all important physical phenomena: **phase-change and surface tension**.
CH equation is a fourth-order non linear partial differential equation.

$$\frac{\partial \phi}{\partial t} + \mathbf{u} \cdot \nabla \phi = \frac{1}{Pe_\phi} \nabla^2 \mu_\phi$$

Chemical potential (Ginzburg-Landau theory)

$$\mu_\phi = \phi^3 - \phi - Ch^2 \nabla^2 \phi$$

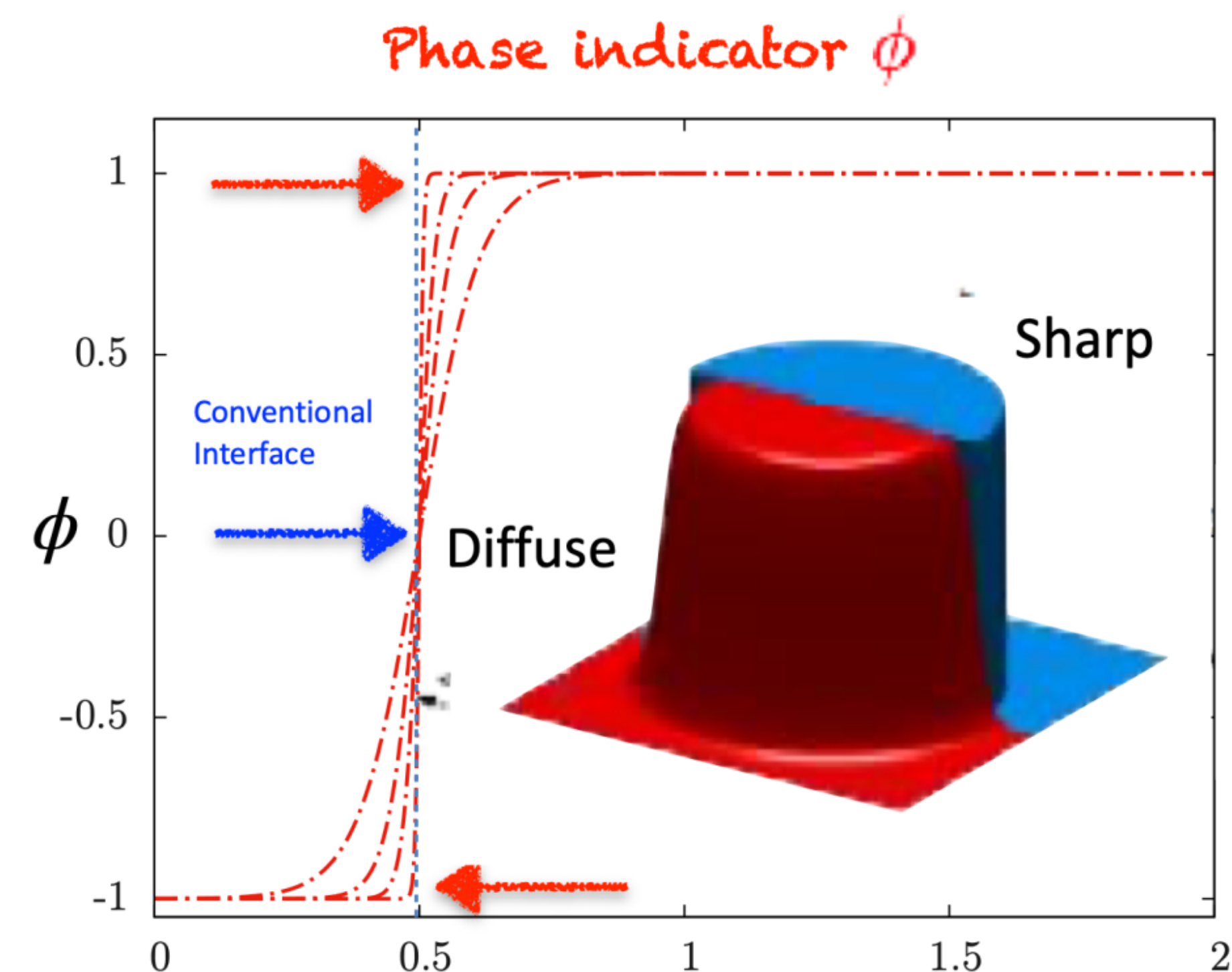
Dimensionless parameters:

$$Ch = \frac{\epsilon}{h} \quad Pe_\phi = \frac{u_\tau h}{M\beta}$$

$$Ch = \mathcal{O}(10^{-9}) \quad Pe = \mathcal{O}(10^9)$$

Cahn number *Peclet number*

To reduce the computational effort, the interface must be fictitiously enlarged to the point that it becomes computationally tractable (3-5 grid poir



At equilibrium:

$$\phi = \tanh \left(\frac{x}{\sqrt{2}Ch} \right)$$

Numerical method:

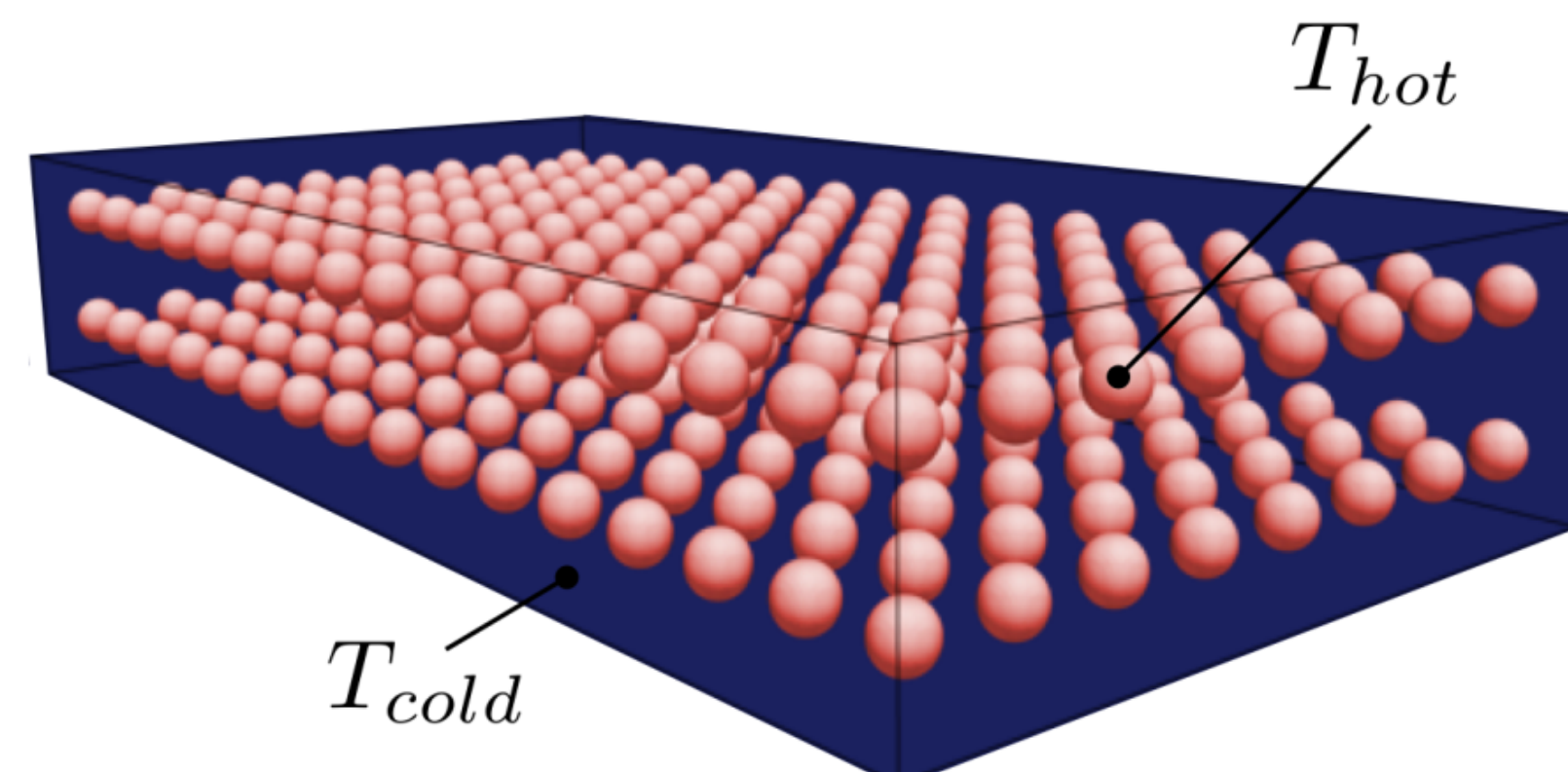
- Wall-normal velocity formulation for the Navier-Stokes equations.
- Pseudo-spectral method (Fourier for the homogenous directions and Chebychev for the wall-normal direction)
- For Cahn-Hilliard equation, splitting technique (recasted in two 2nd order equations)

Parallelization strategy:

- First layer of parallelization that relies on MPI (2D domain decomposition), in-house library for pencil rotations. Used for CPU-based machines (Discoverer, LUMI-C, etc.) + FFTW.
- Second layer of parallelisation that relies on openACC directives and CUDA Fortran instructions for GPU-based machines (Leonardo) + cuFFT.

Initial conditions:

- Flow Field:
Fully developed turbulent channel flow (Shear Reynolds $Re = 300$)
- Phase Field and temperature:
256 spherical **hot** drops in a **cold** channel (adiabatic)



Simulation parameters:



Four different Prandtl numbers:

- $Pr = 1, 2, 4, 8$ (obtained reducing therm. diff.)

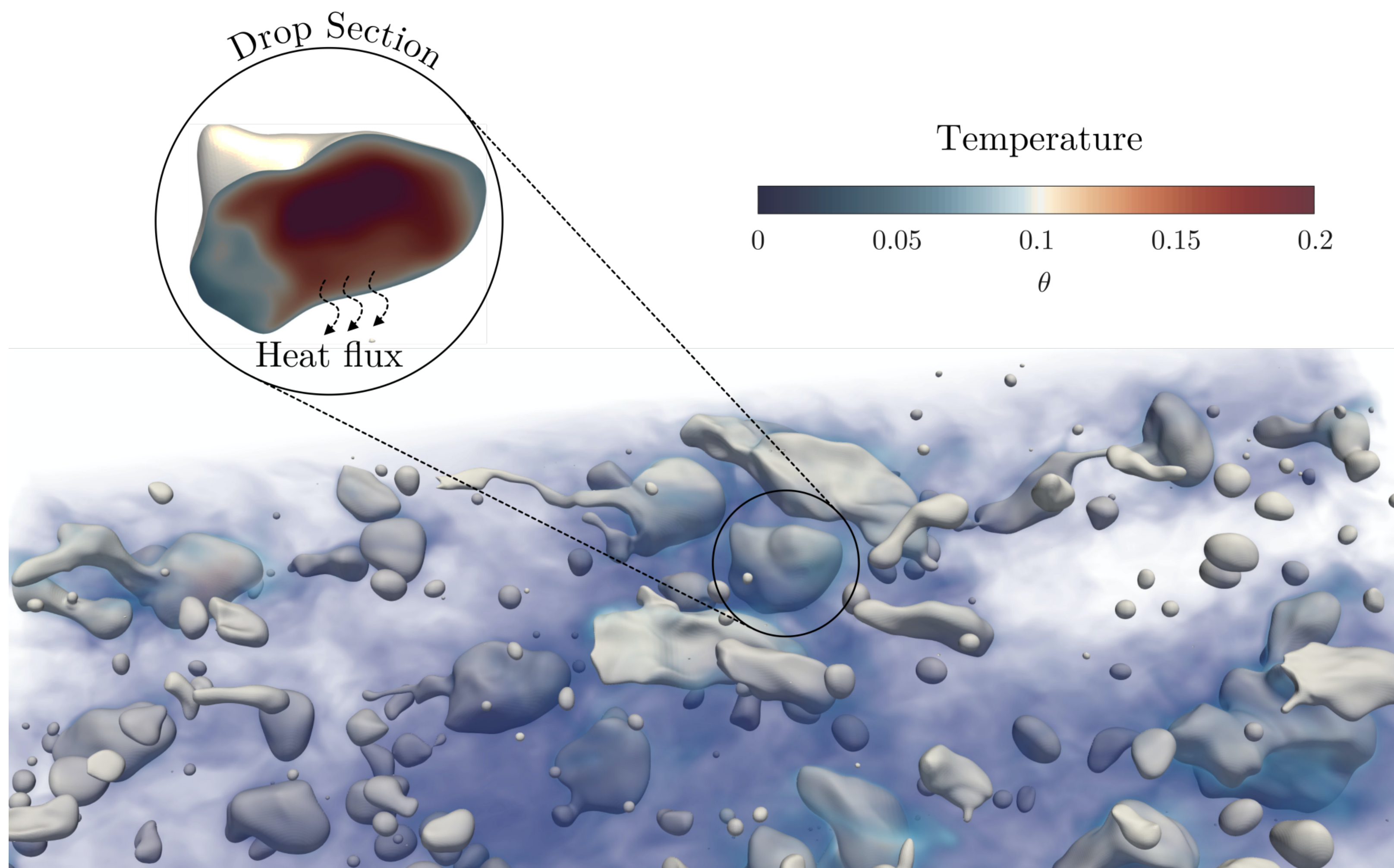
Multi resolution strategy to resolve the Batchelor scale.

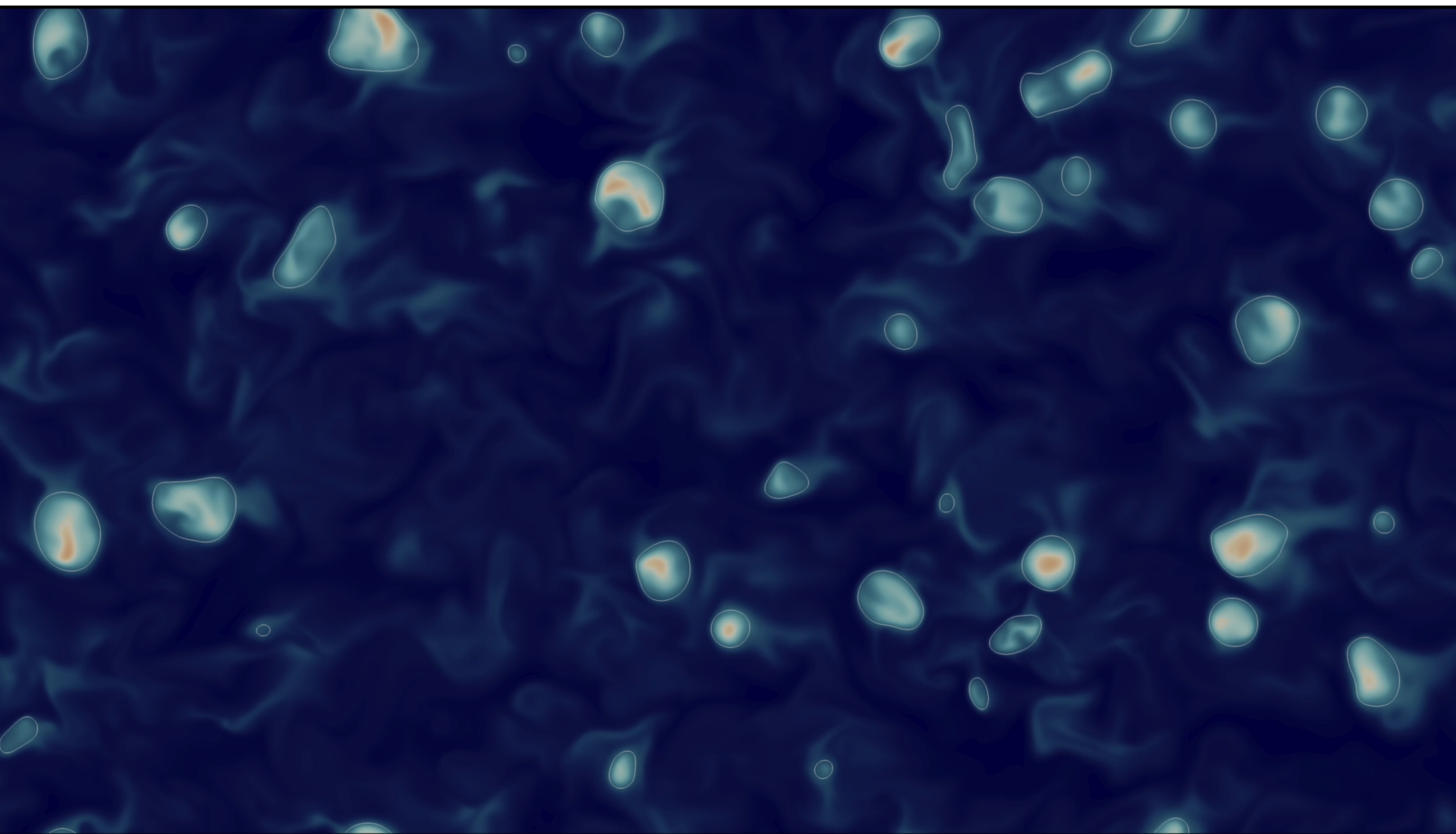
Pr	Batchelor scale		
	Pr	η_B	
1	1	η_k	} grid 1
	2	$0.71\eta_k$	
4	4	$0.50\eta_k$	} grid 2
	8	$0.35\eta_k$	

$$\eta_B = \frac{\eta_k}{\sqrt{Pr}}$$

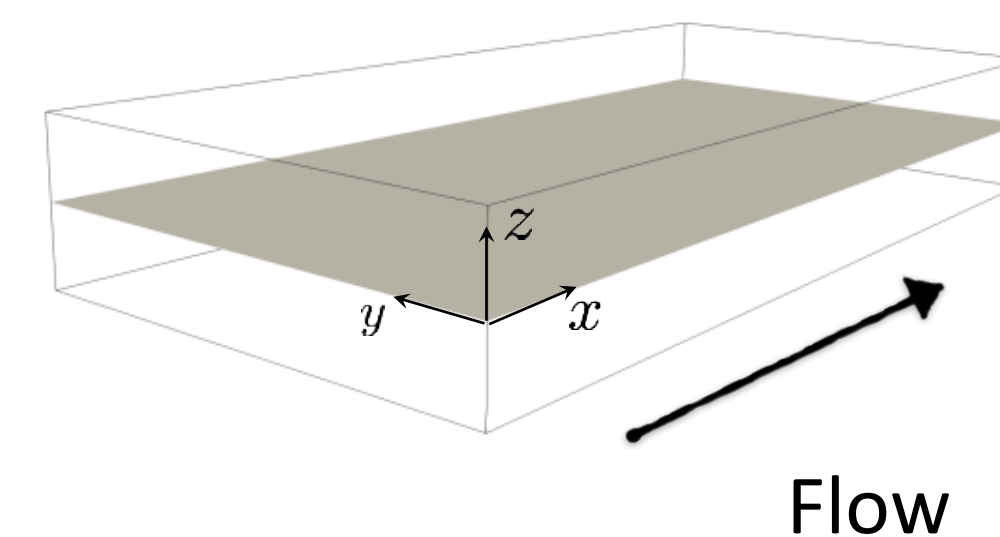
Grid 1: 1024 x 512 x 513

Grid 2: 2048 x 1204 x 513





Channel mid plane

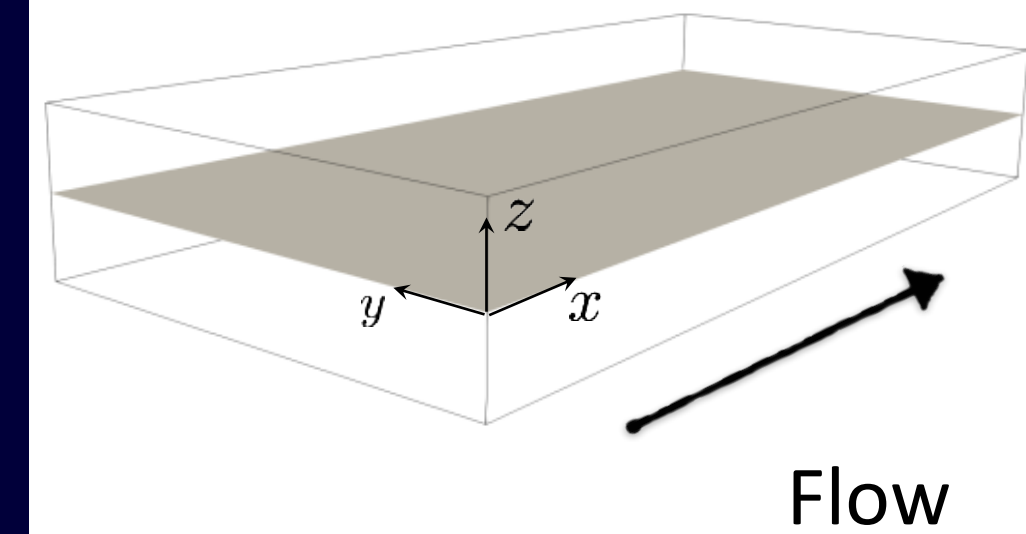


Roccon et al., "Phase-field modeling of complex interface dynamics in drop-laden turbulence, PRF (2023).
Mangani et al., "Heat-transfer in drop-laden turbulence", JFM (2023)

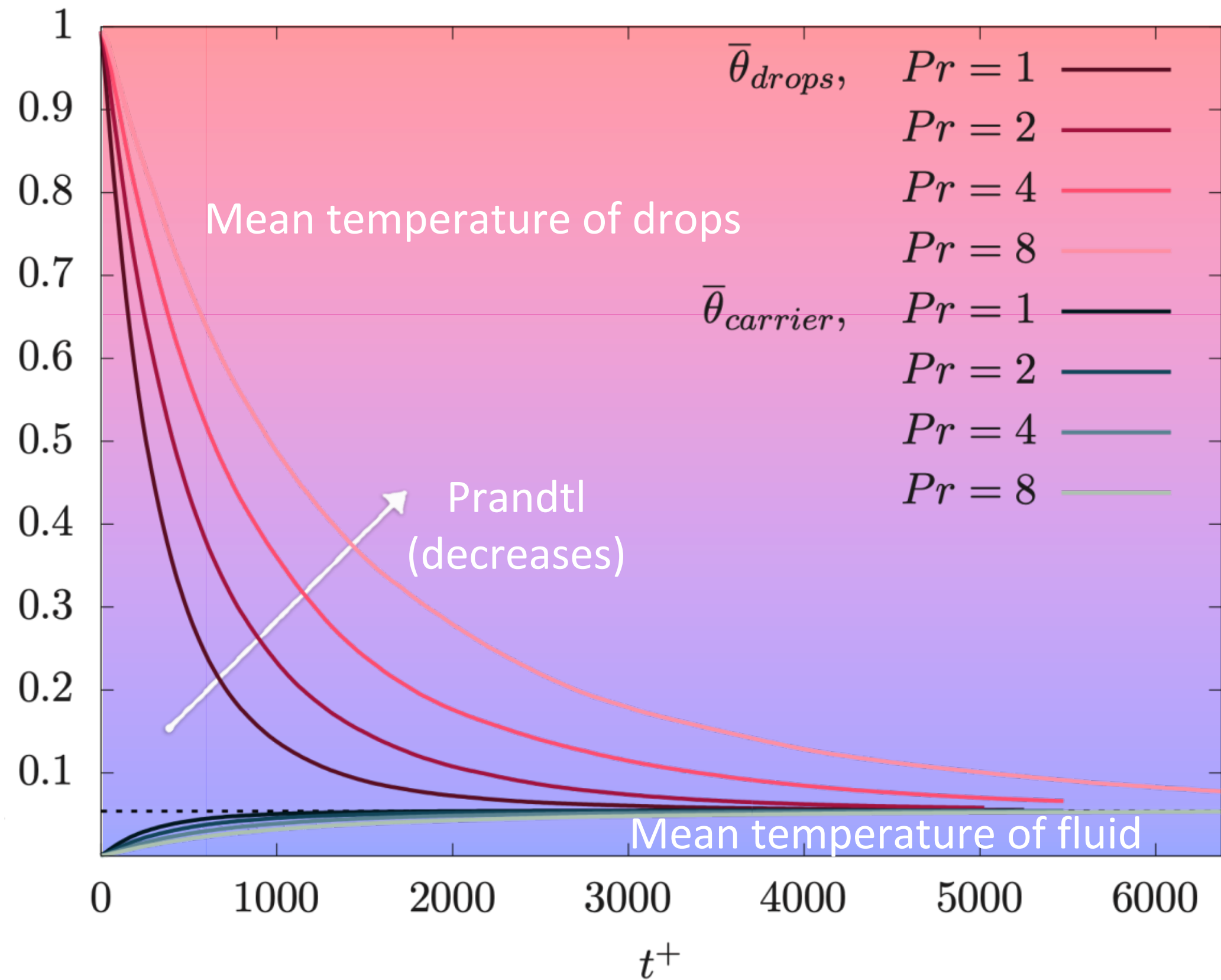
$$Pr = \frac{\nu}{a} = \frac{\text{Momentum diffusivity}}{\text{Thermal diffusivity}}$$



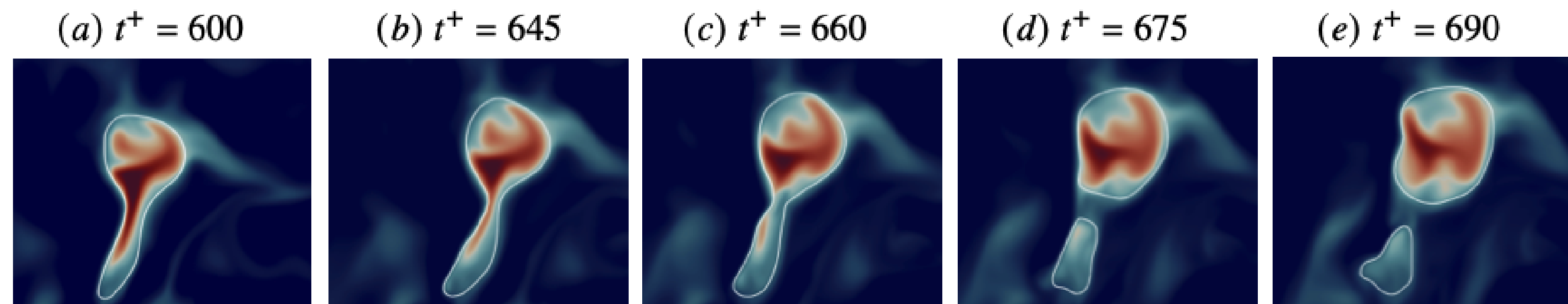
Channel mid plane



$$Pr = \frac{\nu}{a} = \frac{\text{Momentum diffusivity}}{\text{Thermal diffusivity}}$$



Drops can coalesce and break, and thus can have different sizes..
 What is the effect of drop size on temperature evolution?



Small drops tend to cool down faster (small heat capacity).

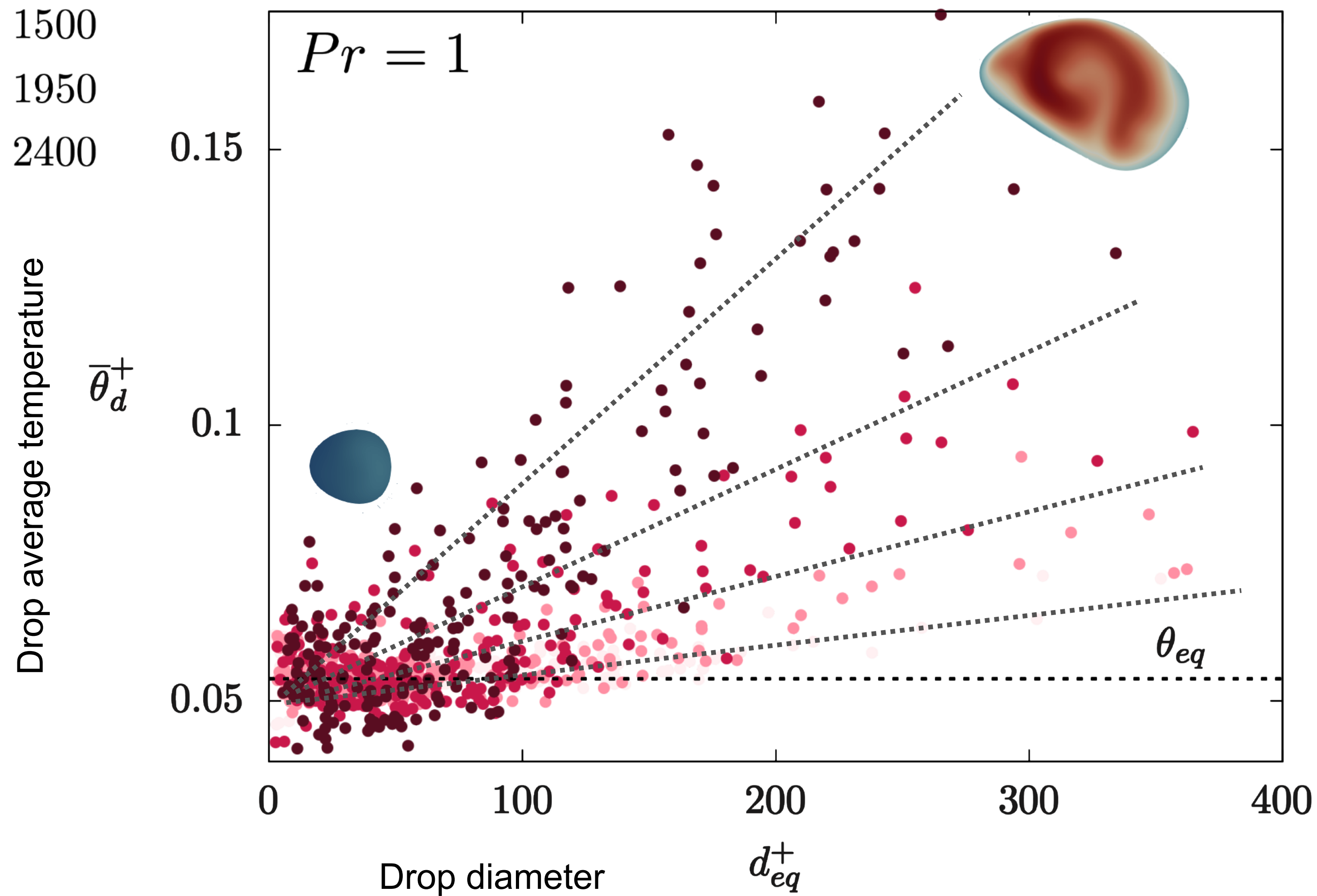
Steady average temperature of the mixture

$$\theta_{eq}^+ = \theta_{c,0}^+ (1 - \Phi) + \theta_{d,0}^+ \Phi$$

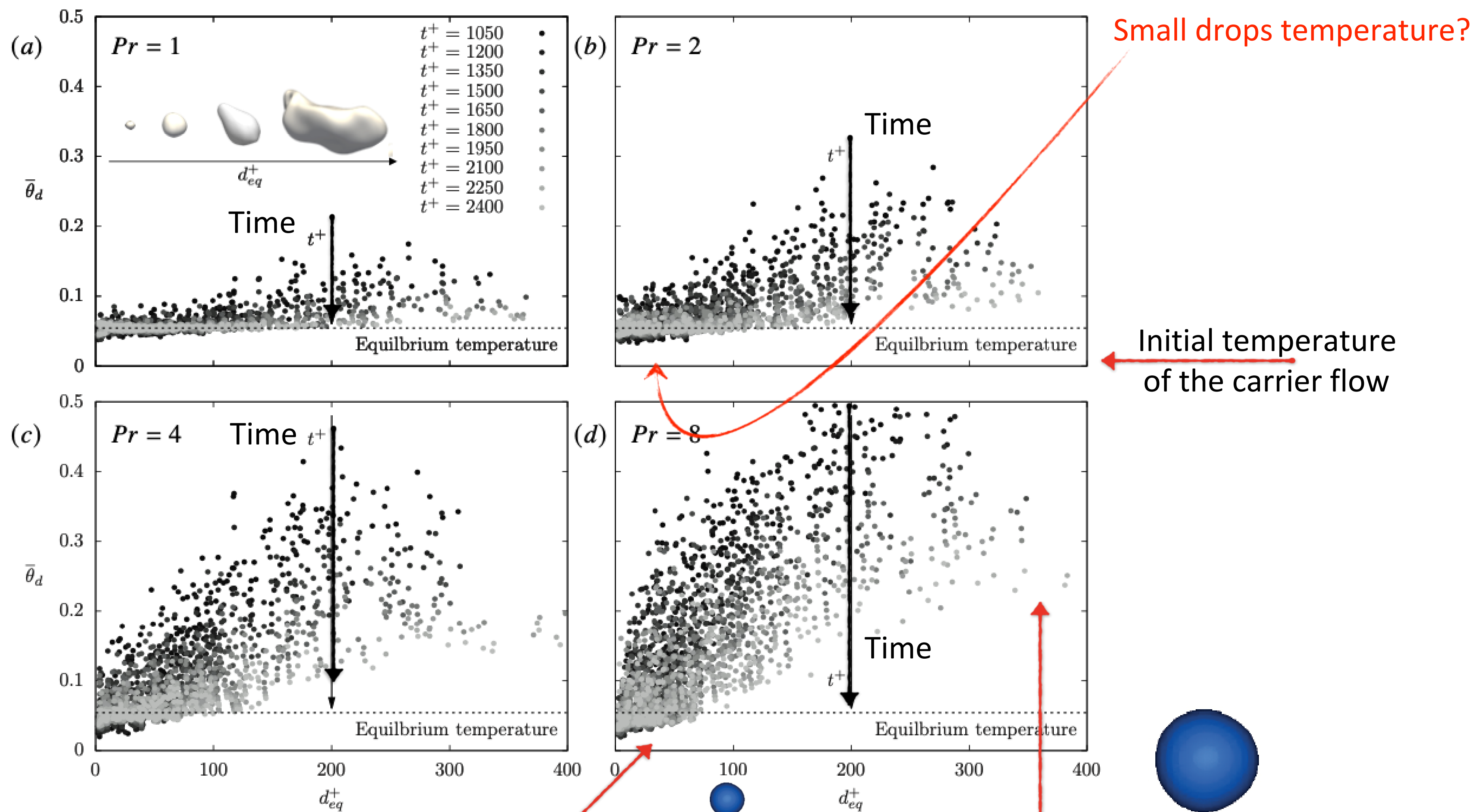
Volume fraction: $\Phi = 5.4\%$

$$Pr = \frac{\nu}{a} = \frac{\text{Momentum diffusivity}}{\text{Thermal diffusivity}}$$

- single drop at $t^+ = 1050$
- single drop at $t^+ = 1500$
- single drop at $t^+ = 1950$
- single drop at $t^+ = 2400$



Time evolution of average drop temperature for different drop sizes.



Small drops temperature?

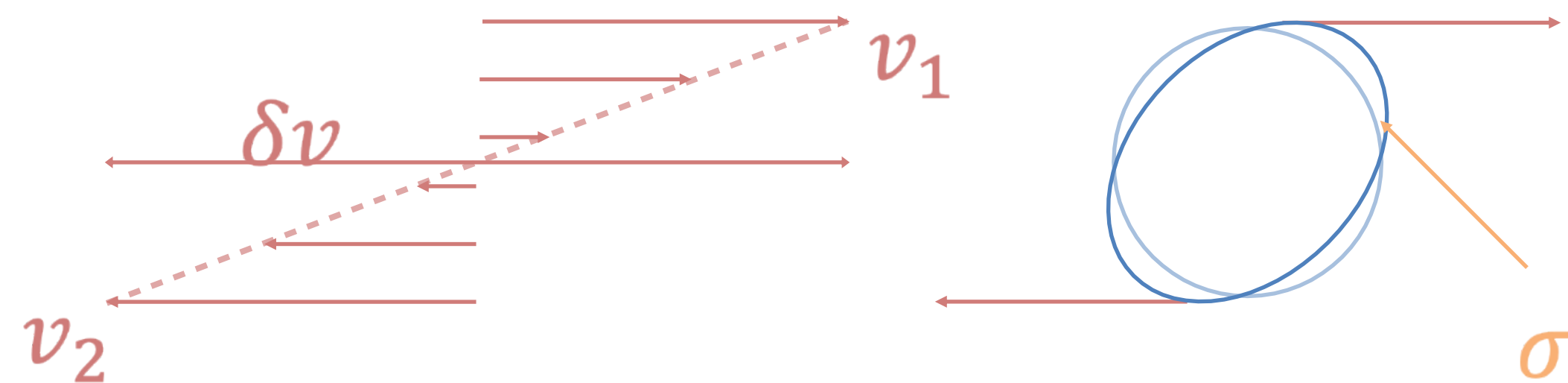
Initial temperature of the carrier flow

Small drops: low heat capacity; cool down is faster

Large drops: large heat capacity cool down is slower.

$$Pr = \frac{\nu}{a} = \frac{\text{Momentum diffusivity}}{\text{Thermal diffusivity}}$$

Bubbles/Drops break if stresses win over restoring surface tension



Kolmogorov-Hinze Critical radius

$$r_H \propto \left(\frac{\rho}{\sigma}\right) \varepsilon^{-2/5} \propto We^{-3/5} \varepsilon^{-2/5}$$

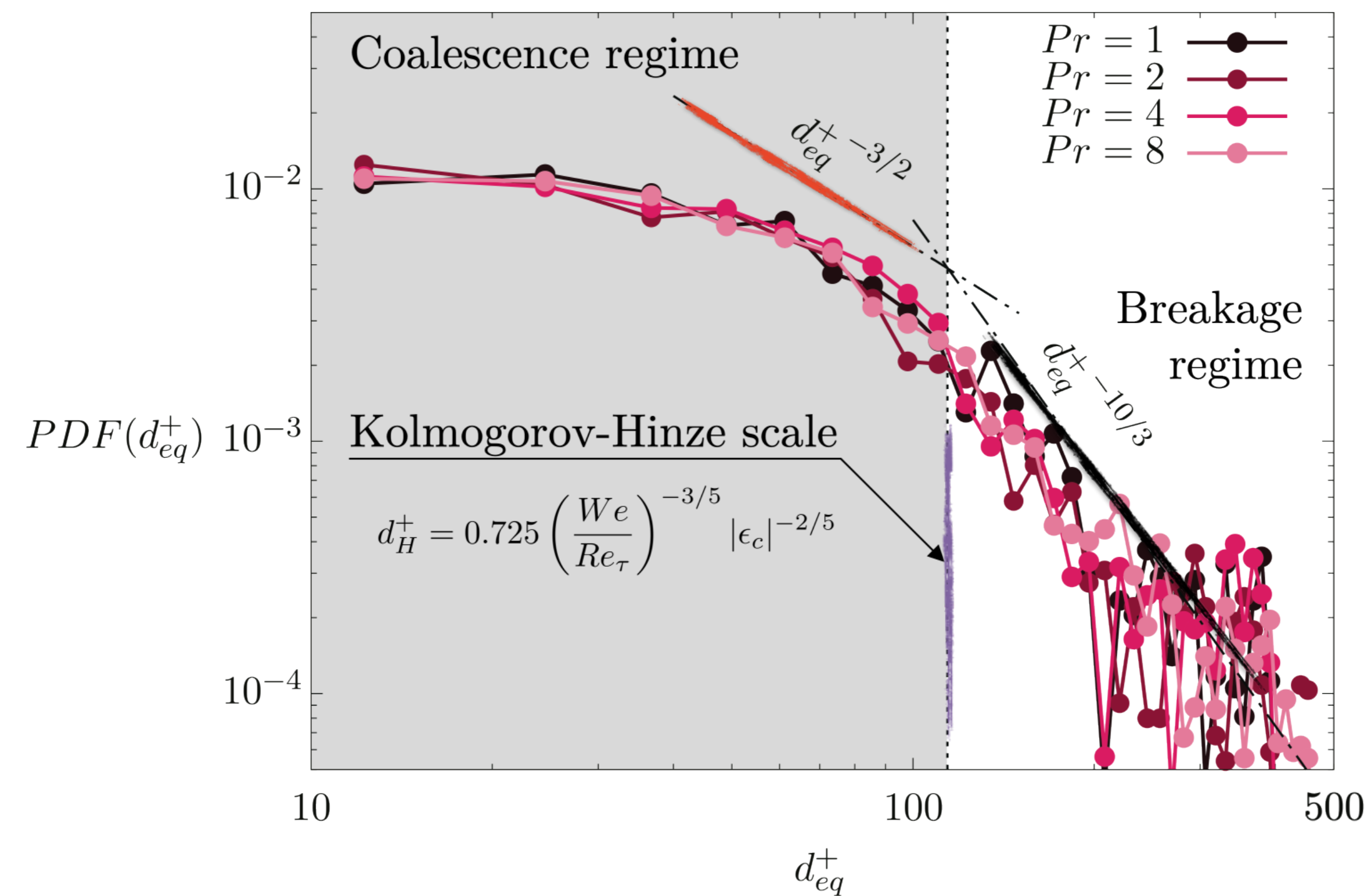
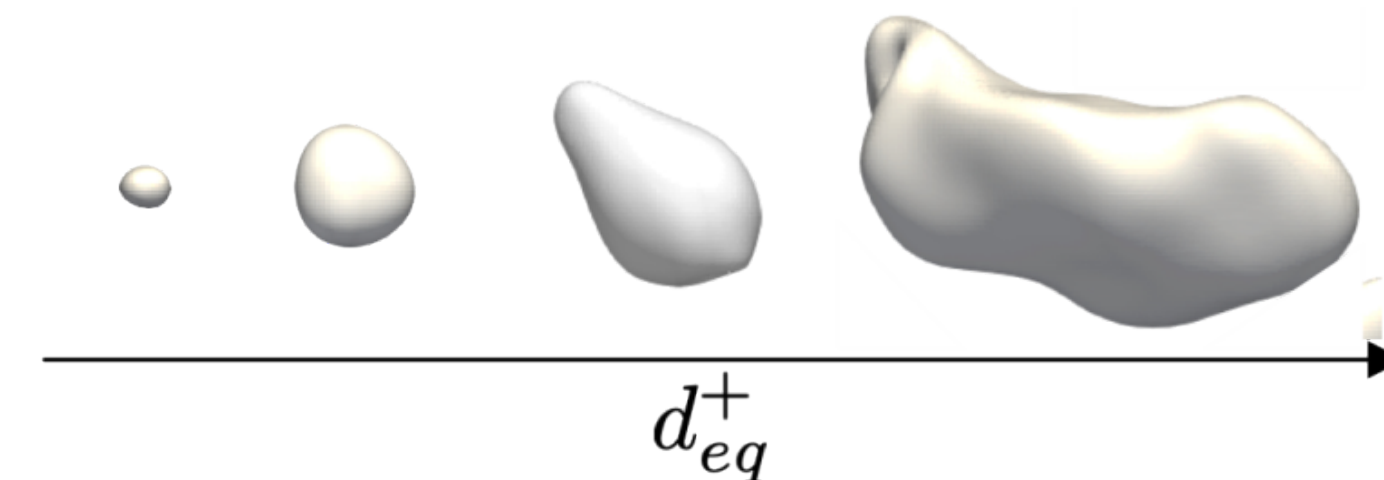
$$We = \rho u_\tau^2 h / \sigma_0$$

Small drops/bubbles

$$N(r) \propto Q \left(\frac{\sigma}{\rho}\right)^{-3/2} u^2 r^{-3/2}$$

Large drops/bubbles

$$N(r) \propto Q \varepsilon^{-1/3} r^{-10/3}$$



Thermal balance for an isolated drop:

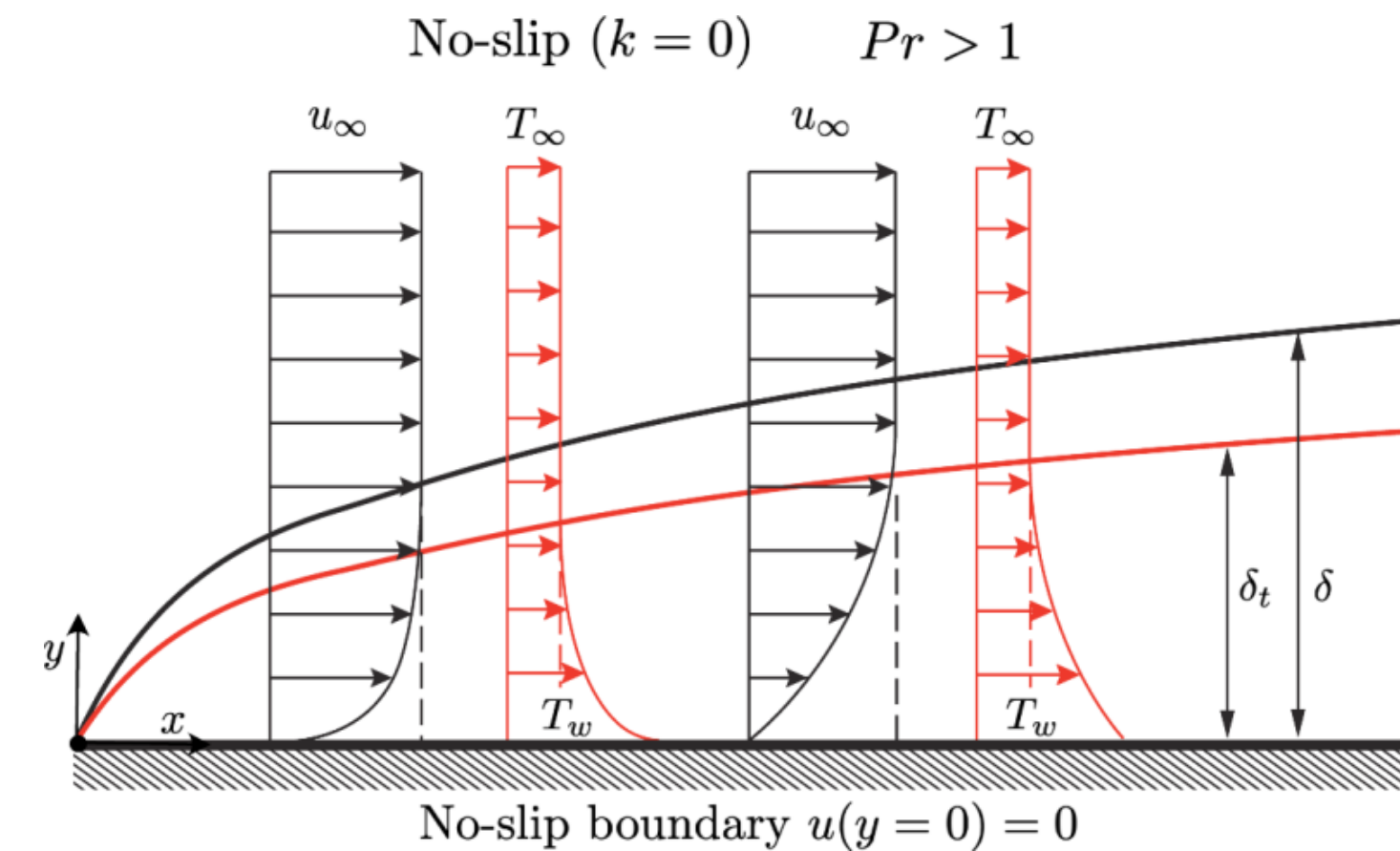
$$m_d^* c_p^* \frac{\partial \theta_d^*}{\partial t^*} = \mathcal{H}^* A_d^* (\theta_c^* - \theta_d^*)$$

$$\frac{\partial \theta_d^*}{\partial t^*} = \frac{6\nu^* \rho_c^*}{\rho_d^* d^* \delta_t^* Pr} (\theta_c^* - \theta_d^*)$$

Boundary layer theory (heat transfer coefficient):

$$\mathcal{H}^* \sim \lambda^* / \delta_t^*$$

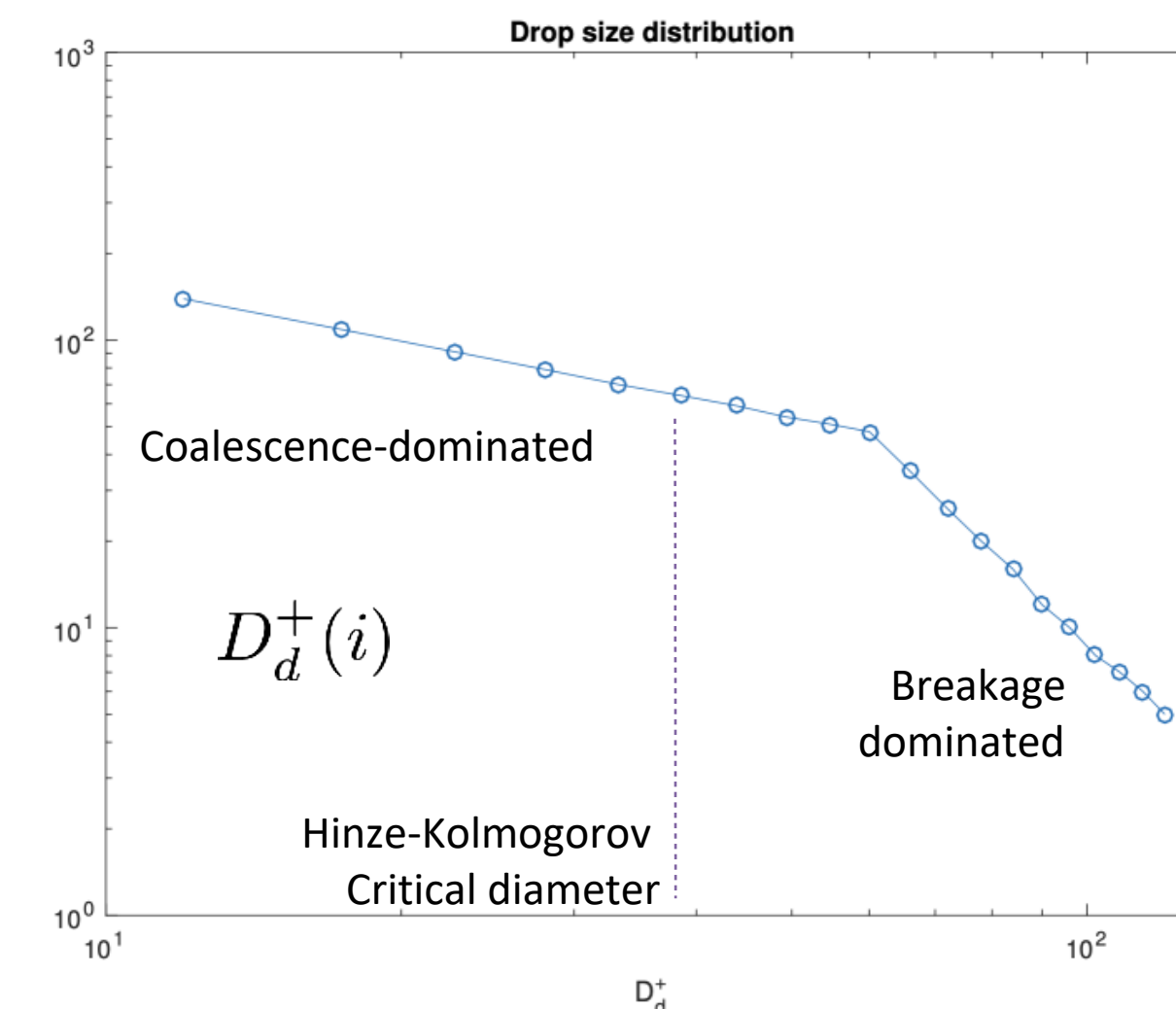
$$\delta_t = \delta Pr^{-1/3}$$



Temperature evolution for a single droplet:

$$\frac{\partial \theta_d^+}{\partial t^+} = C Pr^{-2/3} (D_d^+)^{-1} (\theta_f^+ - \theta_d^+)$$

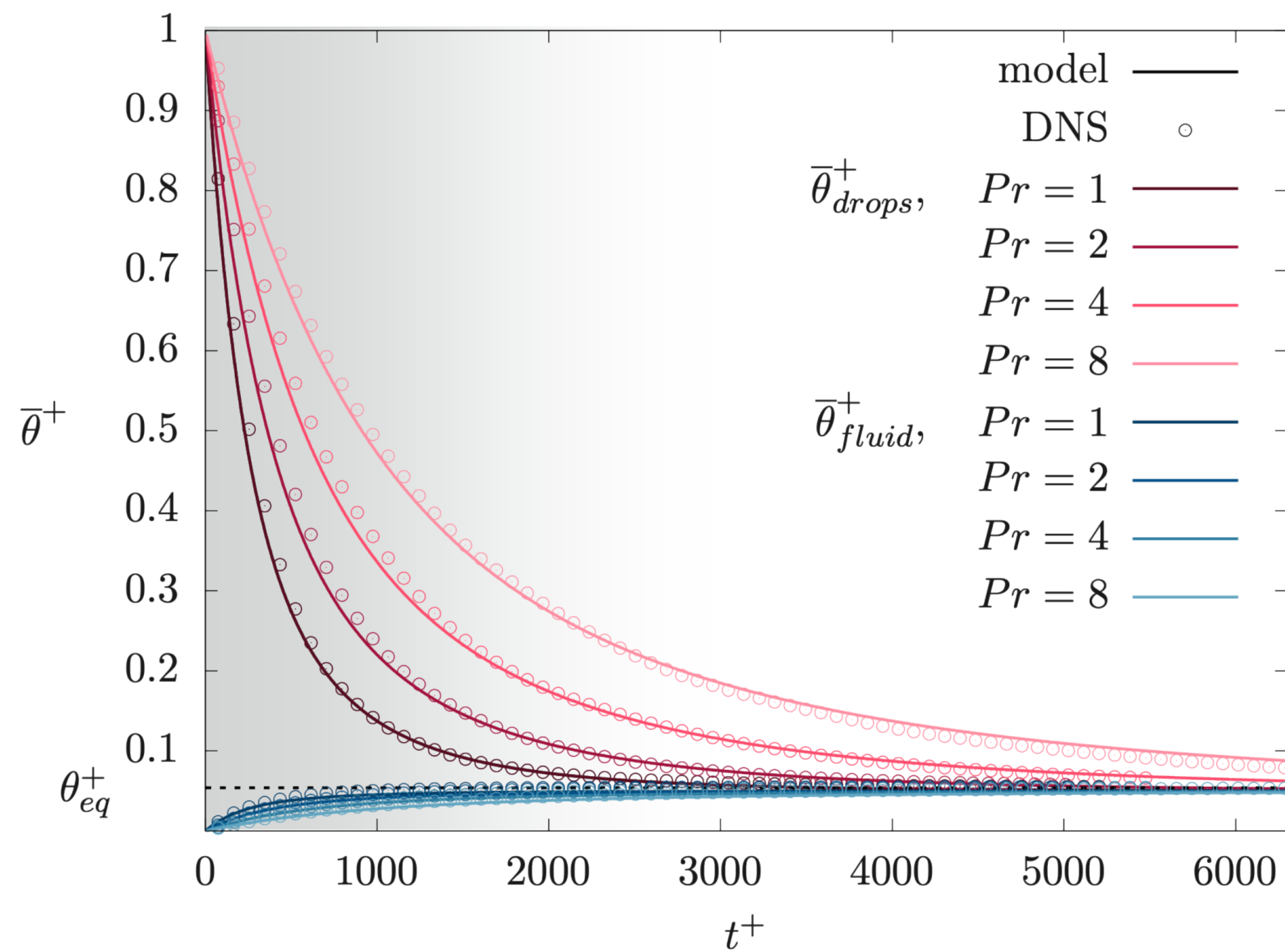
Drop size distribution:



We can now integrate this temperature evolution equation over different class of diameters (DSD) so as to obtain the evolution of the mean temperature of the drops and of the carrier flow.

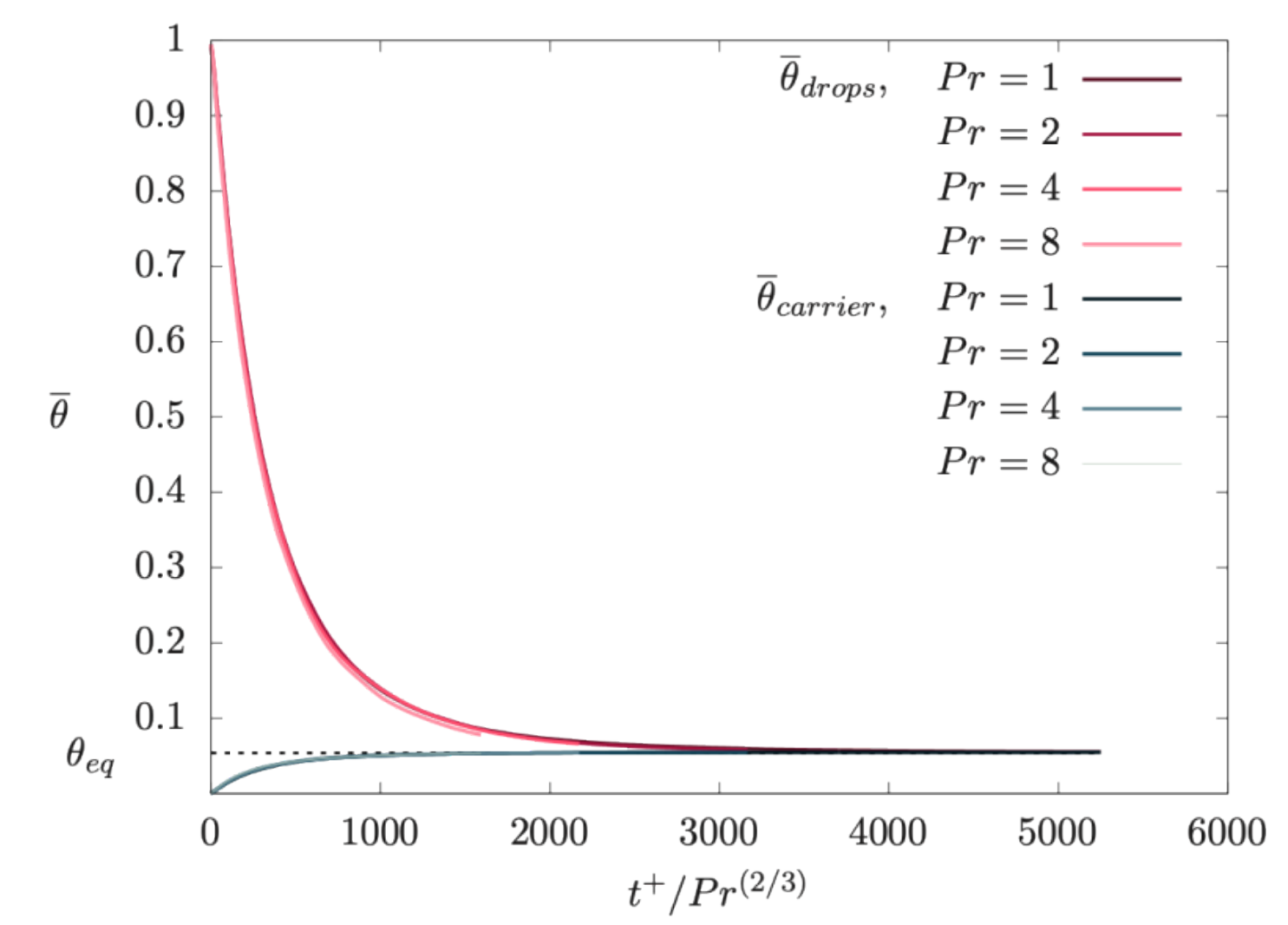
$$Pr = \frac{\nu}{a} = \frac{\text{Momentum diffusivity}}{\text{Thermal diffusivity}}$$

Simple model for mean temperature evolution (II)



Excellent agreement between the numerical results and the phenomenological model...!!

We can also rescale everything using the $Pr^{2/3}$ exponent and collapse all the curves:



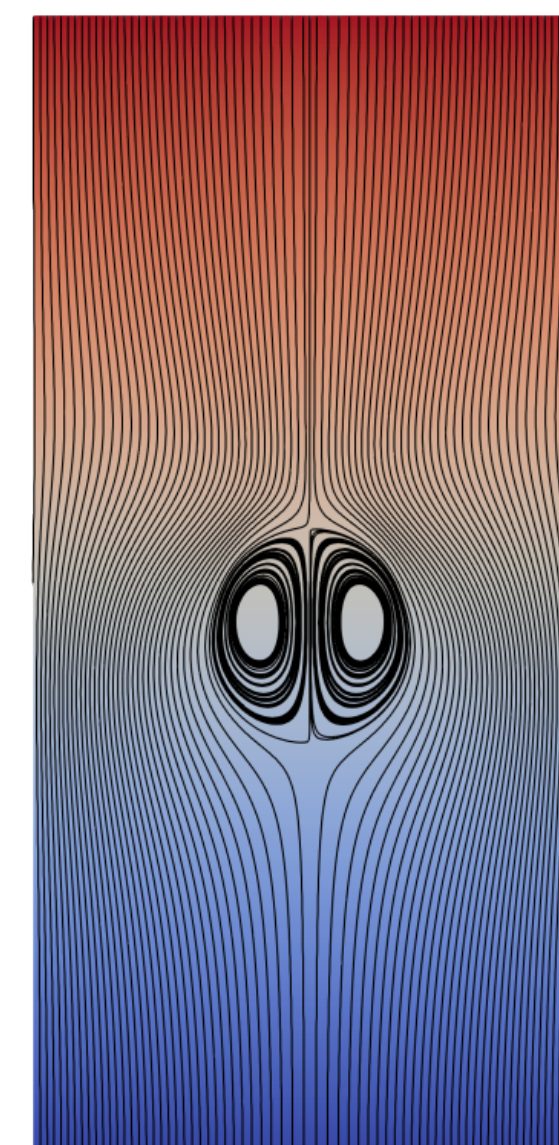
Conclusions:

- The heat transfer from the drops to the carrier fluid shows an expected dependency on **Prandtl**: the higher is the Pr, the slower is the diffusion and thus the heat transfer between the phases
- We developed an analytical model which can well predict the average temperature of the two phases
- We found a scaling for the time (diffusive time)
- We found a correlation between the diameter and the average temperature

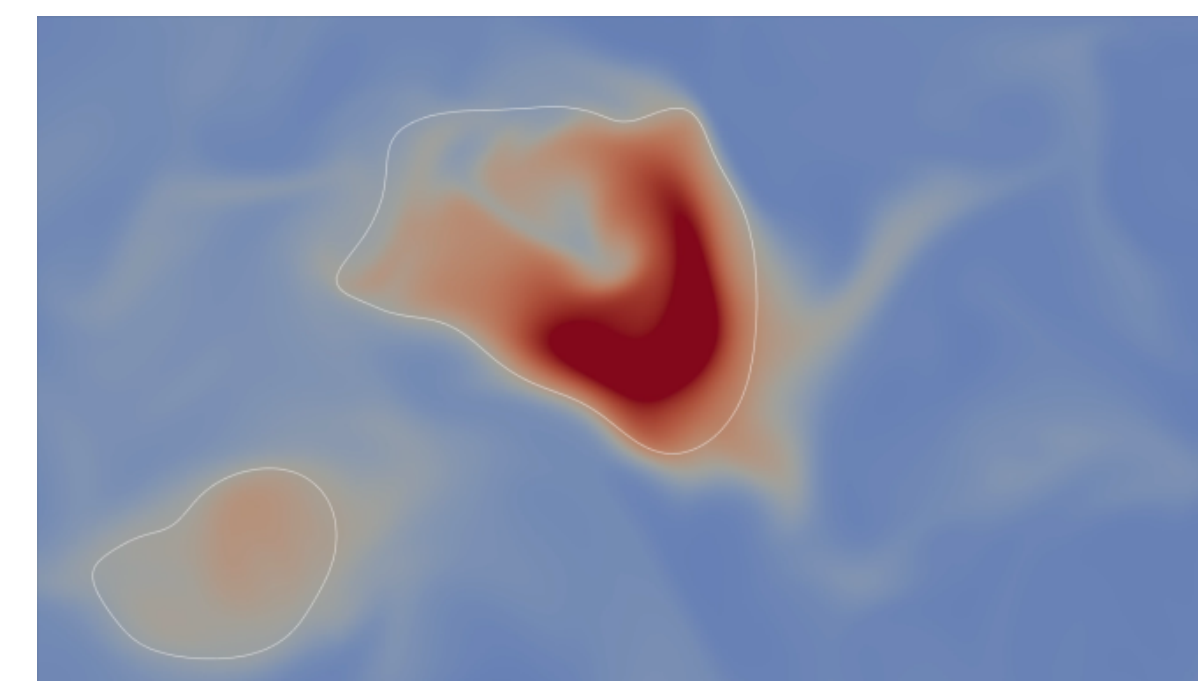
Future developments:

- Extend the simulations to mass/species transfer.
- Thermocapillary Marangoni effects
- Phase Change/Boiling (MIT Collaboration)

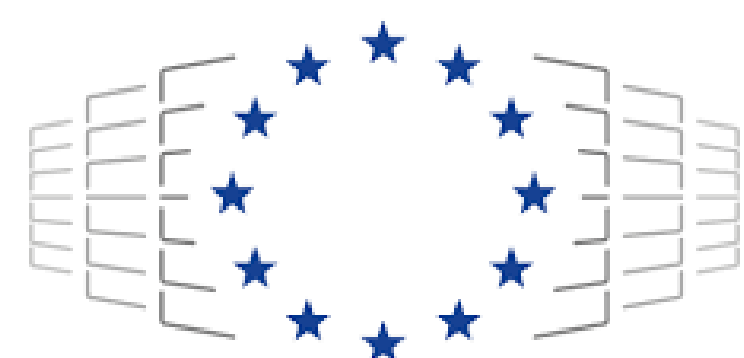
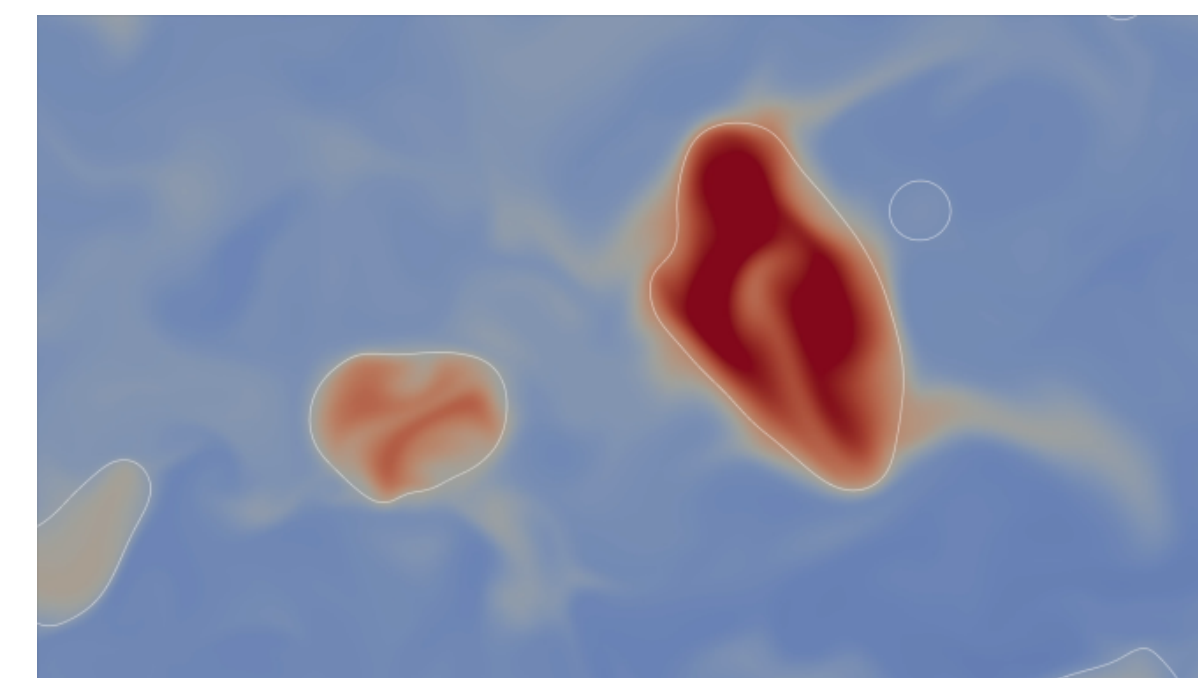
Thermocapillarity



Breakup



Coalescence



EuroHPC
Joint Undertaking



Funded by the European Union
NextGenerationEU

We acknowledge the EuroHPC Joint Undertaking for awarding this project access to the EuroHPC supercomputer Discoverer, Sofiatech (Bulgaria)